SPECTRAL ANALYSIS OF FIELD EMISSION FLICKER (1/f) NOISE

Mark Alan Gesley
B.A. Reed College, 1977

A dissertation submitted to the faculty
of the Oregon Graduate Center
in partial fulfillment of the
requirements for the degree
Doctor of Philosophy
in
Applied Physics

June, 1985

The dissertation "Spectral Analysis of Field Emission Flicker (1/f) Noise" by Mark Alan Gesley has been examined and approved by the following examination committee

Lynwood W. Swanson, Thesis Advisor
Professor

J. Fred Holmes
Professor

Richard Elliott
Professor

M. A. K. Khalil
Professor

This thesis is dedicated to the memory of my brother Mead

"The stone which the builder refused is become the headstone of the corner."

Psalm 118:21-23

Acknowledgements

La vem a força, la vem a magia que me incendie o corpo da alegria ...
la vem a santa maldita euforia que me luzia me joge me rodopia
la vem o canto do berro da fera, la vem a voz de qualquer primavera
la vem a unha rasgando a garganta, a fome a fúria em sangue que já se levante
de onde vem esta coisa tão minha que me aquece e me faz carinho?
de onde vem esta coisa tão crua que me acorde me põe no meio da rua?
é o lemento o canto mais puro que me ilumina na casa escure
é minha força e nosso energia que vem de longe pra nos fazer companhia
é são francisco bone e cachimbo me ensinando que a luta e mesmo comigo
Milton Nascimento

I am most grateful to Professor Swanson for encouraging me to undertake this research. Our many discussions and his thoughtful commentary have enhanced the quality of this work. I have also benefited from his support, which included the opportunity of attending several conferences and discussing this work with a larger circle of scientists. I thank Professors Swanson, Elliott, Holmes, and Khalil for serving on my examination committee. It is a pleasure to thank Dr. Michael Tringides at the University of Chicago for numerous communications concerning field emission noise phenomena. This dialogue has especially stimulated a much improved version of chapter II. To my friend Professor V. Rao Gudimetla I express many thanks for our wide ranging discussions, particularly helpful have been those concerning harmonic analysis and probability theory. I am indebted to Professor Richard Elliott for discussing a number of mathematical points required by this work. I thank Professor J. Fred Holmes for a very useful introduction to the theory of random variables and stochastic processes. The course provided essential groundwork for much of this study particularly chapters I and IV. I have benefited from informative discussions with Dr. A.E. Bell concerning field emission physics. I thank Professor Jon Orloff for his interest and support allowing me the chance to discuss my work with the Darmstadt group. I appreciate Professor R. Meclewski of the University of Wroclaw, Poland and Dr. J. Beben of the Karl Marx University in Leipzig, DDR reading chapter I and

providing several useful comments. Jack Biles has been a source of encouragement through our many discussions especially those concerning correlation theory. To my fellow students Sun Li Bo, Rick DeFreez, and Jia Zheng Li go many thanks for their questions and friendship. The excellent drafting of all of the graphs and figures by Barbara Ryall is gratefully acknowledged. The assistance of librarians Maureen Seaman, Chris Lightcap, and Judy Bar-Tzur has been a very useful aid to this research. I am indebted to the Computer Science and Engineering department for the opportunity of using the VAX computer, which has considerably eased the work of revision and produced a very nice copy of the manuscript. I also wish to thank Professors Jean Delord and Mike Gold for their overall encouragement during the pursuit of this degree.

Very special thanks go to my wife Gail for her love, patience and understanding, to my son Joseph for being such a great inspiration, and to my parents for their many years of support and encouragement which has helped bring me to this point. I thank my family and friends for having helped make this all worthwhile.

Table of Contents

List of Figures

List of Tables

ABSTRACT

Spectral Analysis of Field Emission Flicker ($1/f$) Noise

Mark Alan Gesley, Ph.D.
Oregon Graduate Center, 1985

Supervising professor: *Lynwood W. Swanson*

Spectral analysis of field emission noise induced by emitter surface equilibrium density fluctuations is developed. The noise spectrum factors as $S(\omega) = S_\infty(\omega) + S_B(\omega)$ for a canonical ensemble, which characterizes adsorbate covered emitters. $S_\infty(\omega)$ and $S_B(\omega)$ correspond to unbounded diffusion and the boundary effect respectively. Chemical diffusivity D_c is defined by Fick's first law. Its equilibrium limit, termed hydrodynamic D_h, is derived from $S(\omega)$ and related to the adsorbate fluctuations. These diffusivities are compared using irreversible thermodynamic and Kubo relations. Their equality is ensured by evaluation of the excess entropy production only when the density gradient is small and no phase change occurs. Two dimensional adsorbate phase transitions are identified by correlating incipient nonlinearity in the Arrhenius plot of diffusivity with the onset of a temperature dependent total noise power, which is proportional to adsorbate isothermal compressibility. Examples using K/W, Xe/W, and H/W are given. Thermal field emission noise is characterized by a grand canonical ensemble (GCE). Here the diffusive fluctuation mechanism includes adatom creation and defect vacancy formation resulting from surface free energy minimization. Adatom dynamics are governed by a stochastic diffusion equation. A multidimensional version of Carson's theorem is formulated, which leads to $S(\omega) \approx C(x=0, \omega)\, N_c^{-1}(\omega)$, where (hkl) geometry affects $C(x=0, \omega)$

and $N_c(\omega)$ accounts for probe spatial averaging. From this factorization of $S(\omega)$ an outstanding noise power divergence problem for diffusive equilibrium fluctuations within a GCE is solved. The solution requires finite fluctuation lifetime, which is also proved to be a necessary equilibrium condition. The other part of the solution leads to a new method of measuring the resolution of the microscope. Derived values agree well with a calculation that considers the transverse momentum distribution of the field emitted electrons. The $S(\omega)$ characteristics of tungsten thermal field emission from W(112), W(310), and W(100) planes are explained in detail. Diffusivity values, their corresponding activation energies, and the defect vacancy formation activation energy agree well with other experimental data. Conditions for the broadest band $S(\omega) \propto \omega^{-1}$ are given and a hypothesis is proposed explaining its frequent occurrence for diffusive equilibrium systems.

Introduction

Bend down low, let me tell you what I know
Cold ground was my bed last night
and rock was my pillow too
Robert Nesta Marley O.M.

Noise analysis in its entirety is a vast field with a number of approaches. One is confronted with a probability problem as the random nature of the fluctuating signal requires statements based on statistical averages. Then the general properties of the system may emerge from the initially perceived chaotic nature of the observed signal. For field electron emission the mean value of the current is well described by the Fowler-Nordheim equation. Answering the question, what is the probability that the current will have given values at two points in time? leads directly to the noise theory as it is studied here. The answer to this question requires analysis of the autocorrelation function. The resolution of this expression into a form that determines the weight of the fluctuations for a given interval of time, in a sense being a probabilistic snapshot of the system dynamics, introduces a second mathematical problem whose solution originated with the work of Norbert Wiener and A. Khinchin. A fundamental problem in classical Fourier analysis is that the transform of a fluctuating signal itself does not exist, i.e. cannot be resolved into frequency components, because the function does not decay to zero as time progresses. They joined probability theory to Fourier analysis by first realizing the transform of the autocorrelation exists and is the spectral density, which also has become known as the noise power spectrum.

Wiener stated the study of Brownian motion by Einstein and Smoluchowski inspired his own research. The work of these men created two closely intertwined fields; the more mathematical course leading through Wiener's functional integration methods to Feynman's path integral technique, while Smoluchowski's research was continued by the physicists Fürth, Ornstein, Uhlenbeck, Wang, and Rice also inspired

the mathematicians Doob, Kac, and Ito. The analysis of Brownian motion is of direct importance to the present work as density fluctuations are the object of study in both cases. Here they occur on the surface of a field emitter and induce the observed electron current fluctuations by varying the potential within a few angstroms of the surface. Furthermore the use of the field emission microscope in a configuration that is optically similar to those of the earlier investigators at the turn of the century, such as Westgren and Svedberg, yields related mathematical expressions for the autocorrelation function.

Two events occurred in close succession which encouraged me to pursue this research. In the spring of 1982 Professor Swanson suggested that several unresolved questions existed concerning the nature of field emission noise and specifically the relation between Professor Gomer's autocorrelation measurements of field emission flicker noise due to adsorbate covered emitters in the time domain and his own noise measurements using a thermal field emitter, which were carried out in the frequency domain with a spectrum analyzer. By chance I had found L. Bliek's article in *"Recent Advances in Condensed Matter Physics"* on a diffusion model for flicker $1/f$ noise. I felt this work might contain some clue as to how the field emission noise analysis might be done even though it was not concerned with the specific topic of field emission noise.

By fall of 1982 I began the research that has led to chapter IV, which interestingly became the final one. Initially I thought this model could be applied almost directly to the thermal field noise measurements even though some of Bliek's ideas could not be accepted. These initial ideas were reported in part at the August 1983 Field Emission Symposium.

Two problems continued to bother me at that time. The first was finding the relation between Bliek's analysis and Gomer's autocorrelation theory of field emission fluctuations. The second was how these studies related to Voss and Clarke's equilibrium *1/f* noise theory, which represents the most recent significant contribution to *1/f* noise theory based on a diffusion mechanism.

Because Gomer's work was directly involved with field emission noise the first problem stated was the most important to resolve. I came to understand two things. One was that his paper was really part of a larger school of thought, which dated back to the beginning of this century involving the work of Einstein and Smoluchowski. The reason being that field emission noise is related to surface density fluctuations occurring on the emitter. The formalism used by Gomer is analogous to Smoluchowski's theory of concentration fluctuations. This allowed me to draw on a large literature in developing the spectral analysis of Gomer's theory, which resulted in chapter I.

The second thing I realized was that Bliek's analysis was not formally similar in a mathematical sense to Gomer's. Physically this distinction is due to Gomer's adsorbate diffusion model being constrained to have the total particle number on a single *(hkl)* plane constant, whereas Bliek's study allowed for the total particle number to fluctuate about a mean value.

I next looked at what comes out of the chapter I analysis of adsorbate induced noise in terms of physically significant information. The principal variable that is extracted is the adsorbate diffusion coefficient. Although this term is frequently the first term dropped from further discussion when evaluated by a mathematician, it contains much information concerning the mass transport energetics and many body properties of the adsorbate viewed as a dynamical system. I then learned that even for a

single component system there are many diffusion coefficients and many methods of measurement. Chapter II sorts out my view on what is the mutual relationship of these different coefficients and where field emission noise studies stand with respect to the associated techniques of obtaining them. Diffusion processes occur in many different systems and the field emission noise measurement is a relatively new method for studying them. Before Gomer's group began performing such measurements the field of equilibrium diffusivity studies was restricted to thermal neutron scattering of liquids and light scattering by dilute liquid suspensions. Field ion microscopy is restricted to low densities and traditional nonequilibrium measurements were generally accepted as yielding the same diffusion coefficient as the noise measurement. This latter idea bothered me as it was not clear under what circumstances a diffusion experiment carried out under equilibrium conditions could be compared with one of the same system but which derived a diffusion coefficient from observation of the nonequilibrium decay of a density gradient. However these concerns are not yet widely shared by other workers with one important exception. The monograph by Glansdorff and Prigogine develops nonequilibrium thermodynamic stability theory and my own understanding of this work has been partly incorporated in chapter II. This chapter has since been accepted for publication in Surface Science. I believe there is still much to be done in this field; both experimentally, as there is yet no definitive test of the analysis, and also theoretically, as the general kinetic and thermodynamic description of a system has not rigorously delimited the range of validity of this work for all cases.

The diffusion coefficient reflects the dynamics of the adsorbate and is derived from analysis of the time dependence of the current fluctuations as shown in detail in chapters I and II. Yet noise analysis also provides insight to the thermodynamics of

the adsorbate via the static response of the system, which is measured by the total noise power. Analysis of experimental data in the literature appeared to me not to fully exploit this observation. Chapter III considers how surface adsorbate thermodynamics is studied by analysis of the temperature dependence of the field emission noise power. This chapter is currently under review for publication. Besides pointing out connections between the static and dynamic response of an adsorbate system undergoing a phase change, as measured by field emission noise experiments, this chapter also extends the calculation of kinetic expressions using the idea of a two level thermodynamic system in a manner not previously undertaken.

By the end of 1984 I returned to Chapter IV. I believe that it represents a completed classical equilibrium fluctuation theory, excluding critical phenomena, within the grand canonical ensemble, which is based on a Langevin approach to the modeling of density fluctuations. It incorporates elements of Bliek's and Voss and Clarke's theories. It solves certain divergence problems existing within these previous works in a consistent manner. The elements of the theory have direct physical significance as evidenced by its success in describing the tungsten thermal field measurements described therein, particularly its ability to estimate the spatial resolution of the field emission microscope and the extraction of the diffusion coefficient and defect vacancy activation energy. Its ultimate critical reception awaits publication in the literature, which I intend to pursue in the near future. I feel excited about its prospects and the possibility it affords in opening up a new class of experiments.

Finally a few words concerning the overall justification for pursuing this research. This is always an important consideration, certainly when there is emphasis on applying science to solving technological problems. For the engineer noise is typically something to be rid of as it interferes with the signal carrying the desired information. Yet

to control an effect requires an understanding of the factors that cause it. As soon as this point is accepted a model containing those factors believed important is necessary to guide further experimentation. In noise analysis one is immediately confronted with nontrivial mathematical concepts involving Fourier analysis and probability theory not to mention the particular details of the system under study.

Also given an understanding of how the relevant variables affect the observed noise it is possible to then use this understanding as an extremely fine probe of additional related phenomena that otherwise may be inaccessible by more traditional detection strategies. One then enters more into the realm of basic research, which is sometimes signaled in the literature by a replacement of the word "noise" with the term "fluctuations". At this point one might then say that the "noise" is the "signal". The full value of such measurements cannot be appreciated unless a well developed theory exists. It is remarkable that from a noise measurement atomic properties, of for example a field emitter surface, can be so detected.

I have enjoyed developing an understanding of this field and hope that this interest is communicated to those who read it. Behind even the most random phenomenon may lie an ordered world, which is revealed by patience and imagination.

I. Field Emission Flicker Noise - Canonical Ensemble.

"Who would have thought the old man to have had so much blood in him?

Shakespeare *Macbeth*

A. Introduction

Numerous mechanisms have been proposed to explain flicker ($1/f$) noise. Theories have developed spectral density functions from: nonstationary processes [1], motion in a random potential [2], and diffusion mediated two site switching [3,4]. Investigations of contact noise in semiconductors by Richardson [5], MacFarlane [6], and van der Ziel [7] led to the development of 1/f type spectra from diffusion processes. These analyses were in turn based on Smoluchowski's theory of density fluctuations [8,9]. Since then many studies have developed autocorrelation functions that are proportional to Smoluchowski's probability after-effect factor

$$P_s = 1 - A_p^{-1} \int_{A_p} \int_{A_p} d\vec{r}_1 \, d\vec{r}_2 \; G(\vec{r}_1, t\,; \vec{r}_2),$$

where the density or temperature is taken as the random variable, $G(\vec{r}_1, t\,; \vec{r}_2)$ is the Green function for the diffusion equation, and A_p is the probed region [10-20]. These theories implicitly assume fluctuations occur at equilibrium and are linear and time reversible on a microscopic scale.

Kleint's adsorption-desorption theory [21] attempted to explain the early experimental measurements of field emission flicker noise by Kleint and Gasse [22]. Timm and van der Ziel provided the first spectral analysis of adsorbate induced noise that included the Fowler-Nordheim (FN) equation [11]. They considered diffusive adsorbate

motion over an infinite planar surface with site exclusion interactions only. The use of a probe technique to detect adsorbate density fluctuations on a single (hkl) plane along with a more precise analysis of the FN equation and field emission noise in the time domain has since been carried out by Gomer and Chen [12,13]. Mazenko, Banavar, and Gomer extended the fluctuation theory to include fully interacting systems [14]. Their study demonstrated that a density dependent surface diffusion coefficient $D(n)$ is derivable from the field emission current autocorrelation function $R(t)$ measurement of equilibrium density fluctuations.

The present study develops the spectral analysis of field emission $1/f$ noise associated with adsorbate diffusion over a single (hkl) plane of the emitter including the effect of net plane boundaries and anisotropic diffusion. Systems belonging to a canonical ensemble are considered, i.e those that are closed with respect to the number of net plane particles. Only totally reflecting boundaries are considered consistent with the assumption of equilibrium density fluctuations occurring on a finite size net plane. To maintain equilibrium with absorbing or partially reflecting boundaries would require additional sources in the diffusion equation. Introducing these would fundamentally change the process assumed to cause the noise, e.g. an additional mechanism such as evaporation-condensation would then have to be included.

Factors related to the FN equation, and thus specific to the field emission process, are considered in section B where an integral equation for $R(t)$ is developed analogous to ones derived by Lax [15] and van Vliet and Fassett [16]. This equation involves the two point covariance of the density fluctuation $C(\vec{r}_1,\vec{r}_2) = < \delta n(\vec{r}_1)\ \delta n(\vec{r}_2) >$ and the Green function $G(\vec{r}_1,t\,;\vec{r}_2)$ for the diffusion operator $L = \partial/\partial t - D\nabla^2$. Critical fluctuations affect both $G(\vec{r}_1,t\,;\vec{r}_2)$ and $C(\vec{r}_1,\vec{r}_2)$. It is well known that $C(\vec{r}_1,\vec{r}_2)$ involves a correlation length ρ whose size

becomes significant near the critical point where $G(\vec{r}_1, t\,; \vec{r}_2)$ is also no longer derivable from the diffusion equation. The system is assumed not to be dominated by critical fluctuations and thus the noise spectrum $S(\omega)$ can be evaluated using $G(\vec{r}_1, t\,; \vec{r}_2)$ and a simplified version of $C(\vec{r}_1, \vec{r}_2)$. In this regime interactions affect $D(n)$ but do not alter the time dependence of $G(\vec{r}_1, t\,; \vec{r}_2)$. Therefore a dimensionless expression for $S(\omega)$ can be written that is not explicitly dependent on the interactions.

The influence of probe-net plane geometry on the structure of $R(t)$ and $S(\omega)$ is investigated in section C by their decomposition in terms of eigenfunctions of $C(\vec{r}_1, \vec{r}_2)$. Certain geometries simplify the expressions for $R(t)$ and $S(\omega)$ and also affect the form the total noise power takes. A reduction of the integral equation for $R(t)$ occurs with a special representation of $G(\vec{r}_1, t; \vec{r}_2)$. The existence and completeness of the basis set $\{\phi_n\}$ corresponding to this representation is demonstrated by recognizing $C(\vec{r}_1, \vec{r}_2)$ to be a nondegenerate symmetric kernel of a homogeneous Fredholm integral equation. Representing $G(\vec{r}_1, t\,; \vec{r}_2)$ by this particular basis is equivalent to a Karhunen-Loève (KL) expansion of the density fluctuation $\delta n(\vec{r})$. The result is a linear transformation to a correlationless pair covariance. In general finding the explicit representation is difficult. However a closed solution is derived for the spectral density when the probed and net plane regions are concentric circles.

The dependence of the noise power on probe radius is considered in section D where the net plane is modeled as a square and $G(\vec{r}_1, t\,; \vec{r}_2)$ is represented by a trigonometric eigenfunction expansion. This version of $R(t)$ is equivalent to one developed by Gomer and coworkers [13,17]. For a square geometry a natural decomposition of $G(\vec{r}_1, t\,; \vec{r}_2)$ as a KL series does not occur. This modifies the integral equation involving $R(t)$. The physical consequence of this change is related to the

requirement that total noise power be zero when the probed and net plane areas are equal. This condition is independent of probe-net plane geometry and characteristic of a closed system.

In the absence of net plane boundaries the autocorrelation functions for both circular and square probe geometries are reduced to one proportional to the after-effect factor P_s. The solution for P_s was originally stated by Smoluchowski for the case of a circular probed region [8]. An explicit derivation of P_s is provided in section E to eliminate confusion resulting from an erroneous formulation by Chandrasekhar [9] that was later adopted by MacFarlane in his analysis of the corresponding $S_\infty(\omega)$ [6]. MacFarlane's $S_\infty(\omega)$ has also been used by Saitou et al. in their study of field emission noise [23]. Excluding the prefactor specific to the field emission process the correct spectrum for unbounded diffusion $S_\infty(\omega)$ is similar to one stated by Burgess [10] and subsequently used in Timm and van der Ziel's study [11]. The $S_\infty(\omega)$ derived in the present work corresponds precisely to the autocorrelation function employed by Gomer and coworkers in their study of the diffusion coefficient [12-14,24].

The expression for $S(\omega)$, including the boundary effect, is derived in section F. Its functional form eliminates criticisms that the diffusion process is inadequate for describing flicker noise of certain adsorbate systems [4,25]. It is also noted that early experiments have often not conformed to the assumptions of the theory. More recent spectral density measurements of K/W(111) using the probe-hole method are found consistent with the diffusion mechanism [26].

Anisotropic diffusion is considered in section G. Here the limiting case of purely one dimensional motion is solved analytically and found to increase the low frequency portion of $S(\omega)$.

B. The field emission autocorrelation function

The field emission current density $j(amps/cm^2)$ is described by the Fowler-Nordheim equation

$$j = B F^2 \exp\left\{\frac{-6.8\times10^7 v}{F}\ \phi^{3/2}\right\}, \tag{I.1}$$

where F is the electric field in V/cm, v is an image correction term, ϕ the work function in eV, $B = 6.2 \times 10^6(\mu/\phi)^{1/2}/v^2(\phi+\mu)$, and μ is the Fermi level [27]. The factor B is insensitive to work function fluctuations compared to the exponential term and henceforth is considered constant.

From Eq.(1) the current fluctuation $\delta i(t) \equiv i(t) - <i>$ is given by

$$\frac{\delta i(t)}{<i>} = e^{-a\left[\phi(t)^{3/2} - <\phi>^{3/2}\right]} - 1, \tag{I.2}$$

where $<i> = <j> A_p$ is the equilibrium current and $a = -6.8 \times 10^7 v/F$.

The work function $\phi = \phi(F,n)$ is dependent on the field F and adatom density $n = N/A_p$, N is the number of adatoms in probed area $A_p = \pi r_p^2$,

$$\phi = \phi_n + 2\pi\alpha F n, \tag{I.3}$$

ϕ_n is the zero field work function, and α is the polarizability per adatom.

With the work function fluctuation $\delta\phi \equiv \phi - <\phi>$, Eq.(2) is approximated to first order as

$$\frac{\delta i}{<i>} = \frac{3}{2} a <\phi>^{1/2} \delta\phi, \tag{I.4}$$

assuming $\delta\phi \ll <\phi>$. Noting from Eq.(3) that

$$\delta\phi = \delta\phi_n + c_\alpha \delta n, \tag{I.5}$$

where $c_\alpha = 2\pi\alpha F$, the relative current fluctuation

$$\frac{\delta i}{<i>} = \left[\frac{(c_1 + c_2 \partial\phi/\partial n)}{A_p} \right] \delta N \tag{I.6}$$

follows from Eq.(2) with $c_1 = c_\alpha c_2$, $c_2 = \frac{3}{2} a <\phi>^{1/2}$, and $\delta\phi_n = (\partial\phi/\partial n)\delta n$. By using Eq.(6) the relative field emission current autocorrelation $R(t) \equiv \frac{<\delta i(t)\, \delta i(0)>}{<i>^2}$ becomes

$$R(t) = \left[\frac{(c_1 + c_2\, \partial\phi/\partial n)}{A_p} \right]^2 <\delta N(t)\, \delta N(0)>, \tag{I.7}$$

where $\delta N(t)$ is the equilibrium fluctuation in particle number of the probed area A_p at time t.

Several comments are necessary about the term $(\partial\phi/\partial n)$. Gomer has noted that since field emission is governed by the potential to $\sim$ 5.0 Å from the surface it is possible to have an adatom outside the probed region influence emission within it [12]. This effect can be approximated by

$$\delta\phi = [\, \bar{w}\, h(n) + c_\alpha \,]\, \delta n, \tag{I.8}$$

where the factor $\bar{w}$ is the average contribution per adparticle to the potential energy $\sim$ 5.0 Å above the probed region and $|\, h(n)\,| \leq 1$ is a dimensionless function describing dipole depolarization. In Gomer's analysis $\bar{w}$ appears inside the particle number autocorrelation <N(t) N(0)> because it is really a function of position within the probed area A_p. If density fluctuations outside A_p do not affect the probed current then $\bar{w}$ can be written in the simple form, $\bar{w} = 2\pi\mu$, where μ is the permanent dipole moment of the adatom. The approximation becomes exact when the probed radius $r_p >> 5.0$ Å [12] or when the permanent dipole moment is small, in which case the

polarizability term dominates. This happens for a physisorbed system such as Xe/W [24].

In general $\overline{w}$ influences the value of $D(n)$ by increasing the effective probed radius r_p, but does not change the time dependence of the autocorrelation [12]. Therefore keeping in mind that a systematic error may exist in the estimation of $D(n)$, Eq.(7) can be written

$$R(t) = C_{FN} < \delta N(t)\, \delta N(0) >, \tag{I.9}$$

where $C_{FN} = \left[\frac{(c_1 + 2\pi\mu h(n) c_2)}{A_p}\right]^2$.

For a fixed value of adsorbate density $h(n)$ is constant and does not influence the spectral analysis. Several models relate mutual depolarization to work function and so an expression for $h(n)$ could be included in Eq.(8), [28,29]. Although the density dependence of the autocorrelation function as expressed through $h(n)$ is not of primary importance here there is one significant effect on the noise worth noting. For a chemisorbed system, e.g. an alkali metal adsorbate on a refractory metal substrate, $\phi(n)$ exhibits a distinct minimum, i.e. $\partial\phi/\partial n|_{\phi_{min}} = 0$ and $h(n_{min}) = 0$. Under this condition Eq.(7) implies

$$\frac{< (\delta i)^2 >}{< i >^2} = c_1^2 < (\delta n)^2 >.$$

The relative mean square current fluctuation is greatly reduced since the polarizability term c_1 is usually much smaller than the other term involving the dipole moment. An example of this reduction in noise power at the work function minimum can be found in a study of K/W (Fig.1 of ref.[30]).

The particle number in probed area A_p, expressed in terms of the local density $n(\vec{r},t)$, is

$$N(t) = \int_{A_p} n(\vec{r},t)\, d\vec{r}. \tag{I.10}$$

Hence Eq.(9) becomes

$$R(t) = C_{FN} \int_{A_p}\int_{A_p} < \delta n(\vec{r}_1,t)\, \delta n(\vec{r}_2,0) > \; d\vec{r}_1\, d\vec{r}_2, \tag{I.11}$$

where the integrand of Eq. (11) is the two point (pair) autocovariance of the density fluctuation. The classical expression is

$$< \delta n(\vec{r}_1,t)\, \delta n(\vec{r}_2,0) > = \int_{A_T} G(\vec{r}_1, t\,;\vec{r}_3)\; C(\vec{r}_2,\vec{r}_3)\;\; d\vec{r}_3 \tag{I.12}$$

where $G(\vec{r}_1\,, t\,;\vec{r}_3)$ is the Green function for the diffusion equation, the integration is over the net plane area A_T, and

$$C(\vec{r}_2\,,\vec{r}_3) \equiv <\delta n(\vec{r}_2)\;\, \delta n(\vec{r}_3)> \tag{I.13}$$

is the pair covariance function [15,16]. Combining Eqs. (11) and (12) leads to the following general form of the field emission autocorrelation function

$$R(t) = C_{FN} \int_{A_p}\int_{A_p} d\vec{r}_1\, d\vec{r}_2 \int_{A_T} d\vec{r}_3\;\, G(\vec{r}_1\,, t\,;\vec{r}_3)\; C(\vec{r}_2,\vec{r}_3). \tag{I.14}$$

C. Karhunen-Loève expansion

This section evaluates $R(t)$, as expressed by Eq.(14), in terms of its properties as an integral equation. The analysis will show that, excluding critical fluctuations, a correlationless pair covariance always exists. This simplifies the form of $R(t)$, although in practice it is often difficult finding the proper linear transformation. However a specific example is given in section F that yields a closed expression for the spectrum $S(\omega)$. The analysis shows how the structure of $R(t)$ is related to system geometry and the calculation of the total noise power.

Consider the following homogeneous Fredholm equation of the second kind,

$$\phi_n(\vec{r}_1) = \int_{A_T} d\vec{r}_2 \; C(\vec{r}_1, \vec{r}_2) \; \phi_n(\vec{r}_2), \tag{I.15}$$

and note that the kernel $C(\vec{r}_1, \vec{r}_2)$ as defined by Eq.(13) is real valued and symmetric, i.e.

$$C(\vec{r}_1, \vec{r}_2) = C(\vec{r}_2, \vec{r}_1). \tag{I.16}$$

Given that the system is not at the critical point, $C(\vec{r}_1, \vec{r}_2)$ is continuous. To prove continuity the inequality

$$< (\delta n)^2 > \; \geq \; C(\vec{r}_1, \vec{r}_2)$$

is used, which is a general property of stationary or homogeneous random functions [31]. By considering $C(\vec{r}_1, \vec{r}_2)$ to be a linear functional $T[\delta n(\vec{r}_2)]$ with parameter $\vec{r}_1$ on $\delta n(\vec{r}_2)$, i.e.

$$T[\delta n(\vec{r}_1)] = < \delta n(\vec{r}_1) \; \delta n(\vec{r}_2) >,$$

and noting the thermodynamic fluctuation theory result

$$< (\delta n)^2 > = < n >^2 kT \kappa_T / A_p, \tag{I.17}$$

one can find a constant $c = \left[< n >^2 kT \kappa_T / A_T A_p \right]^{1/2}$, such that for all $\delta n(\vec{r}_1)$,

$$| T [\delta n(\vec{r}_1)] | \leq c \, \| \delta n(\vec{r}_1) \|, \tag{I.18}$$

where the norm is defined

$$\| \delta n(\vec{r}_1) \| \equiv \left[\int_{A_T} d\vec{r}_2 < (\delta n)^2 > \right]^{1/2} = \left[A_T < (\delta n)^2 > \right]^{1/2}$$

and κ_T is the isothermal compressibility. Eq.(18) demonstrates that T is bounded as long as κ_T is finite. Using the theorem that boundedness and continuity are equivalent for linear functionals [32] ensures that $C(\vec{r}_1, \vec{r}_2)$ is continuous.

The kernel is nondegenerate as it is not expressible as a finite sum of separable functions

$$C(\vec{r}_1, \vec{r}_2) \neq \sum_{i=1}^{m} \alpha_i(\vec{r}_1) \, \beta_i(\vec{r}_2).$$

The multivariable density function implicit in $< \delta n(\vec{r}_1) \, \delta n(\vec{r}_2) >$ is not of this form because for bounded regions $\vec{r}_1$ is statistically dependent on $\vec{r}_2$ even in the absence of critical fluctuations.

The following theorem can then be applied to the kernel $C(\vec{r}_1, \vec{r}_2)$ [33]

"Every continuous, symmetric kernel that does not vanish identically possesses eigenvalues and eigenfunctions; their number is denumerably infinite if and only if the kernel is nondegenerate. All eigenvalues of a real symmetric kernel are real."

Therefore the set $\{\phi_n\}$ exists, is denumerably infinite, and can serve as a basis for functions defined over the area A_T. Given the existence of a basis set $\{\phi_n\}$ over A_T the Green function in Eq.(14) can be expanded as

$$G(\vec{r}_1, t; \vec{r}_3) = \sum_{n=1}^{\infty} a_n \ \phi_n(\vec{r}_3). \tag{I.19}$$

Substituting Eq.(19) into (14) leads to

$$R(t) = C_{FN} <(\delta N)^2> A_p^{-1} \int_{A_s} \int_{A_s} d\vec{r}_1 \, d\vec{r}_2 \ \ G(\vec{r}_1, t; \vec{r}_2). \tag{I.20}$$

This decomposition is equivalent to a KL expansion [31,34,35] of $\delta n(\vec{r}_2)$ as shown by writing,

$$\delta n(\vec{r}_2) = \sum_{n=1}^{\infty} \mathsf{b}_n \ \phi_n(\vec{r}_2). \tag{I.21}$$

The random coefficients b_n have the properties: $< \mathsf{b}_n > = 0$ and $< |\mathsf{b}_n|^2 > = 1$. They are orthogonal since solutions $\{\phi_n\}$ exist which satisfy Eq.(15) [31]. The right side of Eq. (21) converges in the mean square sense to $\delta n(\vec{r}_2)$ if the kernel is of the form [31]

$$C(\vec{r}, \vec{r}) = \sum_{n=1}^{\infty} \ | \ \phi_n(t) \ |^2. \tag{I.22}$$

The kernel $C(\vec{r}_1, \vec{r}_2)$ satisfies Mercer's theorem, which states [33]

> *"If $C(\vec{r}_1, \vec{r}_2)$ is a definite continuous kernel then the expansion given by Eq.(22) is valid and converges absolutely and uniformly."*

This theorem ensures the convergence of Eq.(21). Eq.(20) is similar to that used by van Vliet and Chenette in their spectral analysis (excluding the constant C_{FN}) (Eq.(4) of ref.[20]), although they assumed that zero correlation for $|\vec{r}_1 - \vec{r}_2| \gg \rho$, where ρ is the correlation length, is a sufficient condition for its derivation [16]. Here we see that one must also check that the eigenfunctions used correspond to a basis set of a KL expansion. However their original analysis remains valid because a circular probe was

assumed and section F shows that the conditions leading to Eq.(20) are satisfied for this geometry.

D. Correlation effects

The influence of net plane boundaries and critical fluctuations on the pair covariance $C(\vec{r}_1, \vec{r}_2)$ is now considered assuming reflecting boundaries exist on the perimeter of the net plane and that they exert a negligible effect on the critical fluctuations. The pair covariance is then written

$$C(\vec{r}_1, \vec{r}_2) = C_\beta + C_\rho \,, \tag{I.23}$$

where

$$C_\beta = A_\rho^{-1} < (\delta N)^2 > \left[\delta(\vec{r}_1 - \vec{r}_2) - A_T^{-1} \right] \tag{I.24}$$

is the correlation boundary effect [16]. Critical fluctuations are excluded from the present study, which implies $C_\rho = 0$. To find the condition under which this assumption is valid the Fourier transform of the two dimensional density fluctuation

$$\delta n(\vec{r}) = \sum_k e^{i\vec{k}\cdot\vec{r}} \, \delta n(\vec{k}), \tag{I.25}$$

and the probability density function for the Fourier component $\delta n(\vec{k})$ in mean field approximation [36]

$$f\left(\delta n(\vec{k})\right) = d_o \, e^{-\frac{1}{2}(d_1 + d_2 k^2) |\delta n(\vec{k})|^2} \tag{I.26}$$

is used, where d_o is a normalization constant and d_1, d_2 are coefficients resulting from the density fluctuation expansion of the thermodynamic potential. Using the defining

relation for the k-space covariance of the density fluctuation and Eq.(26) leads to

$$< | \delta n(\vec{k}) |^2 > = (d_1 + d_2 k^2)^{-1}. \tag{I.27}$$

Eqs.(17) and (27) yield

$$d_1^{-1} = < n >^2 kT \kappa_T / A_p. \tag{I.28}$$

The Fourier transform of Eq.(27) is

$$C_\rho(R) = (2\pi d_2)^{-1} K_0(R/\rho), \tag{I.29}$$

where the area is assumed large enough to replace summation by integration, $R = |\vec{r}_1 - \vec{r}_2|$, K_0 is the zero order modified Bessel function, and $\rho = (d_2/d_1)^{1/2}$. The asymptotic expansion of Eq.(29) is

$$\lim_{(R/\rho)\to\infty} C_\rho \sim (\rho/R)^{1/2} \; e^{-R/\rho}.$$

Thus critical fluctuations are negligible when $A_p \gg \rho^2$. Assuming this holds then $C_\rho = 0$ and substitution of Eq.(24) into (14) yields

$$R(t) = C_{FN} A_p^{-1} < \delta N^2 > \Big\{ \int_{A_p} \int_{A_p} d\vec{r}_1 \, d\vec{r}_2 \left[G(\vec{r}_1, t; \vec{r}_2) - A_T^{-1} \int_{A_T} d\vec{r}_3 \; G(\vec{r}_1, t; \vec{r}_3) \right] \Big\} \tag{I.30}$$

If the net plane, with reflecting boundary, and probed region are squares of area $4b^2$ and $4a^2$ respectively and centered at the origin then the Green function is

$$G(\vec{r}_1, t; \vec{r}_2) = \prod_{i=1}^{2} \left[\sum_{n=0}^{\infty} e^{-\lambda^2 D t} \; \gamma_n(x_{i1}) \, \gamma_n(x_{i2}) \right], \tag{I.31}$$

where $\lambda^2 = (\pi n/b)^2$, $\gamma_n(x) = (\epsilon_n / 2b)^{1/2} \cos(\pi n x / b)$, and $\epsilon_n \equiv 1(2)$ if $n = 0 (n \neq 0)$ is the Neumann factor. Combining Eqs.(31) and (30) results in

$$R(t) = C_{FN} < (\delta N)^2 > \left[A_p^{-1} \int_{A_p} \int_{A_p} G(\vec{r}_1, t; \vec{r}_2) \, d\vec{r}_1 \, d\vec{r}_2 - (A_p / A_T) \right]. \tag{I.32}$$

Eq.(32) is equal to the autocorrelation function Gomer and coworkers obtained by other means [13,14,17].

The factor (A_p/A_T) is a result of the boundary effect. Its physical significance is clarified by considering the relative noise power $P \equiv \int_0^\infty S(f)df$, which is also given by

$$P = 2R(0). \tag{I.33}$$

Using Eqs.(32) and (33) the relative field emission flicker noise power becomes

$$P = 2C_{FN} < (\delta N)^2 > \left[1 - (A_p/A_T)\right]. \tag{I.34}$$

Thus, in the limit $A_p \rightarrow A_T$, the noise power approaches zero. The reason is that fluctuations occur in this system only when particles diffuse in or out of the probed region A_p, which is impossible when $A_p = A_T$. This condition holds whenever adsorbate induced flicker noise occurs in a closed system and will be used in section F to check the validity of the spectral density derived for the case of a circular net plane. The autocorrelation function derived by Reed and Ehrlich does not have this property [37]. That the autocorrelation functions given by Eqs.(20) and (32) are not equivalent is due to the system geometry. The $\gamma_n(x)$ in Eq.(31) constitute a Fourier series, which do not form a basis in a Karhunen-Loève expansion [31]. Thus one cannot substitute Eq.(31) into (20) and obtain the proper expression for the noise power, Eq.(34), since the factor (A_p/A_T) would be missing.

It is also noted in passing that the total field emission noise power is really a sum of Eq.(34) and the shot noise term $2eI\Delta f_{BW}$, where Δf_{BW} is the bandwidth of the spectrum analyzer. However this last term will be dropped from further discussion.

E. Unbounded diffusion spectrum.

The noise spectrum $S(\omega)$ is now developed in the absence of net plane boundaries. First an explicit derivation of the after-effect factor P_s is provided to disprove several erroneous formulations [6,9,23]. Then the correct form of $S(\omega)$ is given when site exclusion occurs for an otherwise noninteracting adsorbate lattice gas. Also another method is suggested for deriving $D(n)$ from $S(\omega)$ for a fully interacting adsorbate system.

In the limit $A_T \rightarrow \infty$, Eqs.(20) and (32) become identical and are related to Smoluchowski's probability after-effect factor since $R(t) = C_{FN} < (\delta N)^2 > \left[1 - P_s(t)\right]$. Specifically,

$$R(t) = \frac{C_{FN} < (\delta N)^2 >}{A_p \, 4\pi D t} \int_{A_p} \int_{A_p} d\vec{r}_1 \, d\vec{r}_2 \; e^{-|\vec{r}_1 - \vec{r}_2|^2/4Dt}. \tag{I.35}$$

Eq.(35) can be evaluated in closed form by transforming to polar coordinates. The factor P_s becomes

$$P_s(t) = \frac{1}{\alpha^2} \int_{\alpha^2}^{\infty} dx \; e^{-x} \int_0^{\alpha^2} dw \; e^{-w} I_0\left(2\sqrt{xw}\right), \tag{I.36}$$

where $\alpha^2 = r_p^2/4Dt$ and I_0 is the zeroth order modified Bessel function.

The integrand of Eq.(36) can be expressed as the Bessel function J_0 hence,

$$P_s = \frac{1}{\alpha^2} \int_{\alpha^2}^{\infty} dx \int_0^{\alpha^2} dw \; e^{-(x+w)} \, J_0\left(2\sqrt{x(-w)}\right). \tag{I.37}$$

Expanding the α^{th} order Bessel function as a sum of Laguerre polynomials [38]

$$e^z J_\alpha\left(2\sqrt{xz}\right) = (xz)^{\alpha/2} \sum_{n=0}^{\infty} \left[\Gamma(n+\alpha+1)\right]^{-1} L_n^\alpha(x) \, z^n, \tag{I.38}$$

casts Eq.(37) in the form

$$P_s = \sum_{n=0}^{\infty} \frac{(-\alpha^2)^n}{(n+1)!} \int_{\alpha^2}^{\infty} dx\, e^{-x} L_n(x). \tag{I.39}$$

The integral in Eq.(39) is given by

$$\int_{x}^{\infty} e^{-y} L_n^{\alpha}(y)\, dy = e^{-x}\left[L_n^{\alpha}(x) - L_{n-1}^{\alpha}(x)\right]. \tag{I.40}$$

Combining Eqs.(40) and (39) leads to

$$P_s = e^{-\alpha^2}\Big\{ 1 + x + \sum_{n=1}^{\infty} \frac{(-\alpha^2)^n}{(n+1)!} \left[(n+1) L_n(x) + n L_{n-1}(x) + (x-n) L_n(x)\right]\Big\}. \tag{I.41}$$

With the aid of the recursion relation

$$x\, L_n^1(x) = n\, L_{n-1}(x) + (x-n) L_n(x), \tag{I.42}$$

Eq.(41) becomes

$$P_s = e^{-\alpha^2}\Big\{ \sum_{n=0}^{\infty} \frac{(-\alpha^2)^n}{n!} L_n(\alpha^2) + \alpha^2 \sum_{n=0}^{\infty} \frac{(-\alpha^2)^n}{(n+1)!} L_n^1(\alpha^2)\Big\}. \tag{I.43}$$

Substituting Eq.(38) into (43) yields

$$P_s = e^{-2\alpha^2}\left[I_0(2\alpha^2) + I_1(2\alpha^2)\right]. \tag{I.44}$$

As noted in the introduction the value of the argument α has been the source of confusion, although Eq.(44) was first stated long ago by Smoluchowski [8].

Using Eq.(44) the field emission current autocorrelation Eq.(35) can be written

$$R(t) = C_{FN} < (\delta N)^2 > \left\{ 1 - e^{-2\alpha^2}\left[I_0(2\alpha^2) + I_1(2\alpha^2)\right]\right\}. \tag{I.45}$$

The asymptotic expansion of Eq.(45) is

$$\lim_{t\to\infty} R(t) \sim C_{FN} < (\delta N)^2 > (r_p^2/4Dt).$$

This expansion, also derivable directly from Eq.(35), determines $D(n)$ when noise measurements are made in the time domain [12,13,24]. Using the Wiener-Khinchin theorem, the spectral density corresponding to Eq.(45) is

$$S_\infty(\omega) = C_{FN} < (\delta N)^2 > \frac{8r_p^2}{D} \left\{ \frac{ber_1\sqrt{u_p}\, kei_1\sqrt{u_p} + bei_1\sqrt{u_p}\, ker_1\sqrt{u_p}}{-u_p} \right\}. \quad \text{(I.46)}$$

The subscript ∞ is a reminder that the diffusive motion is unbounded, $u_p \equiv \omega r_p^2/D$, and $ber_1, bei_1, kei_1, ker_1$ are Kelvin functions. The term in braces was first given by Burgess [10] and later by van Vliet and Chenette [20]. The Eq.(46) spectrum also corresponds to the field emission current autocorrelation function developed by Mazenko, Banavar, and Gomer [14].

If the adsorbate is represented as a noninteracting lattice gas with site exclusion, then

$$< (\delta N)^2 > = < n > A_p \, (1-\lambda), \quad \text{(I.47)}$$

where $\lambda \equiv n\, a_o^2$ and a_o is the lattice constant. Note that $\lim_{\lambda\to 0} < (\delta N)^2 > = < N >$, which is characteristic of ideal gas behavior. In this case Eq.(46) yields a spectrum similar to Timm and van der Ziel's [11] except they mistakenly inserted an additional factor of λ into Eq.(47).

The low and high frequency limits of Eq.(46) are respectively,

$$\lim_{\omega\to 0} S_\infty(\omega) = C_{FN} < (\delta N)^2 > r_p^2 \, D^{-1} \ln (D/r_p^2 \omega) \quad \text{(I.48)}$$

and

$$\lim_{\omega\to\infty} S_\infty(\omega) = 2^{3/2} \, C_{FN} < (\delta N)^2 > D^{1/2} \, r_p^{-1} \, \omega^{-3/2}. \quad \text{(I.49)}$$

Recent measurements of K/W(111) show a good fit to Eq.(46) [26]. Comparison of the theoretical and experimental curves allows a value of $D(n)$ to be obtained in two ways. The most direct method is to compare abscissas, which assuming r_p is known, leads directly to $D(n)$. The second method is to compare ordinates and introduce a value for $C_{FN} < (\delta N)^2 >$, which is obtainable by a measurement of the total noise power P. This determines $D(n)$ as it is the only remaining variable.

F. Bounded diffusion spectrum

In this section a closed form solution for the spectral density function including the boundary effect is derived. The net plane and probed region are taken to be concentric circles with radii r_t and r_p respectively. Physically the bounded plane corresponds to the radius of the chosen (hkl) plane of the emitter. For this geometry the form of the Green function is shown to be equivalent to a KL expansion of δn. The spectral density will then be given as the Fourier transform of Eq.(20)

$$S(\omega) = 4C_{FN}<(\delta N)^2>A_p^{-1}\,\mathrm{Re}\int_{A_p}\int_{A_p} G(\vec{r}_1,\omega;\vec{r}_2)\,d\vec{r}_1\,d\vec{r}_2, \tag{I.50}$$

where $G(\vec{r}_1,\omega;\vec{r}_2) = \int_0^\infty G(\vec{r}_1,t;\vec{r}_2)\,e^{i\omega t}\,dt$. To prove that the representation of $G(\vec{r}_1,\omega;\vec{r}_2)$ yields a correlationless $C(\vec{r}_1,\vec{r}_2)$ it is sufficient to show

$$\mathrm{Re}\int_{A_T} d\vec{r}_3\; G(\vec{r}_1,\omega;\vec{r}_3) = 0. \tag{I.51}$$

Then the spectrum derived from Eq.(30) will be equal to that obtained from Eq.(20).

The function $G(\vec{r}_1, t; \vec{r}_2)$ satisfies

$$\left(\partial/\partial t - D\nabla^2\right) G(\vec{r}_1, t; \vec{r}_2) = \delta(\vec{r}_1 - \vec{r}_2)\delta(t), \tag{I.52}$$

and $G(\vec{r}_1, \omega; \vec{r}_2)$ solves

$$\left(\nabla^2 + k^2\right) G(\vec{r}_1, \omega; \vec{r}_2) = -\frac{1}{D}\,\delta(\vec{r}_1 - \vec{r}_2), \tag{I.53}$$

with Neumann boundary condition

$$\frac{\partial}{\partial n} G(\vec{r}_1, \omega; \vec{r}_2) = 0, \tag{I.54}$$

where $k^2 = -i\omega/D$ and $\partial/\partial n$ is the normal derivative evaluated at the boundary. Expanding $G(\vec{r}_1, \omega; \vec{r}_2)$ as

$$G(\vec{r}_1, \omega; \vec{r}_2) = \frac{1}{2\pi} \sum_{m=-\infty}^{\infty} p_k^{(m)}(r_1; r_2)\, e^{i m(\phi_1 - \phi_2)} \tag{I.55}$$

and then substituting Eq.(55) into (53) leads to,

$$\frac{1}{2\pi} \sum_{m=-\infty}^{\infty} e^{i m(\phi_1 - \phi_2)} \left[\frac{\partial^2 p_k^{(m)}}{\partial r^2} + \frac{1}{r}\frac{\partial p_k^{(m)}}{\partial r} - \left(\frac{m^2}{r^2} - k^2 \right) p_k^{(m)} \right] \tag{I.56}$$

$$= \frac{-\delta(r_1 - r_2)\delta(\phi_1 - \phi_2)}{D\, r_1}.$$

Operating on Eq.(56) with $\int_0^{2\pi} d\phi\; e^{-n\phi}$ and defining $p_m(z_1, z_2) = p_k^{(m)}(r_1, r_2)$, where $z_1 = k\, r_1$ and $z_2 = k\, r_2$ results in

$$p_m'' + \frac{1}{z_1} p_m' + \left(1 - \frac{m^2}{z_1^2} \right) p_m = \frac{-1}{D\, k\, z_1}\, \delta(r_1 - r_2). \tag{I.57}$$

Here the primes ($'$ and $''$) represent $\partial/\partial z$ and $\partial^2/\partial z^2$ respectively, and p_m satisfies

Bessel's equation. The Eq.(55) expansion must also be substituted into the Eq.(54) boundary condition which yields

$$\frac{\partial}{\partial n}\ p_m(z_1, z_2)\Big|_{r=r_t} = 0. \tag{I.58}$$

The reciprocity relation for the Green function requires the solution to Eq.(57) be written

$$p_m(z_1, z_2) = \frac{-1}{D\, r_2\, W(y_1,y_2)}\ y_1(kr_<)\, y_2(kr_>), \tag{I.59}$$

where $r_<(r_>)$ is the lesser (greater) of r_1 and r_2. The Wronskian $W(y_1,y_2)$ is evaluated at $r_1=r_2$ and y_1 and y_2 must satisfy the boundary conditions at $r_<=0$ and at $r_>=r_t$. The finiteness of G at $r_<=0$ implies

$$y_1 = J_m(kr_<). \tag{I.60}$$

The function y_2 must be bounded as $r_>\rightarrow\infty$, which requires y_2 to have the form

$$y_2(kr_>) = A\ J_m(kr_>)\ +\ B\, H_m^{(1)}(kr_>), \tag{I.61}$$

where $H_m^{(1)}$ is the m^{th} order Hankel function of the first kind. A and B are determined by the boundary condition, $\frac{\partial}{\partial r}\ y_2(r)\,\big|_{r=r_t} = 0$, and so

$$A\ = -B\left\{\frac{k\, H_{m-1}^{(1)}(kr_t) - (m/r_t\,)H_m^{(1)}(kr_t)}{k\, J_{m-1}(kr_t) - (m/r_t\,)\, J_m(kr_t)}\right\}. \tag{I.62}$$

The Wronskian is then equal to

$$W(y_1,y_2) = \frac{2\,i\,B}{\pi\, r}. \tag{I.63}$$

Eq.(59) becomes

$$p_m(k\, r_1, k\, r_1) = \tag{I.64}$$

$$\frac{\pi i}{2D}\left\{ J_m(kr_<)H_m^{(1)}(kr_>) - J_m(kr_<)J_m(kr_>)\left[\frac{k\,H_{m-1}^{(1)}(kr_l) - (m/r_l)\,H_m^{(1)}(kr_l)}{k\,J_{m-1}(kr_l) - (m/r_l)\,J_m(kr_l)}\right]\right\}.$$

Combining Eqs.(55) and (64) leads to

$$\int_{A_T} d\vec{r}_3\; G(\vec{r}_1,\omega;\vec{r}_3) = \pi/\imath\omega. \tag{I.65}$$

Thus Eq.(51) holds, which proves that the expression for $G(\vec{r}_1,\omega;\vec{r}_2)$, as given by Eqs.(55) and (64), does correspond to a Karhunen-Loève expansion of $\delta n(\vec{r})$. Substituting Eqs.(55) and (64) into (50) leads to the following expression for the spectral density,

$$S(\omega) = S_\infty(\omega) + S_B(\omega), \tag{I.66}$$

where

$$S_\infty(\omega) = \frac{8\pi^2 C_{FN}<(\delta N)^2>}{A_T D}\,\mathbf{Re}\; i\int_0^{r_\rho} dr_>\, r_>\, H_0^{(1)}(kr_>)\int_0^{r_>} dr_<\, r_<\, J_0(kr_<) \tag{I.67}$$

and

$$S_B(\omega) = \frac{8\pi^2 C_{FN}<(\delta N)^2>}{A_T D}\,\mathbf{Re}\left[\frac{iH_1^{(1)}(kr_l)}{J_1(kr_l)}\right]\int_0^{r_\rho} dr_>\, r_>\, J_0(kr_>)\int_0^{r_>} dr_<\, r_<\, J_0(kr_<). \tag{I.68}$$

Evaluation of Eq.(67) leads to Eq.(46). Eq.(68) represents the affect of the boundary on $S(\omega)$. The Eq.(66) factorization is a general result independent of the net plane geometry, which arises from the possibility of separating the Green function into a source and boundary term [39]. Performing the integrations in Eq.(68) yields

$$S_B(\omega) = \left[\frac{4\pi r_\rho^2 C_{FN}<(\delta N)^2>}{D}\right]\mathbf{Re}\left\{\left[\frac{i\,H_1^{(1)}(kr_l)}{J_1(kr_l)}\right]\left[\frac{J_1(kr_\rho)}{kr_\rho}\right]^2\right\}. \tag{I.69}$$

A check on $S_B(\omega)$ is obtained by noting,

$$\lim_{r_t \to \infty} S_B(\omega) = 0. \tag{I.70}$$

Equation (69) reduces to

$$S_B(\omega) = \begin{array}{l} \left(8C_{FN}<\delta N^2> r_p^2 u_p^{-1} D^{-1}\right)\left(ber_1^2\sqrt{u_t} + bei_1^2\sqrt{u_t}\right)^{-1} \\ \times \left[\begin{array}{l} \left(ber_1^2\sqrt{u_p} - bei_1^2\sqrt{u_p}\right)\left(kei_1\sqrt{u_t}\, ber_1\sqrt{u_t} - ker_1\sqrt{u_t}\, bei_1\sqrt{u_t}\right) \\ + \\ 2\left(ber_1\sqrt{u_p}\, bei_1\sqrt{u_p}\right)\left(ker_1\sqrt{u_t}\, ber_1\sqrt{u_t} + kei_1\sqrt{u_t}\, bei_1\sqrt{u_t}\right) \end{array}\right] \end{array}, \tag{I.71}$$

where $u_t = \omega r_t^2/D$. Comparing Eqs.(46) and (71) shows that for all frequencies

$$\lim_{r_p \to r_t} S(\omega) = 0. \tag{I.72}$$

As discussed earlier with regards to the total noise power Eq.(72) is a necessary condition that must be obeyed by a closed diffusive system. Furthermore,

$$\lim_{\omega \to 0} S_B(\omega) = C_{FN}<(\delta N)^2> r_p^2 D^{-1} \ln u_T. \tag{I.73}$$

Combining Eqs. (48),(66), and (73) results in

$$\lim_{\omega \to 0} S(\omega) = 2C_{FN}<(\delta N)^2> r_p^2 D^{-1} \ln (r_t/r_p). \tag{I.74}$$

Eq.(74) shows that in the low frequency limit, the spectrum for a bounded net plane is constant. This conclusion has also been arrived at by different means for the case of one dimensional diffusion by van Vliet and Fassett [16] and by van Vliet and van der Ziel [40], who argued within the general framework of Richardson's theory that a constant low frequency spectrum would result from placing a lower bound on vectors in k-space.

The presence of the boundary removes the low frequency logarithmic divergence of $S(\omega)$. This negates the argument that a diffusion process cannot produce a constant

low frequency spectrum such as found experimentally for K/W [4,25]. However it must be noted that a clear refutation of the model was never really provided by these experiments as they did not conform to the assumptions of the theory. Neither study probed a portion of a single crystal plane and in one case the adsorbate was in equilibrium with its vapor [25], which requires analysis using a grand canonical ensemble.

With the aid of Eqs.(49) and (66) the asymptotic expansion of Eq.(71) yields

$$\lim_{\omega\to\infty} S(\omega) = 2^{3/2} D^{1/2} C_{FN} <(\delta N)^2> r_p^{-1} \omega^{-3/2} \left\{ 1 - e^{-(r_t - r_p)\sqrt{2\omega/D}} \right\}. \qquad (I.75)$$

When $u_p \gg 1/2(1-r_t/r_p)^2$ then $S(\omega)\to S_\infty(\omega)$, i.e., Eq.(75) reduces to a $\omega^{-3/2}$ dependence equivalent to Eq.(49) for the unbounded system. Physically this is because appreciable adatom interaction with the boundary is not allowed on such a small time scale.

Fig. 1 graphs the spectra $S_\infty(\omega)$ and $S(\omega)$ given respectively by Eqs.(46) and (66). $S(\omega)$ is plotted for several different ratios of the net plane to probed area radii $r_t/r_p =$ 1.5,2,3, and 10. The presence of the boundary reduces the noise power in the low frequency regime.

G. Anisotropic diffusion

The preceding sections assume two dimensional adsorbate diffusion is isotropic. However certain substrate systems exist, e.g. bcc (211) planes, that are known to induce anisotropy in the diffusive adatom motion. The relation between a diffusion tensor and the field emission autocorrelation function has been worked out by Bowman et al. [41]. This section considers what influence such behavior has on the unbounded spectral density.

If a square region of the net plane is probed the Eq.(35) autocorrelation can be factored as

$$R_{\infty}^{\square}(t) = R_{\infty}^{x}(t) \times R_{\infty}^{y}(t). \tag{I.76}$$

The $\square$ superscript is a reminder that a square probe is used,

$$R_{\infty}^{i}(t) = \left[\frac{C_{FN} < (\delta N)^2 >}{l_i^2 4\pi D_i t}\right]^{1/2} \int_0^{l_i} \int_0^{l_i} dx_1\, dx_2\, e^{-(x_1 - x_2)^2/4D_i t},$$

and l_i is the length of the probed region in the i^{th} direction, $(i = x, y)$. D_i denotes the corresponding diffusion coefficient. The spectrum is then

$$S_{\infty}^{\square}(\omega) = S_{\infty}^{x}(\omega) \; * \; S_{\infty}^{y}(\omega), \tag{I.77}$$

where * denotes the convolution product and $S_{\infty}^{i}(\omega)$ is the spectrum corresponding to the one dimensional $R_{\infty}^{i}(t)$. In general this results in a complicated expression for $S_{\infty}^{\square}(\omega)$. By treating the limit of one dimensional diffusion, i.e., $D_y/D_x = 0$, with no boundaries the effect of channeled motion on the noise can be demonstrated. Restricting adatom motion to the x-direction reduces Eq.(76) to

$$R_{\infty}^{1D}(t) = \sqrt{C_{FN} < (\delta N)^2 >}\; R_{\infty}^{x}(t).$$

The superscript 1D shows the spectrum results from one dimensional motion. Application of the Wiener-Khinchin theorem yields

$$S_{\infty}^{1D}(\Omega) = C_{FN} < (\delta N)^2 > l_x^2 D^{-1} \Omega^{-3} \left[1 - e^{-\Omega}(\cos\Omega + \sin\Omega)\right], \tag{I.78}$$

and $\Omega \equiv l_x(\omega/2D)^{1/2}$. The frequency dependence due to one dimensional diffusion has been given previously by Burgess [10] and Voss and Clarke [18]. Eq.(78) is graphed in Fig.1 assuming $l_x = \pi r_p^2$. This results in equality of the scaled noise power $P/<(\delta N)^2>$ for circular and square probed regions. The normalization allows for

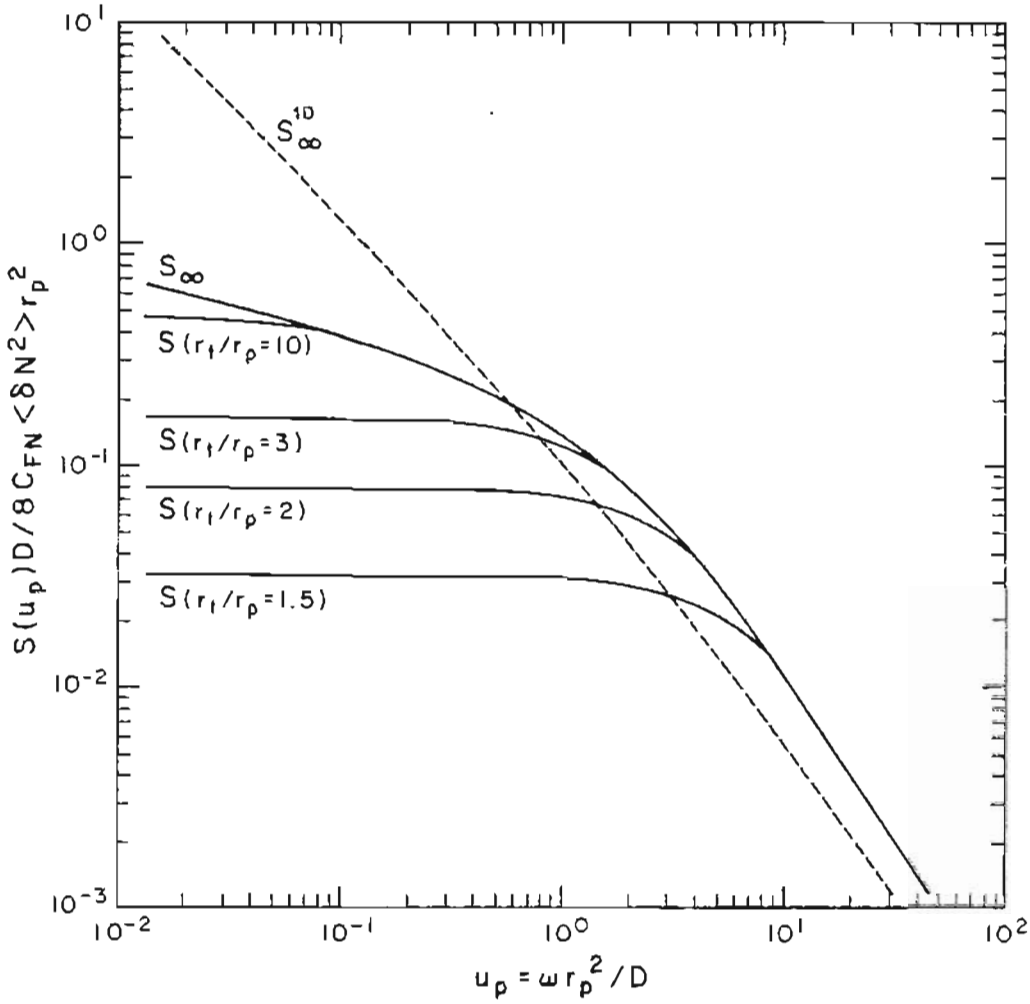

Fig. 1. Graph of the normalized spectra for: unbounded diffusion $S_\infty(u_p)$ with probe radius r_p, bounded diffusion $S(u_p\,;\, r_t/r_p = 1.5, 2, 3, 10)$ with net plane radius r_t, and unbounded one dimensional diffusion $S_\infty^{1D}(u_p)$ with a square probe of length l_x. The latter quantity is plotted assuming $l_x = \pi r_p^2$. $u_p \equiv \omega r_p^2/D$. See Eqs.(46), (66), (71), and (78) for the functional forms.

possible anisotropy in $<(\delta N)^2>$, which has been observed by measuring $R(0)$ with a narrow rectangular probe [42].

To compare one and two dimensional motion using S_∞^{1D} and S_∞ respectively it is necessary to show that the probe geometry has a negligible effect on the frequency dependence of S_∞, because in the latter case a circular probe was assumed for the calculation. The ambiguity is removed by first noting

$$\lim_{\omega\to 0} S_\infty^{1D}(\omega) = 4C_{FN}\ \frac{<(\delta N)^2> l_x}{3(D\omega)^{1/2}} \tag{I.79}$$

and

$$\lim_{\omega\to\infty} S_\infty^{1D}(\omega) = C_{FN}<(\delta N)^2>\Big(\frac{8D}{l_x^2\omega^3}\Big)^{1/2}. \tag{I.80}$$

Comparing Eqs.(49) and (80) yields

$$\lim_{\omega\to\infty} \frac{S_\infty(\omega)}{S_\infty^{1D}(\omega)} = \frac{l_x}{r_p}. \tag{I.81}$$

Thus, excluding a numerical factor, the high frequency dependence of the flicker noise is geometry independent. This is a characteristic property of diffusion processes [19]. The high frequency noise component is one dimensional in nature.

It is now shown that the low frequency limit of Eq.(77), i.e. the spectrum corresponding to a square probe, is the same as that obtained in Eq.(48) for the case of a circular probe. For a square probe $A_p = l_x^2$ and Eq.(77) becomes

$$S_\infty^{\square}(\omega) = \frac{C_{FN}<(\delta N)^2>}{A_p}\ \frac{8}{\pi D}\int_0^{l_x} dx \int_0^{x} dz \int_0^{l_x} dy \int_0^{y} dv\ ker\left[\sqrt{\omega(z^2+v^2)/D}\ \right]. \tag{I.82}$$

Eq.(82) can be written

$$S_\infty^{\square}(\omega) = \frac{C_{FN}<(\delta N)^2>}{A_p}\ \frac{16}{\pi D}\int_0^{l_x} dx \int_0^{l_x} dy \int_0^{\tan^{-1}(y/x)} d\theta \int_0^{x/\cos\theta} dr\ r\ ker(ar), \tag{I.83}$$

where $a \equiv \sqrt{\omega/D}$ and $r \equiv \sqrt{z^2+v^2}$. For low frequencies Eq.(83) becomes

$$\lim_{\omega \to 0} \frac{S_{\infty}^{\square}(\omega) D}{8 C_{FN} < (\delta N)^2 > r_p^2} = \frac{1}{4} \log \left[\frac{4}{\pi} \frac{D}{\omega r_p^2} \right]. \qquad \text{(I.84)}$$

Comparison of Eqs.(48) and (84) coupled with Eq.(81) demonstrates that probe geometry has a negligible effect on the spectra and therefore one can use S_{∞}^{1D} and S_{∞} to represent the limiting cases of one and two dimensional diffusion. Fig. 1 illustrates that one dimensional motion increases the noise power in the low frequency band of the spectrum.

H. Summary

The aim of this paper has been to analyze the spectrum of field emission flicker noise induced by equilibrium adsorbate density fluctuations in a canonical ensemble. The relative field emission current autocorrelation function $R(t)$ is a product of two factors. One contains terms related to the Fowler-Nordheim equation C_{FN} and the second is the autocorrelation of the total adparticle number within the probed region $<\delta N(t)\,\delta N(0)>$, Eq.(9). A general expression for $R(t)$ has been derived that contains the Green function for the diffusion equation $G(\vec{r}_1, t\,; \vec{r}_2)$ and the pair covariance of the density fluctuations $C(\vec{r}_1, \vec{r}_2)$, Eq.(14). This expression is simplified using several results from the theory of integral equations where $C(\vec{r}_1, \vec{r}_2)$ is taken as the kernel. The procedure is equivalent to a Karhunen-Loève expansion of the density fluctuation $\delta n(\vec{r})$, section C. The presence of boundaries and critical fluctuations on $C(\vec{r}_1, \vec{r}_2)$ has also been discussed, although subsequent analysis assumes the system is not influenced by critical fluctuations, section D. A form of $R(t)$ studied by Gomer was obtained by considering a square probed region on a square net plane, Eq.(32). This

formulation yields an expression for the flicker noise power that is a product of the constant C_{FN}, the mean square particle number fluctuation $< (\delta N)^2 >$ within the probed region, and the factor $(1 - A_p / A_T)$. The latter term relates the noise power to the ratio of the probed to net plane area, Eq.(34). For unbounded diffusion the autocorrelation function is proportional to Smoluchowski's probability after-effect factor, Eq.(36), and the spectral density function $S_\infty(\omega)$ is analogous to one derived by Burgess for contact noise in semiconductors, Eq.(46). A closed expression was found for diffusion on a circular net plane with a circular probe. The form of $S(\omega)$ explains several characteristics of field emission noise measurements. It was shown that the existence of finite net plane area produces a flat low frequency spectrum, Eq.(74). The affect of anisotropic diffusion on $S(\omega)$ in the limit of one dimensional motion was considered in section G. The qualitative result of such motion is to increase the noise power in the low frequency band in contrast to the boundary effect which decreases it. The high frequency dependence of $S(\omega)$ is affected by neither the finite size of the net plane nor by anisotropic motion.

I. Appendix. Wiener-Khinchin theorem.

The specific pupose of this appendix is to derive Eq.(I.33), which requires use of the Wiener-Khinchin theorem. A detailed analysis is provided for several reasons. First, although there are many expositions of this theorem, alas, not all are mutually consistent. The derived relation between the autocorrelation $R(t)$ and the spectral density $S(\omega)$ can vary by a factor of two or four. Second, the theorem is applied frequently throughout this dissertation and a clear understanding of its origins provides a more secure basis upon which these results can be placed. Third, certain elements of the derivation are used in the Fourier analysis presented in chapter IV, section E. Fourth, a technique used here provides a quick alternate calculation of $R(t)$ evaluated by Gomer in reference [12], although this point is not shown here. Finally it was done so that every step would be clear to myself. The construction of the proof is nontrivial and many authors either state the result or go only part way in deriving it. For example even van der Ziel's relatively thorough analysis [43] excludes a necessary section concerning arguments related to Fig.(2) below.

Historically this theorem arose from the inability of classical Fourier analysis to deal with a random function $\mathrm{I}(t)$, which does not approach zero as its argument tends to infinity. Gouy, Rayleigh, and Schuster preceeded Wiener in considering this type of function in their investigations of various systems, e.g. white light, stock market fluctuations, and weather forecasting. For a discussion of the early history see the classical reference [44]. Wiener's contemporary, J.R. Carson, a communication engineer at Bell labs, also provided important insights into calculating the spectrum of a random function, see reference [45] and chapter IV. Khinchin, working in Russia independently of Wiener and Carson, found the relation between $R(t)$ and $S(\omega)$ four

years after Wiener [46]. His research was concerned more with questions of existence and the measure theoretic aspects of the functions.

The original and most general version due to Wiener himself can be found in reference [44]. His result appears as

$$S'(u) = \frac{1}{2\pi} \int_{-\infty}^{\infty} \phi(x)\, e^{ixu}\, dx \tag{A.1}$$

or

$$S(u) = \frac{1}{2\pi} \int_{-\infty}^{\infty} \phi(x) \left[\frac{e^{ixu} - 1}{i\, x} \right] dx, \tag{A.2}$$

where $\phi(x) = \lim_{T\to\infty} \frac{1}{2T} \int \mathrm{I}(x+t)\, \mathrm{I}^*(t)\, dt$ is the autocorrelation. S' is the spectral density function named $S(\omega)$ here. Eq.(A.2) was called the integrated periodogram of $\mathrm{I}(t)$. A problem with reading the early literature is that the δ function had not been developed and use of Stieltjes integration techniques was required. Although Eq.(A.1) is the most general result, Wiener does not discuss several of the more specialized versions. He does consider the case where $\mathrm{I}(t)$ is vector valued as does Reichl [47]. For the present purposes this extension is not necessary and we consider $\mathrm{I}(t)$ to be a scalar valued function. The present account follows more along the lines of Lax [15].

The random function $\mathrm{I}(t)$ is assumed stationary

$$< \mathrm{I}(t+t')\, \mathrm{I}(t') > = < \mathrm{I}(t)\, \mathrm{I}(0) > \tag{A.3}$$

with $< \mathrm{I}(t) > = 0$. Although $\lim_{T\to\infty} \mathrm{I}(t) \neq 0$, one begins by defining $\mathrm{I}(t) \neq 0$ only in the interval $0 \leq t \leq T$ and later taking the limit $\mathrm{T} \to \infty$. Then it may be expressed in a Fourier series

$$\mathrm{I}(t) = \sum_{n=-\infty}^{\infty} \mathbf{a}_n \, e^{i\omega_n t} \tag{A.4}$$

where $\omega_n = \frac{2\pi n}{T}$, $n = 0, \pm 1, \pm 2$, etc., with

$$\mathbf{a}_n = \frac{1}{T} \int_0^T \mathrm{I}(t) \, e^{-i\omega_n t} \, dt. \tag{A.5}$$

The noise power per frequency at $f_n = \omega_n / 2\pi$ is defined

$$S(f_n) \equiv \lim_{T\to\infty} 2T < \mathbf{a}_n \, \mathbf{a}_n^* > = \lim_{T\to\infty} \frac{2}{T} < \left| \int_{-T/2}^{T/2} \mathrm{I}(t) \, e^{-i\omega_n t} \, dt \right|^2 >. \tag{A.6}$$

The factor 2 arises from the convention that the total dissipated power $P \equiv < \mathrm{I}^2 >$ is given by

$$< \mathrm{I}^2 > = \lim_{T\to\infty} \frac{1}{T} \int_{-T/2}^{T/2} \mathrm{I}^2(t) \, dt = \int_0^\infty S(f) \, df. \tag{A.7}$$

Proof of Eq.(A.7).

$$S(f) = \lim_{T\to\infty} \frac{2}{T} \int_{-T/2}^{T/2} \int_{-T/2}^{T/2} < \mathrm{I}(t) \, \mathrm{I}(t') > e^{-2\pi i f (t-t')} \, dt \, dt'. \tag{A.8}$$

Integrating Eq.(A.8)

$$\int_0^\infty S(f) \, df = \lim_{T\to\infty} \frac{2}{T} \int_{-T/2}^{T/2} \int_{-T/2}^{T/2} dt \, dt' < \mathrm{I}(t) \, \mathrm{I}(t') > \int_0^\infty e^{-2\pi i f (t-t')} df \tag{A.9}$$

and using

$$\delta(f) = 2 \int_0^\infty e^{2\pi f \tau} d\tau \tag{A.10}$$

yields

$$\int_0^\infty S(f)\,df = \lim_{T\to\infty}\frac{1}{T}\int_{-T/2}^{T/2} dt < \mathrm{I}(t)^2 > = < \mathrm{I}^2 >. \quad Q.E.D. \qquad (A.11)$$

The assumption of stationarity has been used, which makes $< \mathrm{I}(t)^2 >$ time independent.

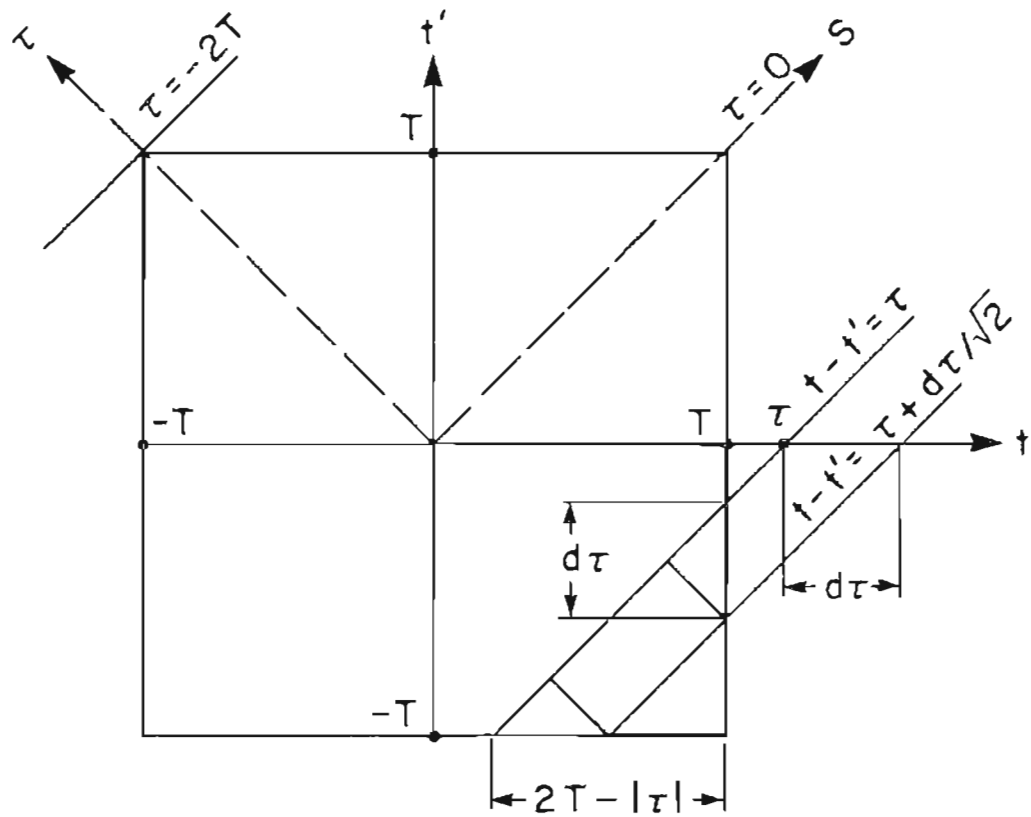

Fig. 2. Diagram of the double integration limits used in Eq.(A.13).

Referring to Fig.(2) the coordinate transformation $t - t' = \tau$, $s = t'$ is applied to Eq.(A.6), which is written as

$$< \mathbf{a}_n \, \mathbf{a}_n^* > = \lim_{T\to\infty} \frac{1}{4T^2} \int_{-T}^{T}\int_{-T}^{T} < \mathrm{I}(t)\, \mathrm{I}(t') > e^{-i\omega(t-t')} dt\, dt'. \qquad \text{(A.12)}$$

It then follows from Eq.(A.12) that

$$< \mathbf{a}_n \, \mathbf{a}_n^* > = \lim_{T\to\infty} \frac{1}{4T^2} \int_{-2T}^{2T} d\tau \int_{0}^{2T-|\tau|} ds\; R(\tau) e^{-i\omega_n \tau}$$

$$= \lim_{T\to\infty} \frac{1}{4T^2} \int_{-2T}^{2T} d\tau \left(2T - |\tau| \right) R(\tau)\, e^{-i\omega\tau}$$

$$= \lim_{T\to\infty} \left[\frac{1}{2T} \int_{-2T}^{2T} R(\tau)\, e^{-i\omega\tau} - \frac{1}{4T^2} \int_{-2T}^{2T} |\tau|\, R(\tau)\, e^{-i\omega\tau}\, d\tau \right], \qquad \text{(A.13)}$$

where $R(\tau) \equiv < \mathrm{I}(\tau)\, \mathrm{I}(0) >$. Hence

$$S(f) = 2 \int_{-\infty}^{\infty} R(\tau)\, e^{-i\omega\tau}\, d\tau - \lim_{T\to\infty} \frac{1}{T} \int_{-T}^{T} |\tau|\, R(\tau)\, e^{-i\omega\tau}\, d\tau. \qquad \text{(A.14)}$$

Consider the last term

$$\lim_{T\to\infty} \frac{1}{T} \int_{-T}^{T} |\tau|\, R(\tau)\, e^{-i\omega\tau}\, d\tau = \lim_{T\to\infty} \frac{1}{T} \left[\int_{0}^{T} \tau\, R(\tau)\, e^{-i\omega\tau}\, d\tau + \int_{-T}^{0} (-\tau)\, R(\tau)\, e^{-i\omega\tau}\, d\tau \right]$$

$$= \lim_{T\to\infty} \frac{1}{T} \left[\int_{0}^{T} \tau \left(R(\tau) + R(-\tau) \right) 2\cos\omega\tau\, d\tau \right]$$

$$= \lim_{T\to\infty} \frac{1}{T} \mathrm{Re} \int_{0}^{T} \tau \left[R(\tau) + R(-\tau) \right] e^{-i\omega\tau}\, d\tau$$

$$= \mathrm{Re} \lim_{T\to\infty} \frac{2}{iT} \frac{d}{d\omega} \int_{0}^{T} \left[R(\tau) + R(-\tau) \right] e^{-i\omega\tau}\, d\tau.$$

Assuming the current is bounded, i.e. $| < I(t) > | \leq M$ then

$$| \lim_{T\to\infty} \frac{1}{T} \int_{-T}^{T} | \tau | \, R(\tau) \, e^{-i\omega\tau} \, d\tau | \leq 2 \frac{d}{d} \lim_{T\to\infty} \frac{1}{T} \int_{0}^{T} | \, R(\tau) + R(-\tau) \, | \, d\tau.$$

Now

$$| \, R(\tau) + R(-\tau) | \, \leq | \, R(\tau) | + | \, R(-\tau) | \, \leq \, 2M^2.$$

Therefore

$$\lim_{T\to\infty} \frac{1}{T} \int_{-T}^{T} | \tau | \, R(\tau) \, e^{-i\omega\tau} \, d\tau = 0. \tag{A.15}$$

Thus Eq.(A.14) becomes

$$S(f) = 2 \int_{-\infty}^{\infty} R(\tau) \, e^{-i\omega\tau} \, d\tau, \tag{A.16}$$

which is the Wiener-Khinchin theorem. The factor of 2 is sometimes omitted as, e.g. in Papoulis [31].

Onsager's hypothesis [47] explains why the field emission $R(t)$ is an even function

$$R(t) = R(-t) \tag{A.17}$$

From Eqs.(A.16-17) it follows that

$$S(-f) = S(f). \tag{A.18}$$

Operating on Eq.(A.16) with $\int_{-\infty}^{\infty} df \; e^{i\omega t'}$ and using the properties of the δ-function leads to

$$R(t) = \frac{1}{2} \int_{-\infty}^{\infty} S(f) \, e^{i\omega t} \, df. \tag{A.19}$$

Using Eq.(A.18) the left side of Eq.(A.19) yields

$$R(t) = \frac{1}{2}\int_0^\infty S(f)\cos\omega t \; df \tag{A.20}$$

and hence

$$R(0) = \frac{1}{2}\int_0^\infty S(f) \; df. \tag{A.21}$$

Combining Eqs.(A.7) and (A.21) yields the desired result

$$P = 2R(0), \tag{A.22}$$

which appears as Eq (I.33).

J. Chapter I references.

[1] B. Mandelbrot, "Some Noises with 1/f Spectrum, a Bridge Between Direct Current and White Noise." *Proc. IEEE*, IT-**13** *(1967) 289.*
M. Keshner, "1/f Noise." *Proc. IEEE* **70** *(1982) 212.*

[2] E. Marinari, G. Parisi, D. Ruelle, and P. Windey, "On the Interpretation of 1/f Noise." *Comm. Math. Phys.*, **89** *(1983) 1.*

[3] L. Bess, "Study of 1/f Noise in Semiconductor Filaments." *Phys. Rev.* **103** *(1956) 72.*

[4] Ch. Kleint, "Surface Diffusion Model of Adsorption-Induced Field Emission Flicker Noise." *Surface Sci.* **25** *(1971) 394.*

[5] J.M. Richardson, "The Linear Theory of Fluctuations Arising from Diffusional Mechanisms- An Attempt at a Theory of Contact Noise." *Bell System Tech. J.* **29** *(1950) 117.*

[6] G.G. MacFarlane, "A Theory of Contact Noise in Semiconductors." *Proc. Phys. Soc.* **B63** *(1950) 807.*

[7] A. van der Ziel, "On the Spectra of Semi-Conductor Noise and of Flicker Effect." *Physica* **16** *(1950) 359.*

[8] M.v. Smoluchowski, "Drei Vorträge über Diffusion, Brownsche Molekular-bewegung und Koagulation von Kolloidteilchen." *Phys. Zeit.* **17** *(1916) 557,585.*

[9] S. Chandrasekhar, "Stochastic Problems in Physics and Astronomy." *Rev. Mod. Phys.* **15** *(1943) 1.*

[10] R.E. Burgess, "Contact Noise in Semiconductors." *Proc. Phys. Soc.* **B66** *(1953) 334.*

[11] G.W. Timm and A. van der Ziel, "Noise in Field Emission Diodes." *Physica* **32** *(1966) 1333.*

[12] R. Gomer, "Current Fluctuations from Small Regions of Adsorbate Covered Field Emitters. A Method for Determining Diffusion Coefficients on Single Crystal Planes." *Surface Sci.* **38** *(1973) 373.*

[13] J.R. Chen and R. Gomer, "Mobility of Oxygen on the (110) Plane of Tungsten." *Surface Sci.* **79** *(1979) 413.*

[14] G. Mazenko, J.R. Banavar, and R. Gomer, "Diffusion Coefficients and the Time Autocorrelation Function of Density Fluctuations." *Surface Sci.* **107** *(1981) 459.*

[15] M. Lax, "Fluctuations from the Nonequilibrium Steady State." *Rev. Mod. Phys.* **32** *(1960) 25.*

[16] K.M. van Vliet and J.R. Fassett, "Fluctuations Due to Electronic Transitions and Transport." In *"Fluctuation Phenomena in Solids"* ed. R.E. Burgess *(Academic Press, New York 1965).*

[17] J.R. Banavar and R. Gomer, "Density Fluctuation Autocorrelation Functions for Surface Diffusion with Various Boundary Conditions." *Surface Sci.* **97** *(1980) L845.*

[18] R.F. Voss and J. Clarke, "Flicker (1/f) Noise: Equilibrium Temperature and Resistance Fluctuations." *Phys. Rev. B* **13** *(1976) 556.*

[19] M. Lax and P. Mengert, "Influence of Trapping, Diffusion, and Recombination on Carrier Concentration Fluctuations." *J. Phys. Chem. Solids,* **14** *(1960) 248.*

[20] K.M. van Vliet and E.R. Chenette, "Noise Spectra Resulting from Diffusion Processes in a Cylindrical Geometry." *Physica* **31** *(1965) 985.*

[21] Ch. Kleint, "Theoretische Betrachtungen zum Funkelrauschen bei Feldemission." "Experimente zum Funkelrauschen bei Feldemission und Vergleich mit Theoretischen Vorstellungen." *Ann. Physik* **10** *(1963) 295,309.*

[22] Ch. Kleint and H.J. Gasse, "Schrot- und Funkelrauschen bei Kalter Elektronen-Emission." *Z. Naturforsch.* **15a** *(1960) 87.*

[23] N. Saitou, S. Yamamoto, and H. Okano, "Power Spectral Density of Field Emission Current Fluctuations." *Shinku (Vacuum)* **21** *(1978) 14.*

[24] J.R. Chen and R. Gomer, "Mobility and Two Dimensional Compressibility of Xe on the (110) Plane of Tungsten." *Surface Sci.* **94** *(1980) 456.*

[25] Ch. Kleint, R. Meclewski, and R. Blaszczyszyn, "Comparison of Experimental Noise Spectral Densities of K- Covered Tungsten Emitters with Field-Emission Flicker-Noise Theories." *Physica* **68** *(1973) 382.*

[26] J. Beben and Ch. Kleint, "Surface Diffusion Activation Energy of the Adsorption System W(111) from Field Emission Current Fluctuations." *8th Seminar on Surface Physics, Karpacz, Poland (May, 1984).*

[27] R.H. Good and E.W. Müller, "Field Emission." In *"Handbuch der Physik" vol.21, ed.* S. Flügge *(Springer, Berlin 1956) p.176.*

[28] J. Topping, "On the Mutual Potential Energy of a Plane Network of Doubles." *Proc. Roy. Soc.* **A114** *(1927) 67.*

[29] J.R. MacDonald and C.A. Barlow,Jr., "Work Function Change on Monolayer Adsorption." *J. Chem. Phys.* **39** *(1963) 412.*

[30] R. Meclewski, Ch. Kleint, and R. Blaszczyszyn, "Correlation of Field Emission Flicker Noise and Work Function for Tungsten Single Crystal Planes with Adsorbed Potassium." *Surface Sci.* **52** *(1975) 365.*

[31] A. Papoulis, *"Probability, Random Variables, and Stochastic Processes" (McGraw-Hill, New York 1965).*

[32] I. Stakgold, *"Boundary Value Problems of Mathematical Physics" vol.1, (Macmillan, New York 1969) p.136.*

[33] R. Courant and D. Hilbert, *"Methods of Mathematical Physics" vol.I, 7th ed., Wiley-Interscience, New York, (1966).*

[34] K. Karhunen, "Uber Lineare Methoden in der Wahrscheinlichkeitsrechnung." *Ann. Acad. Sci. Fennicae Ser. A. I* **34** *(1946); ibid.* **37** *(1947).*

[35] M. Kac and A.J.F. Siegert, "On the Theory of Noise in Radio Receivers with Square Law Detectors." *J. Appl. Phys.* **18** *(1947) 383.*

[36] E.M. Lifshitz and L.P. Pitaevskii, *"Statistical Physics" 3rd ed. part 1, (Pergamon press, Oxford 1980).*

[37] D.A. Reed and G. Ehrlich, "Surface Diffusivity and the Time Correlation of Concentration Fluctuations." *Surface Sci.* **105** *(1981) 603.*

[38] *"Higher Transcendental Functions" vol.II,* ed. Erdelyi, *(McGraw-Hill, New York 1953).*

[39] P.M Morse and H. Feschbach, *"Methods of Theoretical Physics" vol.I (McGraw-Hill, New York 1953) chpt.7.*

[40] K.M. van Vliet and A. van der Ziel, "On the Noise Generated by Diffusion Mechanisms." *Physica* **24** *(1958) 415,556.*

[41] D.R. Bowman, R. Gomer, K. Muttalib, and M. Tringides, "The Determination of Diffusion Tensors in Surface Diffusion by the Fluctuation Method (Theory)." *Surface Sci.* **138** *(1984) 581.*

[42] M. Tringides and R. Gomer, "A Monte Carlo Study of Oxygen Diffusion on the (110) Plane of Tungsten." *Surface Science,* **145** *(1984) 121.*

[43] L.E. Reichl, *"A Modern Course in Statistical Physics", (Univ. Texas, 1980).*

[44] A. van der Ziel, *"Noise: Sources, Characterization, Measurement." (Prentice-Hall, 1970).*

[45] N. Wiener, *"Generalized Harmonic Analysis and Tauberian Theorems," (M.I.T. Press, 1964).*

[46] J.R. Carson, "The Statistical Energy-Frequency Spectrum of Random Disturbances." *Bell System Technical Journal* **10** *(1931) 374.*

[47] A.I. Khinchin, "Korrelationstheorie der Stationären Stochastichen Prozesse" *Math. Annalen* **109** *(1934) 604.*

II. Nature of Diffusion Coefficients and Their Relation to Field Emission Noise

"I don't know nothin' 'bout voltage
I don't know nothin' 'bout watts"
Muddy Waters

A. Introduction

The density dependence of a diffusion coefficient (diffusivity) $D(n)$ provides insight to the influence of many body interactions on the mass transport properties of a system. Gomer's first analysis of field electron emission noise showed how equilibrium surface density fluctuations could be measured [1]. This study related the field electron current to the number fluctuation of noninteracting adatoms within a probed area A_p. Prior to this work surface diffusivities were only obtainable by measuring a nonequilibrium decay of a density gradient. Later Mazenko, Banavar, and Gomer (MBG) extended the fluctuation theory to include fully interacting equilibrium adsorbate systems, with the exception of those influenced by critical fluctuations, using hydrodynamic correlation theory [2]. This allowed a diffusivity $D(n)$ to be measured for a range of densities $n=N/A_p$ with N the particle number in A_p. The measured $D(n)$ was taken to be the chemical D_c defined by Fick's first law.

In the present study it is proposed that surface density fluctuations, such as measured in a field emission noise experiment, be associated with a hydrodynamic D_h defined as the equilibrium limit of D_c. The chemical D_c is placed in the more general context of nonequilibrium systems. The circumstances under which chemical diffusivity is equal to its equilibrium limit, i.e. $D_h(n)=D_c(n)$, are examined in terms of irreversible thermodynamic stability theory [3]. In general these diffusivities are equivalent when local equilibrium is maintained and the density gradient is small, which is the regime of strictly linear irreversible thermodynamics. An exception occurs when an adsorbate phase transition exists within the range of densities probed by the nonequilibrium experiment. In this case equality of the two diffusivities cannot be guaranteed.

The discussion begins in section B by relating phenomenological transport coefficients to each other. Applying these equations to a Langmuir gas in C the results are then readily extended to a fully interacting lattice gas in D where interactions influence both the kinetic coefficient and the thermodynamic response of the system. In section E relations between diffusivities associated with equilibrium fluctuations are found using Kubo equations. Here it is emphasized that the distribution function used to evaluate ensemble averages is the determining factor for distinguishing D_h from the tracer D_t. Section F evaluates the equivalence of $D_h(n)$ and $D_c(n)$ by considering the excess entropy production of a diffusive process.

B. Linear phenomenological equations.

To introduce a consistent notation and provide relations among various mass transport coefficients used in subsequent sections a comparison is made of three phenomenological equations. Linear irreversible thermodynamics relates current density J to thermodynamic force X by

$$J(n) = L(n)X(n), \tag{II.1}$$

where L is the kinetic coefficient and the vectorial nature of the pertinent variables is implicitly understood. The present discussion only considers mass transport and no thermodiffusion effect. The generalized force is defined

$$X(n) = -\nabla\mu(n)/T, \tag{II.2}$$

with μ the chemical potential. Using the chain rule and Eq.(2), Eq.(1) becomes

$$J(n) = -[L(n)/T\chi(n)]\,\nabla n, \tag{II.3}$$

where the isothermal response function $\chi(n) \equiv (\partial n/\partial\mu)_T$ is [4]

$$\chi(n) = n^2\kappa_T(n), \tag{II.4}$$

and κ_T is the isothermal compressibility.

Writing the current density in terms of a local velocity,

$$J(n) = n\,v(n), \tag{II.5}$$

and defining the mobility u as,

$$\mathrm{u}(n) \equiv -v(n)/\nabla\mu(n), \tag{II.6}$$

transforms Eq.(5) to

$$J(n) = -\left[\, n\, \mathrm{u}(n)\, \chi^{-1}(n) \,\right] \nabla n. \tag{II.7}$$

Fick's first law provides a third expression for J and defines the chemical diffusivity $D_c(n)$,

$$J(n) = -D_c(n)\, \nabla n. \tag{II.8}$$

Combining Eqs.(3), (7), and (8) leads to the following relations among L, u, and D_c:

$$L(n) = n\, \mathrm{u}(n)\, T \tag{II.9}$$

$$D_c(n) = n\, \mathrm{u}(n)/\chi(n) \tag{II.10}$$

$$D_c(n) = L(n)/\chi(n)\, T. \tag{II.11}$$

C. Langmuir gas (site exclusion only).

Transport coefficients for a fully interacting lattice gas are most easily developed by first applying equations of the preceding section to a Langmuir gas. The chemical diffusivity is then independent of density and is given by [5,6]

$$D_c^l = \Gamma_o \lambda^2, \tag{II.12}$$

where λ^2 is the mean square jump length and Γ_o is the single particle jump rate. The superscript l is a reminder that a Langmuir gas is being considered.

The chemical potential for this system is [5]

$$\mu^l = \mu_o + kT \ln \theta(1-\theta)^{-1}, \tag{II.13}$$

where $\mu_o = constant$, $\theta \equiv n\, a_o^2$, and Combining Eqs.(3) and (13) leads to

$$J(\theta) = -\left[\, k\, L^{I}(\theta)/\theta(1-\theta)\,\right] \nabla\theta. \tag{II.14}$$

It then follows from Eq.(8) that

$$D_c^I = a_o^2\, k\, L^{I}(\theta)/\theta(1-\theta). \tag{II.15}$$

With the help of Eq.(9), Eq.(15) can be expressed in terms of mobility as,

$$\upsilon^{I}(\theta) = (\,1-\theta\,)\, D_c^I/kT. \tag{II.16}$$

Sadiq and Binder found that the transition probability for a kinetic lattice gas model allows two neighboring atoms to exchange sites without affecting diffusivity [7], i.e. D_c^I remains independent of coverage θ. Eq.(16) is consistent with this site exchange mechanism since the mobility approaches zero as $\theta \rightarrow 1$. This means, by Eq.(6), that for unity coverage the average velocity evaluated at a point between these two sites will also be zero even though each adatom has a nonzero velocity.

D. Fully interacting lattice gas.

To discuss $D_c(n)$ for a fully interacting lattice gas and also to make contact with other studies, Eq.(3) is rewritten as

$$J(n) = -\left[\, k\, n^{-1} L(n) F(n)\,\right] \nabla n, \tag{II.17}$$

where

$$F(n) = n/kT\chi(n) \tag{II.18}$$

is the thermodynamic factor discussed by Reed and Ehrlich [5]. Combining Eqs.(8), (9), and (17) leads to

$$D_c(n) = k\,T\,\mathrm{u}(n)\,F(n). \tag{II.19}$$

Coupling the mobility of an interacting lattice gas, written as $\mathrm{u}(\theta) \equiv \mathrm{u}^{I}(\theta)\,\gamma(\theta)$, with Eq.(16) yields,

$$\mathrm{u}(\theta) = (1-\theta)\,\gamma(\theta) D_c^{I}/kT. \tag{II.20}$$

Substituting Eq.(20) into (19) results in,

$$D_c(\theta) = \lambda^2 \Gamma(\theta) F(\theta), \tag{II.21}$$

where the effective jump rate is defined

$$\Gamma(\theta) \equiv (1-\theta)\,\Gamma_o \gamma(\theta). \tag{II.22}$$

Reed and Ehrlich named D_c, expressed as Eq.(21), kinetic diffusivity [8]. In Monte Carlo MC calculations $\Gamma(\theta)$ is found by taking the ratio of successful to attempted jumps. A problem with all phenomenological formalisms is that analytical expressions for L, u, Γ, or γ occur only in microscopic theories. Thus the degree of approximation made by estimating $\Gamma(\theta)$ as is done in MC experiments is not known. The same problem exists for theories cast in terms of correlation coefficients [6].

Zwerger defined bulk diffusivity as [11],

$$D_b(\theta) \equiv \mathrm{u}(\theta) kT, \tag{II.23}$$

which is a generalization to interacting systems of Einstein's relation between mobility and the free particle diffusivity, $D_o = u_o kT$. Then from Eqs.(19) and (23),

$$D_c(\theta) = D_b(\theta) F(\theta). \tag{II.24}$$

A microscopic derivation of Eq.(24) involving equilibrium fluctuations is discussed in section E.

Zwerger recognized that D_b is associated with the center of mass of the system. Combining Eqs.(12), (20), and (23) yields,

$$D_b(\theta) = (1-\theta)\,\Gamma_o\,\lambda^2\,\gamma(\theta). \tag{II.25}$$

Eq.(25) is consistent with center of mass motion since $\lim_{\theta\to 1} D_b = 0$, i.e. the center of mass does not diffuse at unity coverage.

D_b is also found in Butz and Wagner's study (D^i in their paper) [12]. However they state that this diffusivity describes the motion of a tracer particle within a homogeneous concentration. This interpretation is not correct as Eqs.(39) and (40) show that for an equilibrium system D_b is a sum of the adatom velocity cross-correlation function and the tracer D_t. Furthermore, because D_b is related to D_c by Eq.(24) it is defined for nonequilibrium as well as equilibrium systems.

E. Equilibrium fluctuations and hydrodynamic diffusivity D_h.

Another diffusivity is now introduced, termed hydrodynamic D_h, which is to be associated with field emission noise measurement of surface density fluctuations and defined as the equilibrium limit of D_c. The relationship between D_h and other equilibrium diffusivities is then considered by expressing them as Kubo equations.

The most general first order relation between current flux and particle density is given by

$$J(n(x,t)) = -D_c(n(x,t),x)\,\nabla n(x,t). \tag{II.26}$$

The D_c involved in this version of Fick's law has an explicit spatial dependence

independent of density. The form is valid when diffusion occurs over more than one (hkl) plane, i.e. when the substrate potential profile is spatially inhomogeneous. We shall only consider diffusion on a single plane in which case $D_c = D_c(n)$, assuming $n=n(x)$ is invertible. Application of the mass continuity equation to Eq.(26) yields Fick's nonlinear second law:

$$[\partial/\partial t - \nabla\cdot(D_c\,\nabla)]\, n(x,t) = 0. \tag{II.27}$$

A system at equilibrium is characterized by spatial homogeneity of the density, i.e., $\lim_{t\to\infty} n(x,t) = constant$. This condition means

$$\lim_{t\to\infty} \nabla D_c(n) = 0. \tag{II.28}$$

The hydrodynamic diffusivity is then defined as the equilibrium limit of D_c,

$$D_h(n) = \lim_{t\to\infty} D_c(n), \tag{II.29a}$$

or equivalently,

$$D_h(n) = -\lim_{\nabla n\to 0} (J/\nabla n). \tag{II.29b}$$

The limit in Eq.(29a) indicates a sufficient time has elapsed for the decay of any macroscopic density inhomogeneity. Thus for an equilibrated system Eq.(28) holds and Eq.(27) reduces to the linear diffusion equation,

$$(\partial/\partial t - D_h \nabla^2)\, n(\vec{x},t) = 0. \tag{II.30}$$

The cross-covariance of the equilibrium density fluctuation is,

$$S(\vec{x}-\vec{x}',t) = < \delta n(\vec{x},t)\, \delta n(\vec{x}',0) >, \tag{II.31}$$

where $\delta n(x,t) = n(x,t) - < n >$. Onsager's hypothesis that microscopic density fluctuations decay on the average according to the macroscopic Eq.(30) yields,

$$(\partial/\partial t - D_h \nabla^2) S(\vec{x}-\vec{x}', t) = 0, \tag{II.32}$$

and it is implicitly understood that the average in Eq.(31) is with respect to an equilibrium ensemble.

The relative field emission current fluctuation can be written [2]

$$R(t) = c_0 \int_{A_p} \int_{A_p} d\vec{x}\ d\vec{x}'\ S(\vec{x} - \vec{x}', t), \tag{II.33}$$

where c_0 is a constant related to the Fowler - Nordheim equation. Ignoring boundary effects, a consequence of Eq.(32) is that the asymptotic limit of $R(t)$ is [2]

$$\lim_{t\to\infty} R(t) = (kT \chi A_p^2/4\pi D_h t), \tag{II.34}$$

where D_c of reference [2] has been replaced here by D_h. Thus equilibrium field emission noise experiments are associated with a measurement of the hydrodynamic diffusivity D_h and not D_c. We wish to retain the distinction between equilibrium and nonequilibrium dynamical systems by separately considering D_h and D_c and then evaluating under what conditions they are equal in section F.

The following discussion examines diffusivities for systems at equilibrium. Kubo's expression for diffusivity is derived by considering a weak perturbation on an equilibrium system and its linear response [13],

$$D_h = (2kT A_p \chi)^{-1} \int_0^\infty < \vec{I}(t)\cdot\vec{I}(0) > dt, \tag{II.35}$$

where the total particle flow is defined,

$$\vec{I}(t) = \sum_{i=1}^{N} \vec{v}_i(t). \tag{II.36}$$

Using D_h in Eq.(32) is justified as we have associated it with equilibrium fluctuations. The statistical average is taken with respect to the N-body Liouville operator L_N,

$$< \vec{\Gamma}(t)\vec{\Gamma}(0) > = Z^{-1} \int d\Gamma \, \vec{\Gamma} \, e^{-iL_N} \, e^{-\beta H_N} \vec{\Gamma}, \tag{II.37}$$

where $Z^{-1} \, e^{-\beta H_N}$ is the canonical distribution, H_N is the N-body Hamiltonian, and $\Gamma \equiv \prod_{i=1}^{N} d^2x \, d^2p$.

Tracer (tagged particle) diffusivity is defined

$$D_t(n) \equiv \lim_{t \to \infty} < \vec{x}_1^2(t) > /4t. \tag{II.38}$$

Again the average is with respect to the canonical ensemble Eq.(37). Equivalently, Eq.(38) can be written [14],

$$D_t(n) = \frac{1}{2} \int_0^\infty < \vec{v}_1(t) \cdot \vec{v}_1(0) > \, dt. \tag{II.39}$$

Combining Eqs.(35), (36), and (39) results in

$$kT\chi \, D_h(n) = n \, D_t(n) + \frac{1}{2} \sum_{i \neq j} \int_0^\infty < \vec{v}_i(t) \cdot \vec{v}_j(0) > \, dt. \tag{II.40}$$

Eq.(40) shows $D_h(n)$ is not equivalent to $D_t(n)$. This is well known from neutron scattering within liquids where $D_h(n)$ is related to the sum of coherent and incoherent scattering effects and $D_t(n)$ is due solely to the incoherent contribution. That these diffusivities have different energetics and preexponentials has been demonstrated recently in a MC study of surface diffusion [10]. However the tracer $D_t(n)$ cannot be measured from actual field emission fluctuations as there is no way to distinguish a single particle in an interacting system by this method.

If the adsorbate behaves as an ideal gas with site exclusion omitted then $\chi = <n>/kT$ and Eq.(40) becomes,

$$D_h(n) = D_t(n) + \frac{1}{2N}\sum_{i \neq j} \int_0^\infty <\vec{v}_i(t)\cdot\vec{v}_j(0)>dt. \qquad \text{(II.41)}$$

It is then argued by MBG without further explanation that the corresponding dynamical property of this system is such that the time integral of the velocity cross-correlation function is identically zero, in which case Eq.(41) reduces to

$$D_h(n) = D_t(n). \qquad \text{(II.42)}$$

While an ideal system in the thermodynamic sense is described by the ideal gas law, it is not clear from a dynamical viewpoint that equilibrium fluctuations can occur without some correlation of the velocities. Otherwise there is no mechanism for the response of the system to re-equilibrate the fluctuation.

A slightly weaker version of MBG's implicit statement: $\chi = nkT$ iff $\int_0^\infty < \vec{v}_j(t)\cdot\vec{v}_i(0) > dt = 0$ will now be proved, which then makes the derivation of Eq.(42) more plausible. The proof will also clarify the role of probability density functions (PDF's) in distinguishing D_h from D_t.

It is well known that

$$D_h = \lim_{t\to\infty} < \vec{x}_i(t)^2 >_h /4t \qquad \text{(II.43)}$$

can be derived directly from Eq.(30). An equivalent form of Eq.(43) is given by,

$$D_h = \frac{1}{2}\int_0^\infty < \vec{v}_i(t)\cdot\vec{v}_i(0) >_h dt, \qquad \text{(II.44)}$$

which is found by the same means that led to Eq.(39). Eqs.(43) and (44) are similar to those satisfied by D_t, Eqs.(38) and (39). The difference being that, in Eqs.(43) and (44), $n(x,t)/N$ is used as the PDF rather than the one associated with the canonical ensemble, Eq.(37). This change in PDF is noted by placing the subscript h with the average $< >_h$ in Eqs.(43) and (44). Using the solution to the diffusion equation as a PDF means that the exact time evolution implicit in Eq.(37) is replaced by an approximation which is the hydrodynamic relaxation of local equilibrium. For this reason D_h is termed hydrodynamic diffusivity.

Forster recognized that the N-body distribution function, Eq.(37), can be replaced by the hydrodynamic average $< >_h$ in Kubo's expression for diffusivity evaluated at equilibrium, Eq.(35) [15], i.e.,

$$D_h = (2\,kT\,A_p\,\chi)^{-1} \int_0^\infty < \vec{I}(t)\cdot\vec{I}(0) >_h dt. \tag{II.45}$$

Eq.(45) is obtained by Fourier analysis of Eq.(32). Combining Eqs.(36), (44), and (45) yields,

$$D_h \left[\, 2\,A_p\,(kT\,\chi - n)\,\right] = \sum_{i \neq j} \int_0^\infty < \vec{v}_i(t)\cdot\vec{v}_j(0) >_h dt. \tag{II.46}$$

Eq.(46) shows that the thermodynamic relation for an ideal gas,

$$\chi = n/kT, \tag{II.47}$$

is a necessary and sufficient condition for the time integral of the hydrodynamic velocity field to be uncorrelated:

$$\int_0^\infty < \vec{v}_i(t)\cdot\vec{v}_j(0) >_h dt = 0. \tag{II.48}$$

These results, based on Eq.(45), show in what manner the MBG argument leading to Eq.(41) can be accepted. The present discussion provides a mechanism that allows re-equilibration of equilibrium fluctuations while allowing ideal behavior to occur in the thermodynamic sense.

As a final note concerning equilibrium fluctuations the Kubo equation for bulk diffusivity is given by [11]

$$D_b = \frac{1}{2N} \sum_{i,j=1}^{N} \int_0^{\infty} < \vec{v}_i(t) \cdot \vec{v}_j(0) > dt. \tag{II.49}$$

Combining Eqs.(35), (36), and (49) yields the equilibrium version of Eq.(24), now derived microscopically

$$D_h = (n/kT\chi) D_b. \tag{II.50}$$

Ideal gas behavior reduces Eq.(50) to

$$D_h = D_b. \tag{II.51}$$

Eq.(51) becomes,

$$D_h = D_b/(\,1-\theta\,), \tag{II.52}$$

when site exclusion interaction is introduced. Using Eq.(25) transforms (52) to

$$D_h = \Gamma_o \lambda^2. \tag{II.53}$$

F. Irreversible thermodynamic conditions for $D_c(n)=D_h(n)$.

This section considers the equivalence of $D_c(n)$ and $D_h(n)$ from the standpoint of irreversible thermodynamic stability theory. By defining the entropy production,

$$\sigma[s] \equiv J\,X, \tag{II.54}$$

$D_h(n)$ and $D_c(n)$ are equal over the range of thermodynamic force $0 \leq X \leq X_o$ given,

$$D_h(n) = \sigma/\chi\,T\,X^2. \tag{II.55}$$

The right hand side of Eq.(55) is D_c, which is seen by combining Eqs.(1), (11), and (54). The equality always holds in the $X \rightarrow 0$ limit as this is just the definition of D_h, see Eq.(29). There are several reasons to expect that an upper limit X_o exists beyond which Eq.(55) and hence $D_c(n) = D_h(n)$ breaks down. First, because the theorem of minimum entropy production is inapplicable when the kinetic coefficient is not a constant [3]. This happens when the range of densities probed by ∇n becomes large enough that $\nabla D_c \neq 0$, i.e., when the nonlinear Eq.(27) rather than the diffusion Eq.(32) describes the decay of the density inhomogeneity. Then it is uncertain whether σ will vary quadratically in X. Secondly, the response χ of the system is a thermodynamic property and Eq.(55) implicitly assumes that χ is well defined for all values of X, i.e. local equilibrium occurs, but this may not be the case when X becomes large. These points have not been previously addressed in surface diffusion studies.

The stability of the nonlinear Eq.(27) guarantees the uniqueness of the solution [16] and hence would provide a sufficient condition for $D_h(n)=D_c(n)$. Within the framework of the irreversible thermodynamic stability theory a sufficient condition is that the excess entropy production be positive [3], i.e,

$$P[\delta s] \equiv \int \sigma[\delta s]\, dA = \int \delta J\, \delta X\, dA > 0, \tag{II.56}$$

where δ represents a local variation with respect to the thermodynamic variable, in this case density. Eq.(56) is identically satisfied when the variation of the kinetic coefficient is zero: $\delta L = 0$. This occurs when the range of probed densities is small enough that $D_c \chi$ can be considered a constant with respect to the density fluctuation. It is outside the scope of the present study to provide a complete stability analysis of Eq.(27). However there is one situation, pertinent to surface diffusion studies, that may occur which renders Eq.(56) useless in determining the equivalence of the two diffusivities. Nonequilibrium thermodynamic stability theory is based on the assumption that local equilibrium exists within the system. This ensures that terms appearing in the expression for entropy variation, $T\, \delta s = -\mu\, \delta n$, as well as χ, are well defined and spatially continuous functions. Relative changes in thermodynamic parameters of neighboring points are then required to be of the order of the fluctuation in each cell [16]. The basic criterion for the validity of the local equilibrium assumption is: if there exists a fluctuation in the local variable P, then $\delta P \ll P$. If we let $P = J$ and note

$$\delta J = L\, \delta X + X\, \delta L, \tag{II.57}$$

where

$$\delta L = D\, T\, \delta \chi + \chi\, T\, \delta D,$$

then it follows from Eq.(57) that

$$\frac{\delta X}{X} + \frac{\delta \chi}{\chi} + \frac{\delta D}{D} \ll 1 \tag{II.58}$$

is required for local equilibrium. These three terms describe different properties of the

system, being respectively: imposed external thermodynamic force, thermodynamic response, and mass transport. For the present discussion we show how the form of the thermodynamic response function can result in a breakdown of the local equilibrium assumption. This happens when

$$\delta\chi/\chi \ll 1 \tag{II.59}$$

is no longer true. Evaluating Eq.(59) leads to

$$\left[\nabla\kappa_T/(\kappa_T \nabla n) + 2/n \right] \delta n \ll 1. \tag{II.60}$$

However, as a phase boundary is approached $\nabla\kappa_T$ becomes infinite. At this point the local equilibrium assumption is invalid. Fig.3 illustrates a situation where this occurs. Curve (a) represents a range of coverages θ where the system exists as a single phase and local equilibrium holds. In this case a nonequilibrium system that obeys condition Eq.(56) can be evaluated by the stability theory. Curve (b) represents a situation where an initial concentration $\theta_b \rightarrow \theta_a$ would exhibit phase separation and lead to a breakdown of local equilibrium. Then one could not conclude that the two diffusivities are equivalent.

Comparison of data from surface diffusion studies concerning this point is limited to the O/W(110) system studied under nonequilibrium conditions by Butz and Wagner [12], at equilibrium by Chen and Gomer [17], and with MC modeling by Reed and Ehrlich [9]. These results do not clearly demonstrate $D_h(n)=D_c(n)$ for any experimental system. A simple comparison of D_h from ref.[17] and D_c from ref.[12] is precluded as the experiments were carried out in different temperature regimes. The MC data of ref.[9] shows $D_c(n)\neq D_h(n)$ for long range (type III) interactions with $D_c(n)$ evaluated by Fick's law. From this result Reed and Ehrlich concluded that the equilibrium fluctuation theory was not applicable to the ordered states created by this type of

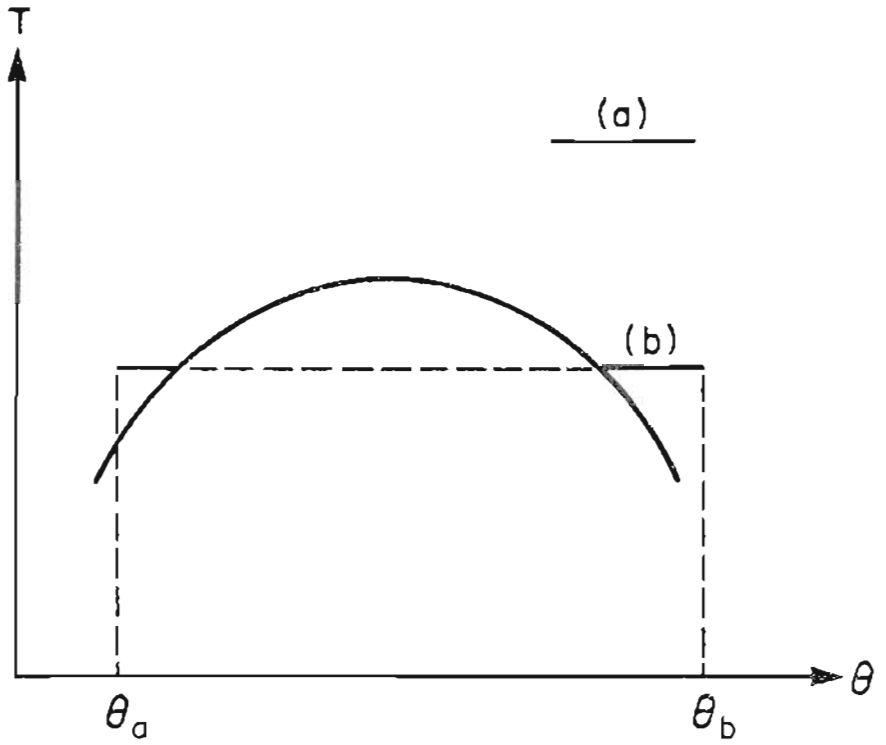

Fig. 3. Thermodynamic phase diagram. Curve (a) represents a coverage range with no phase separation. Curve (b) indicates phase separation as the system proceeds from θ_b to θ_a in coverage.

interaction. However exclusion of a particular adsorbate state is not consistent with the hydrodynamic relaxation theory proposed by MBG that showed a density dependent diffusivity can be derived for all equilibrium systems. Nor does it follow from the discussion of the present section that the two diffusivities are by necessity equivalent. $D_h(n) \neq D_c(n)$ was also found even with $D_c(n)$ evaluated at equilibrium using Eq.(21) [9,10]. The inequality in this case must be due to MC approximation of $\Gamma(\theta)$ because

these diffusivities should be equal as D_h is the equilibrium limit of D_c. Thus it is difficult to properly ascertain whether Reed and Ehrlich's MC result, $D_h(n) \neq D_c(n)$, with $D_c(n)$ evaluated under nonequilibrium conditions is due to a MC artifact or to a phase transition affecting the diffusivity measurement.

G. Summary.

Relations among a number of diffusivities have been analyzed in terms of irreversible thermodynamics and for equilibrium fluctuations in Kubo's formalism. The chemical $D_c(n)$, associated with nonequilibrium systems and defined by Fick's first law, has been distinguished from its equilibrium limit, $D_h(n)$. This latter diffusivity is connected with surface density fluctuations detected by field emission noise measurements. A sufficient condition for their equivalence is that the density gradient probed in the nonequilibrium experiment is small enough that $\nabla D_c \approx 0$. Otherwise if the range of densities is such that a phase boundary is crossed then the irreversible thermodynamic stability theory cannot guarantee their equality. Current experimental evidence does not yet strongly support the equivalence of D_c and D_h under any conditions, although this will probably change as the number of comparative diffusion studies grows. However the distinction between D_c and D_h does not affect the generality of the equilibrium density fluctuation measurement, i.e., a density dependent diffusivity $D_h(n)$ can be found from the long time decay of the autocorrelation function for all adsorbate interactions other than those due to critical fluctuations.

The relations, $D_h = < x^2 >_h / 4t$ and $D_t = < x^2 > / 4t$, show that hydrodynamic and tracer diffusivities are closely related. Their different behavior is determined by the respective probability density functions. The physical origin of this distinction is that measurement of a tracer D_t implies distinguishability of the given particle. Measurement of D_h, as in a field emission noise experiment, arises from current fluctuations within the probed region of indistinguishable particles. A comparison of these diffusivities is only useful for MC studies as $D_t(n)$ cannot be determined from a field emission noise experiment.

We therefore conclude that field emission noise measurements provide a reliable method of measuring D_h. However care must be taken both when D_h is compared with MC data, since $\Gamma(\theta)$ cannot be precisely simulated, and when D_h is compared with D_c, since the latter may depend on the range of densities probed and the phase structure of the adsorbate.

H. Chapter II references.

[1] R.Gomer, "Current Fluctuations from Small Regions of Adsorbate Covered Field Emitters. A Method for Determining Diffusion Coefficients on Single Crystal Planes." *Surface Sci.* **38** *(1973) 373.*

[2] G. Mazenko, J.R. Banavar, and R. Gomer, "Diffusion Coefficients and the Time Autocorrelation Function of Density Fluctuations." *Surface Sci.* **107** *(1981) 459.*

[3] P. Glansdorff and I. Prigogine, *"Thermodynamic Theory of Structure, Stability, and Fluctuations" (Wiley-Interscience, New York 1971).*

[4] E.M. Lifshitz and L.P. Pitaevskii, *"Statistical Physics" 3rd ed. part 1 (Pergamon Press, Oxford 1980).*

[5] D.A. Reed and G. Ehrlich, "Surface Diffusion, Atomic Jump Rates and Thermodynamics." *Surface Sci.* **102** *(1981) 588.*

[6] G.E. Murch and R.J. Thorn, "Isothermal Transport in a Lattice Gas." *Phil. Mag.* **A40** *(1979) 477.*

[7] A. Sadiq and K. Binder, "Diffusion of Adsorbed Atoms in Ordered and Disordered Monolayers at Surfaces." *Surface Sci.* **128** *(1983) 350.*

[8] Denoted D^k in ref.[9] and D_J in ref.[10].

[9] D.A. Reed and G. Ehrlich, "Surface Diffusivity and the Time Correlation of Concentration Fluctuations." *Surface Sci.* **105** *(1981) 603.*

[10] M. Tringides and R. Gomer, "A Monte Carlo Study of Oxygen Diffusion on the (110) Plane of Tungsten." *Surface Sci.*, **145** *(1984) 121.*

[11] W. Zwerger, "The Density Dependence of the Diffusion Constant in Interacting Lattice Gases: Application to Surface Diffusion of O on W(110)." *Z. Physik B (Condensed Matter)* **42** *(1981) 333.*

[12] R. Butz and H. Wagner, "Diffusion of Oxygen on Tungsten (110)." *Surface Sci.* **63** *(1977) 448.*

[13] R. Kubo, "Statistical-Mechanical Theory of Irrevrsible Processes. I. General Theory and Simple Applications to Magnetic and Conduction Problems." *J. Phys. Soc. Japan* **12** *(1957) 570.*

[14] J.P. Boon and S. Yip, *"Molecular Hydrodynamics", (McGraw-Hill, New York 1980).*

[15] D. Forster, *" Hydrodynamic Fluctuations, Broken Symmetry and Correlation Functions" (Benjamin, Reading MA 1975).*

[16] H.J. Kreuzer, *" Nonequilibrium Thermodynamics and its Statistical Foundations" (Clarendon, 1981).*

[17] J.-R. Chen and R. Gomer, "Mobility of Oxygen on the (110) Plane of Tungsten." *Surface Sci.* **79** *(1979) 413.*

III. Detection of Two Dimensional Phase Transitions by Field Emission Noise Measurements

"They move in the void and catching each other up jostle together, and some recoil in any direction that may chance, and others become entangled with one another in various degrees according to the symmetry of their shapes and sizes and positions and order, and they remain together and thus the coming into being of composite things is effected." Simplicius *De Caelo*

A. Introduction

It is now well established that field electron emission current fluctuations induced by diffusive adsorbate motion on single crystal planes at equilibrium yield a measurement of the coverage dependent surface diffusion coefficient D. This quantity is obtained either from the long time limit of the current autocorrelation function $R(t) \equiv < \delta i(t)\delta i(0) > / < i >^2$ [1,2],

$$\lim_{t\to\infty} R(t) \sim C_{FN} < (\delta N)^2 > (r_p^2/4Dt), \tag{III.1}$$

where C_{FN} is a constant containing factors from the Fowler-Nordheim equation, δN is the fluctuation in the number of adparticles appearing in the circular probed region of radius r_p, and it is implicitly assumed that the net plane boundaries are not a factor; or in the low frequency limit of the corresponding spectral density function [3]

$$\lim_{f\to 0} S(f) = 2C_{FN} < (\delta N)^2 > r_p^2 D^{-1} ln(r_t/r_p), \tag{III.2}$$

where the finite size of the net plane with radius r_t is included.

The thermodynamic state of the adlayer is accessible by measuring the current noise power from the probed area A_p since [4],

$$R(0) = C < (\delta n)^2 >, \tag{III.3}$$

where C= $A_p^2 C_{FN}$, $n = N/A_p$, and

$$< (\delta n)^2 > = < n >^2 kT \kappa_T / A_p. \tag{III.4}$$

$\kappa_T = n^{-1}(\partial n/\partial \sigma)_T$ is the isothermal compressibility of the two dimensional adlayer with spreading pressure σ. The relative noise power $P = \int_0^\infty S(f)\, df$ of the field emission current fluctuations is given by,

$$P = 2R(0) \tag{III.5}$$

and the spectral density function S(f) is related to R(t) by the Wiener-Khinchin theorem. Combining Eqs.(3-5) yields,

$$P = a_1 T \kappa_T, \tag{III.6}$$

with $a_1 = 2\, C < n >^2 k/A_p$ a constant. Therefore the isothermal compressibility κ_T is detected by a measurement of the noise power P. This is an alternate statement of Eq.(3).

In this study we demonstrate that the transition temperature of a two dimensional phase change occurring in the thermally activated diffusion regime corresponds to the onset of collective interactions that affect diffusivity and isothermal compressibility as determined by field emission noise measurements. Although not all systems have the simple phase structure modeled here, the correspondence is not specific to a particular adsorbate as shown by examples using chemisorbed K/W, physisorbed Xe/W, and H/W systems. Exceptions appear to be O/W(110) [5] and the β_1 state of H/W(111) [6], which do not show an easily discernible relation between $\kappa_T(T)$ and $D(T)$ and the existence of a phase change. This is apparently due to a significant

deviation from a simple two dimensional lattice gas model as can be inferred from a Monte Carlo study of O/W that was able to qualitatively model the adsorbate thermodynamics by a lattice gas model, but could not reproduce quantitatively the large increase in prefactor of the diffusion coefficient as a function of coverage that was found experimentally [7]. The disparity in the quantitative results was attributed to substrate lattice deformation induced by the adsorbate. This effect also appears related to the anomalous behavior observed when either hydrogen or deuterium were adsorbed on W(111) or W(110) planes [6]. Nevertheless from our analysis we are able to find previously undetected phase transitions for the systems considered here. It is shown that the resulting variation in noise power P is associated with the onset of a nonlinear Arrhenius plot of $D(T)$.

B. Temperature Dependence of κ_T and $D(T)$.

With no adsorbate-adsorbate (ad-ad) interactions a nonlocalized and mobile collection of adatoms behaves as an ideal gas with an equation of state,

$$\sigma A_p = <N> kT, \tag{III.7}$$

where <^N^> is the average number of particles in the probed area A_p. The correponding noise power for a two dimensional ideal gas,

$$P = 2\,C <n> / A_p, \tag{III.8a}$$

is then temperature independent. With site exclusion but no other interaction (Langmuir gas) $<(\delta n)^2> = <n>(1-\theta)A_p^{-1}$ and Eq.(III.8a) becomes,

$$P = 2\,C < n > (\,1-\theta\,)/A_p, \tag{III.8b}$$

where $\theta \equiv n\,a_0^2$ and a_0 is the lattice constant assuming a square lattice geometry, however the noise power remains temperature independent. Eqs.(6) and (8) suggest that incipient temperature dependence of the field emission noise power, or equivalently of the isothermal compressibility, reveals the existence of a phase transition. To show this, it is necessary to find the functional form of $\kappa_T(T)$ when the system undergoes a phase change. Formalisms that use the compressibility equation [8], partition functions for a lattice gas [4], or hole model of a liquid [9] require additional information concerning interaction energies or the radial distribution function. Instead $\kappa_T(T)$ is evaluated for a homogeneous condensed phase and then extrapolated to a temperature where dilute phase behavior occurs. This temperature is taken as the transition temperature.

The procedure is to expand the area to first order in $(T-T_0)$ [9-11]:

$$A(T) = A(T_0)\,[\,1 + \alpha_\sigma(\,T - T_0)\,], \tag{III.9}$$

where T_0 is a fiducial temperature for the homogeneous condensed phase and $\alpha_\sigma \equiv A^{-1}(\,\partial A/\partial T\,)_\sigma$ is the coefficient of thermal expansion. It then follows from Eq.(9) that

$$\kappa_T(T) = \kappa_T^o(\,1 + \alpha_\sigma\,\Delta T\,) \tag{III.10}$$

and $\kappa_T^o \equiv n^{-1}(\,\partial n/\partial\sigma\,)_{T_0}$. When $\alpha_\sigma\,\Delta T \ll 1$ then $\kappa_T(T)$ can be considered constant. For example this condition holds when $\Delta T = 100K$ and $\alpha_\sigma = 3.2\times10^{-4}K^{-1}$, the latter value is for potassium in the bulk liquid state [9]. Assuming the systems studied here exhibit this property then

$$P = a_1\,\kappa_T^o\,T, \tag{III.11}$$

i.e., the noise power is proportional to temperature.

Eqs.(8) and (11) show the noise power-temperature curve has zero slope when the adsorbate exhibits two-dimensional ideal gas behavior and a quasi-linear temperature dependence when condensation occurs. If interphase fluctuations exist then another term must be added to $< (\delta n)^2 >$ which can lead to additional peaks in the noise power curve at intermediate temperatures [4,7]. Other structure can develop at even lower temperatures when tunneling becomes the dominant mechanism for diffusion [6,12]. The nature of these latter phase transitions is outside the scope of the present discussion.

The static response of a phase change, measured by the compressibility of the adlayer, can also be correlated with the adsorbate dynamics by analyzing the temperature dependence of the diffusivity associated with the equilibrium surface density fluctuations. The diffusivity $D(T)$ is given by [13,14]:

$$D(\theta,T) = \lambda^2\, \Gamma(\theta,T)\, F(\theta,T), \qquad \text{(III.12)}$$

where λ^2 is the mean square jump length, the thermodynamic factor

$$F(\theta,T) = n / kT\chi(\theta,T),$$

and the response function $\chi \equiv (\partial n/\partial \mu)_T$ is [15]

$$\chi(\theta,T) = n^2 \kappa_T(\theta).$$

The effective jump rate,

$$\Gamma(\theta) = (1-\theta)\gamma(\theta)\,\Gamma_o,$$

accounts for site exclusion via $(1-\theta)$ and the dimensionless γ represents the influence of interactions on the kinetic coefficient. The jump rate Γ_o is the probability per unit time of a particle passing over an activation energy barrier for a dilute system and is

given by [16]

$$\Gamma_o = \nu e^{-\Delta A_o/kT}, \tag{III.13}$$

where ν is the average vibrational frequency of the particle, $\Delta A_o \equiv A_o^s - A_o^w$ is the difference in the free energy per site for the saddle and well positions of the potential barrier respectively. We follow the usual assumption of transition state theory by expressing the temperature dependence of the effective jump frequency Γ for all coverages θ as [13]

$$\Gamma(\theta,T) = (1 - \theta) \nu e^{-\Delta A(\theta,T)/kT}. \tag{III.14}$$

Combining Eqs.(12) and (14) yields,

$$D(\theta,T) = (1-\theta) F(\theta,T) \lambda^2 \nu e^{\Delta S(\theta,T)/k} e^{-\Delta E(\theta)/kT}, \tag{III.15}$$

where $\Delta A(\theta,T) = \Delta E(\theta) - T\Delta S(\theta,T)$ is expressed as the change in activation energy and entropy per site respectively. Substrate stability is assumed throughout the temperature range of the diffusion experiment, which implies $\Delta E(\theta)$ is temperature independent.

The term $\nu F(\theta,T)$ has only a weak temperature dependence compared to the exponential factors in Eq.(15). To show this, the chemical potential is written as a sum of contributions due to site exclusion plus all other interactions respectively,

$$\mu = kT \ln \left[\theta/(1-\theta) \right] + \mu^*. \tag{III.16}$$

Then

$$F(\theta,T) = (1-\theta)^{-1} + f^*(\theta)/kT, \tag{III.17}$$

where $f^*(\theta)$ is only a function of coverage whose precise form depends on the particular approximation made in the interaction energy of the partition function. For

example, by using the Topping model that includes mutual dipole depolarization [17], in Bragg-Williams approximation this function is of the form:

$$f^*(\theta) = (4\,d^2/a_o^3) \left[\theta/(1+9p\,\theta)^2 \right] \left[1-18p\,\theta/(1+9p\theta) \right] - c\,\theta, \qquad \text{(III.18)}$$

where $p \equiv \alpha/a_o^3$, α is the adatom polarizability, d is the dipole moment, and c is a constant related to the binding energy. Given the system is above the Debye temperature one can assume $\nu = kT/h$ where h is Planck's constant and therefore from Eqs.(15) and (17) find

$$(1-\theta)\,F(\theta,T) = \left[kT + (1-\theta) f^*(\theta) \right]/h\nu.$$

We are then assured that; $\lim_{\theta \to 1} (1-\theta) F \approx 1$ and the T dependence of νF is negligible with respect to the exponential terms in Eq.(15), which can now be written,

$$D(\theta,T) = D_o(\theta)\, e^{\Delta S(\theta,T)/k}\; e^{-\Delta E(\theta)/kT}, \qquad \text{(III.19)}$$

where $D_o(\theta) \equiv \lambda^2 \nu (1-\theta) F(\theta)$.

Eqs.(1) and (2) show that Arrhenius plots of spectral density and autocorrelation functions are equivalent in the sense that

$$\lim_{f \to 0} d[\ln S(f)]/d[1/kT] = \lim_{t \to \infty} d[\ln R(t)]/d[1/kT] = d[\ln D]/d[1/kT]. \qquad \text{(III.20)}$$

Combining Eqs.(19) and (20) leads to,

$$d[\ln D]/d[1/kT] = -(\Delta E(\theta) - T\Delta C_\theta), \qquad \text{(III.21)}$$

where $\Delta C_\theta \equiv C_\theta^s - C_\theta^w$ is the difference in heat capacity per site at constant coverage between saddle and well positions respectively.

To evaluate ΔC_θ the system is divided into two levels and the states are associated either with the well or the saddle position. An adatom at the saddle is always taken to be in the gas phase whereas an adatom in the well may exist in one of two

phases. When the system exists as a single phase for all positions along the potential energy curve we assume the specific heat of the gas phase $c_{\theta,g}$ is constant, in which case,

$$\Delta C_\theta = (P_s - P_w) \theta c_{\theta,g}, \tag{III.22}$$

where $P_s(P_w)$ is the probability the adatom is in the saddle (well) position and $c_{\theta,g}$ is the specific heat per adatom of the gas phase at constant coverage. When $\Delta E(\theta) \gg kT$, $P_w \approx 1$. Hence Eq.(22) is to good approximation given as,

$$\Delta C_\theta = -\theta c_{\theta,g}. \tag{III.23}$$

Thus for a single phase system Eq.(21) becomes

$$d[\ln D]/d[1/kT] = -(\Delta E(\theta) + \theta T c_{\theta,g}). \tag{III.24}$$

Regarding the vapor as an ideal gas implies $c_{\theta,g} = k$ and reduces Eq.(24) to

$$d[\ln D]/d[1/kT] = -\Delta E(\theta). \tag{III.25}$$

In this case a linear Arrhenius plot of diffusivity yields the diffusion activation energy $\Delta E(\theta)$. Eq.(25) is strictly true in the $\lim \theta \rightarrow 0$, but is also valid for all θ given $\Delta E(\theta) \gg kT$ and there is no phase transition.

When the temperature is lowered to a point within the two phase region, i.e., inside the coexistence curve, the specific heat for the well sites is given by [8]

$$c_\theta^w = x_g \left[c_{\theta,g} + (T v_g \alpha^2_{coex,g} / \kappa_{T,g}) \right] + x_l \left[c_{\theta,l} + (T v_l \alpha^2_{coex,l} / \kappa_{T,l}) \right]. \tag{III.26}$$

The symbols g and l refer to the gas and liquid (condensed) phase respectively, $c_{\theta,g} \equiv C_{\theta,g}/N_g$, $x_g \equiv N_g/N$, N_g is the number of adatoms (in the gas phase), $v_g \equiv V_g/N_g$, V_g is the gas phase volume, and $\alpha_{coex,g} \equiv v_g^{-1}(\partial v_g/\partial T)_{coex}$. Eq.(21) is

now transformed with the aid of Eq.(26) to,

$$d[lnD]/d[1/kT] = -\Delta E(\theta) + \theta_l\, T\Big[\, c_{\theta,l} + T(\, \alpha^2{}_{coex,l}\, v_l/\kappa_{T,l}\,)\,\Big], \qquad \text{(III.27)}$$

where $\theta_l \equiv x_l\theta$ and the gas phase at the coexistance line is taken to be ideal. The appearance of the condensed phase as the temperature is lowered then leads to a non-linear Arrhenius plot of diffusivity for a given coverage.

The following section presents several examples where the transition temperature T_t and coverage θ_t of the adsorbate phase, deduced from noise power-temperature curves, corresponds with (θ_t, T_t) determined from the onset of nonlinear Arrhenius behavior of the diffusivity.

C. Experimental results.

1. K/W(112)

K/W(112) is a previously studied chemisorbed system that exhibits a phase transition at submonolayer coverages [18]. Evidence for this behavior is given in Fig.4 where the absolute field emission noise power is plotted as a function of temperature at a coverage $\theta \simeq 0.47$. The graph clearly shows a transition from ideal to condensed behavior at T $\sim$ 385K.

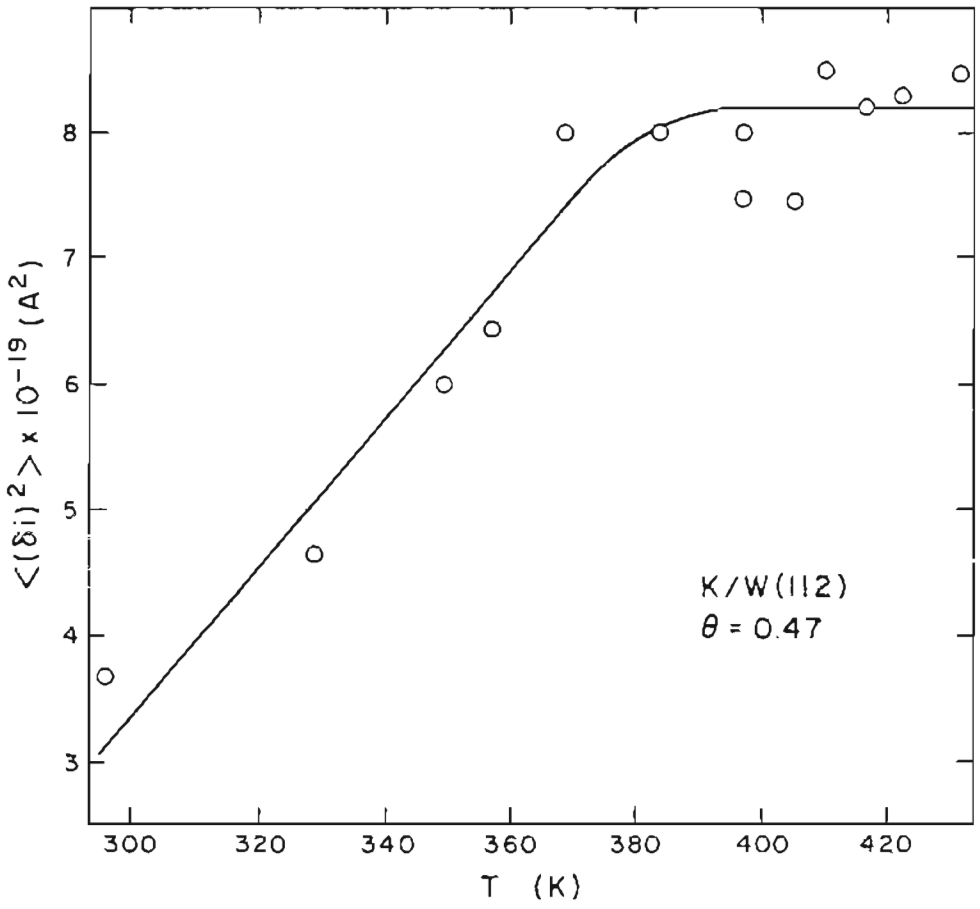

Fig. 4. Plot of noise power temperature dependence of K/W(112) at a coverage $\theta = 0.47$. Data from Fig.2 of reference [18].

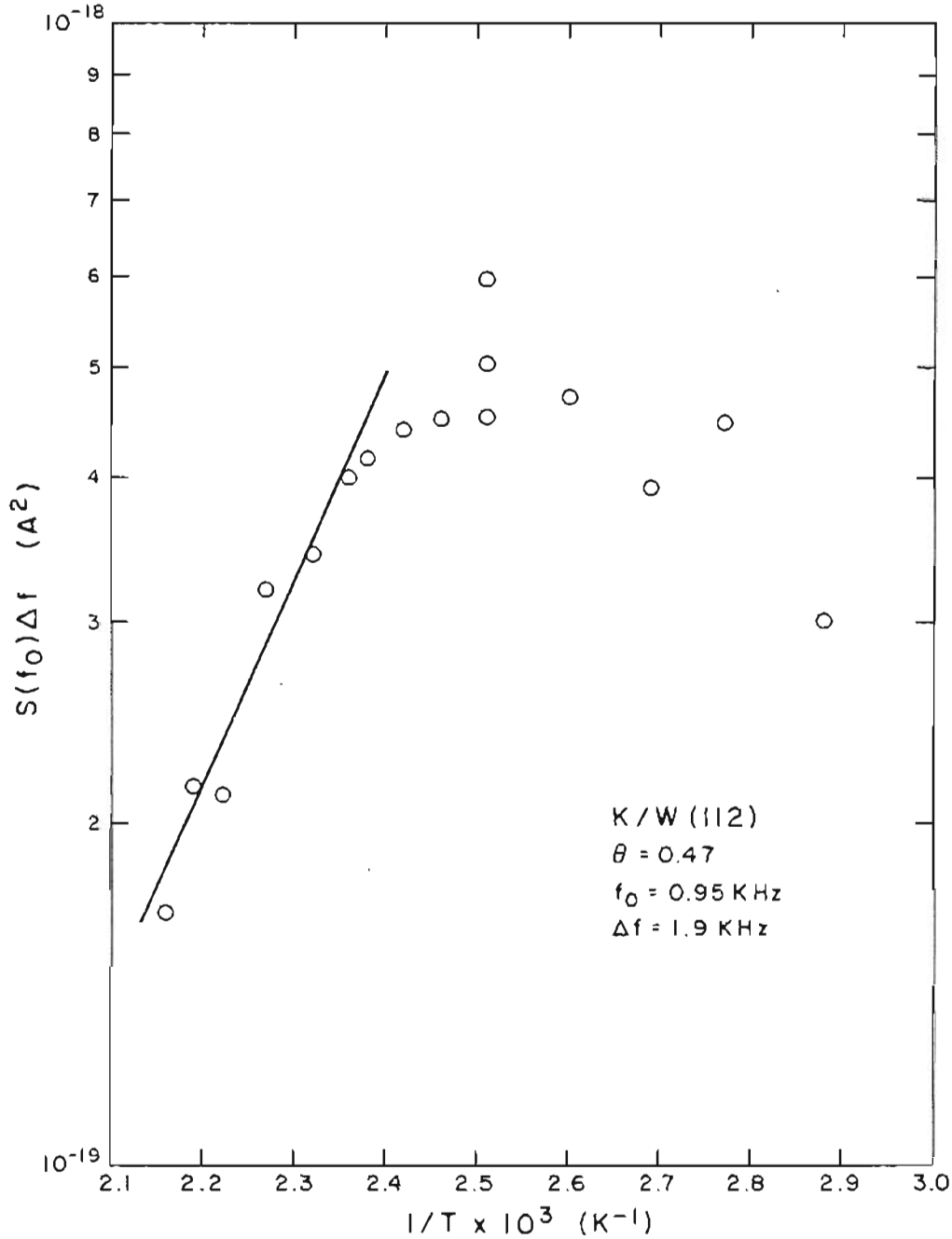

Fig. 5. Arrhenius plot of the noise spectrum $S(f_o)\Delta f$ due to K/W(112) at $\theta = 0.47$. Data from Fig.6 of reference [18].

The transition at $T \sim 385K$ is correlated with incipient nonlinearity of the Arrhenius plot shown in Fig. 5, which graphs $d[\ln S(f_0)\Delta f]/d[1/T]$ and hence by Eq.(2) $-d\ln[D(T)]/d[1/T]$. This curve suggests a phase transition occurs at $T \sim 420K$. This is 35K from the transition temperature as determined by the noise power measurement of Fig.4. A closer agreement between the two transition temperatures would most likely be found if a narrower bandwidth had been used in the determination of $S(f,T)$. From the data in the ideal gas regime of Fig.5 a value of the diffusion activation energy $E_D = 0.20\,eV$ is obtained from an Arrhenius plot of the spectral density for K/W(112). Given the difference in experimental method and the relatively large Δf used this value is comparable to $E_D = 0.28\,eV$ obtained by Schmidt and Gomer in the limit $\theta \rightarrow 0$ [19] and to $E_D = 0.21\,eV$ found by Meclewski at $\theta = 0.2$ [20] from observations of the time dependence for equilibration of adsorbate concentration gradients in the field emission microscope.

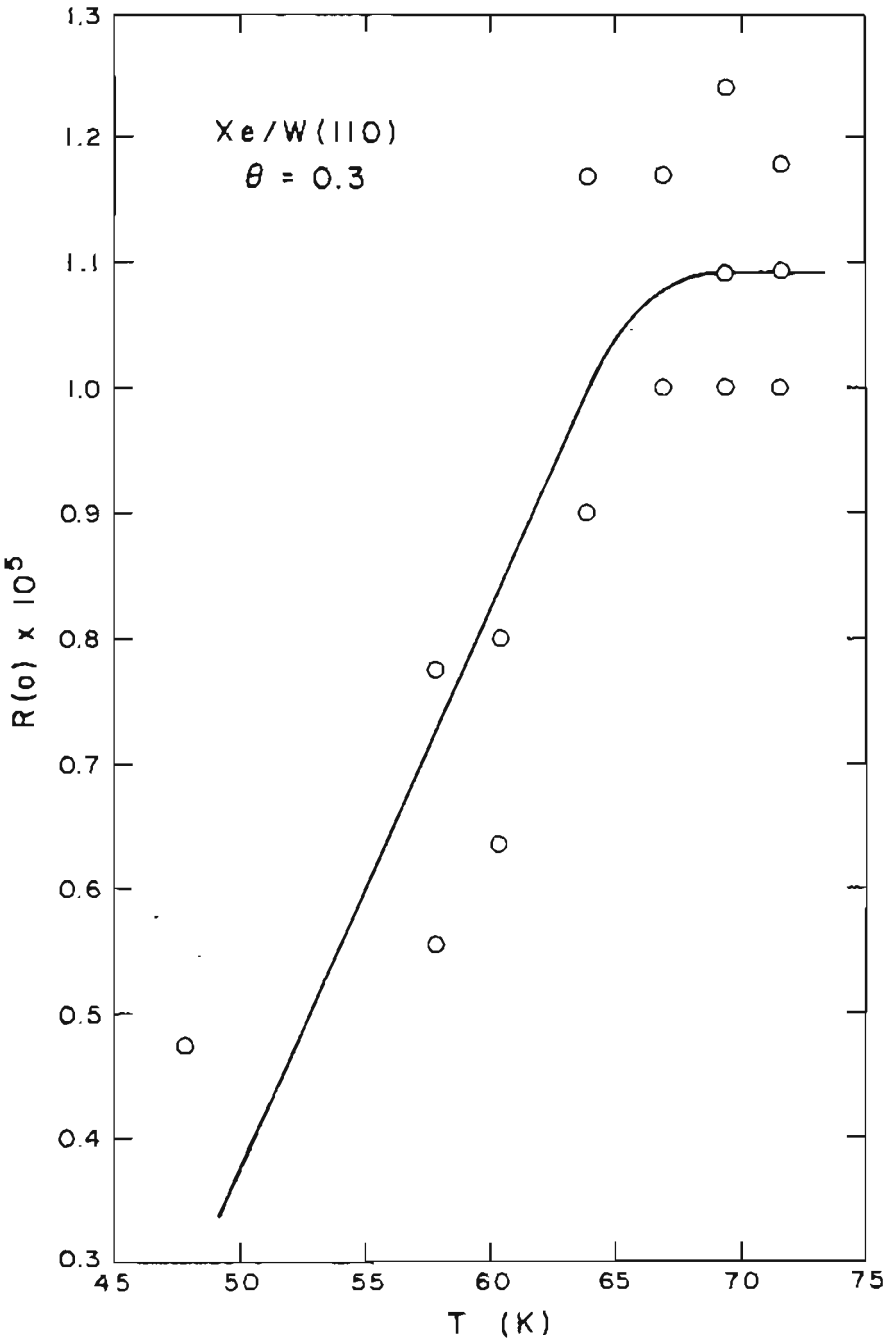

Fig. 6. Plot of noise power temperature dependence of Xe/W(110) at $\theta = 0.3$. Data from Fig.6 of reference [21].

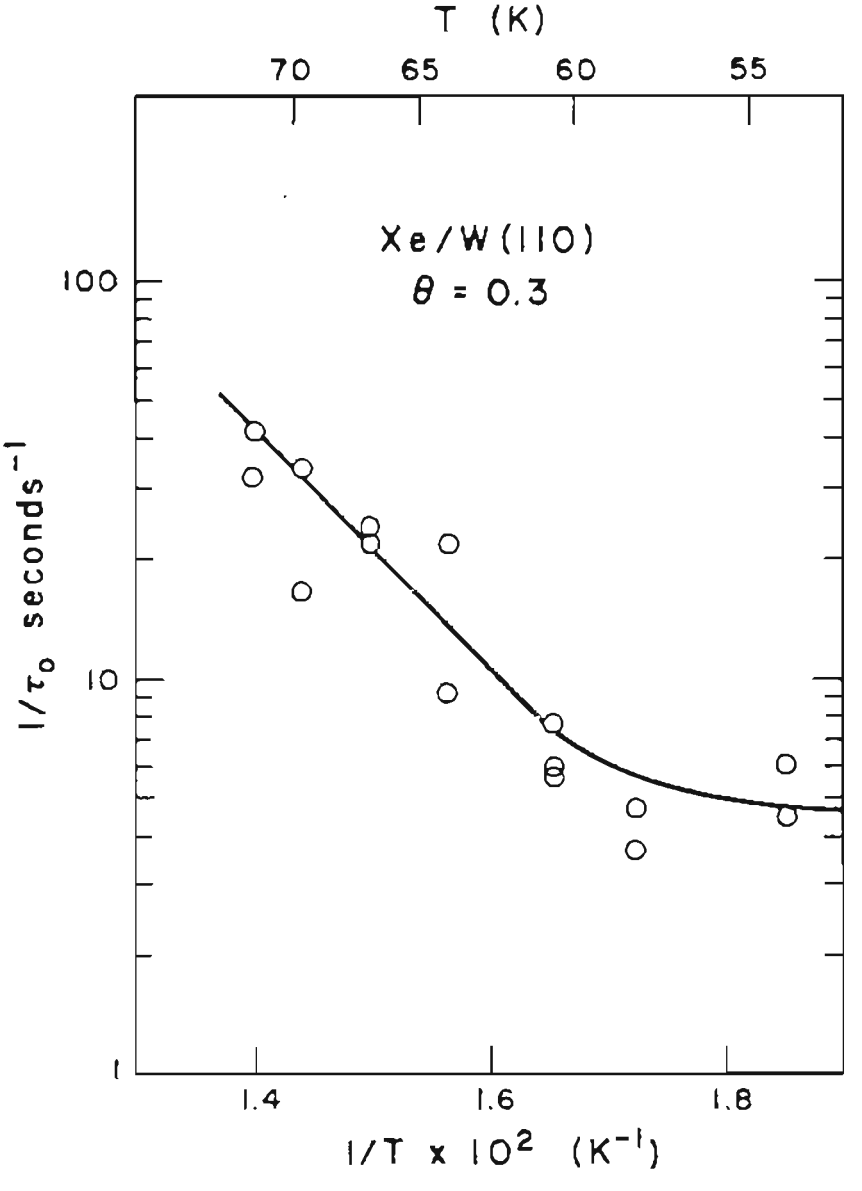

Fig. 7. Arrhenius plot of the diffusivity $D = r_p/4\tau_o$ for Xe/W(110) at $\theta = 0.3$. Data from Fig.3 of reference [21].

2. Xe/W(110)

Fig. 6 shows relative field emission noise power versus temperature data of Xe/W(110) that has been replotted from Fig.6 of reference [21]. Although there is some scatter in the data at high temperatures a phase transition appears to occur at $\theta = 0.3$ and T = 65K for this physisorbed system. This suspected transition corresponds closely to the onset of nonlinearity in the Arrhenius plot of $D(T)$ as shown in Fig.7 where $\tau_0^{-1} = 4D/r_p$. The data implies the transition temperature occurs at about T = 60K, which is 5K from the temperature estimated from the noise power data of Fig.6. Since a transition to nonideal behavior exists at T = 65K and $\theta = 0.3$ it is reasonable to expect this temperature to rise as the coverage is increased. Thus the anomalous behavior found by Chen and Gomer in $\tau_0(T)$ at $\theta = 0.5$ (Fig.4 of [21]) is probably due to condensation of the adlayer, which is consistent with their conclusion that the system had formed an ordered phase at this coverage.

3. H/W(111)

The present analysis can also be applied in certain cases to measurements of H/W(111) in the thermally activated diffusion regime. Fig. 8 shows data taken from reference [6] where deviations from ideal behavior of the compressibility occur for T < 210K and $\theta = 0.5$ of the β_2 state. Fig. 9 shows that this temperature corresponds to the onset of nonlinearities in the Arrhenius plot of $D(T)$.

At a coverage of $\theta = 0.7$ more complicated behavior is found which suggests an isotope effect in the thermally activated diffusion regime. Fig. 10 graphs the noise

power-temperature dependence for both ^1H and ^2H. Interestingly a transition appears for ^1H but not ^2H in this range. For ^1H this occurs at $T = 170K$ where the compressibility goes through a large variation, probably due to interphase fluctuations, before exhibiting a monotonic decrease characteristic of a condensed homogeneous phase. This isotope effect is also reflected in the Arrhenius plots of diffusivity shown in Fig.11. Incipient nonlinearity occurs approximately at $T = 180K$ for ^1H as does the compressibility change. Yet the slope of the ^2H diffusivity plot does not show significant nonlinear behavior in this temperature range corresponding to the behavior found in Fig.7.

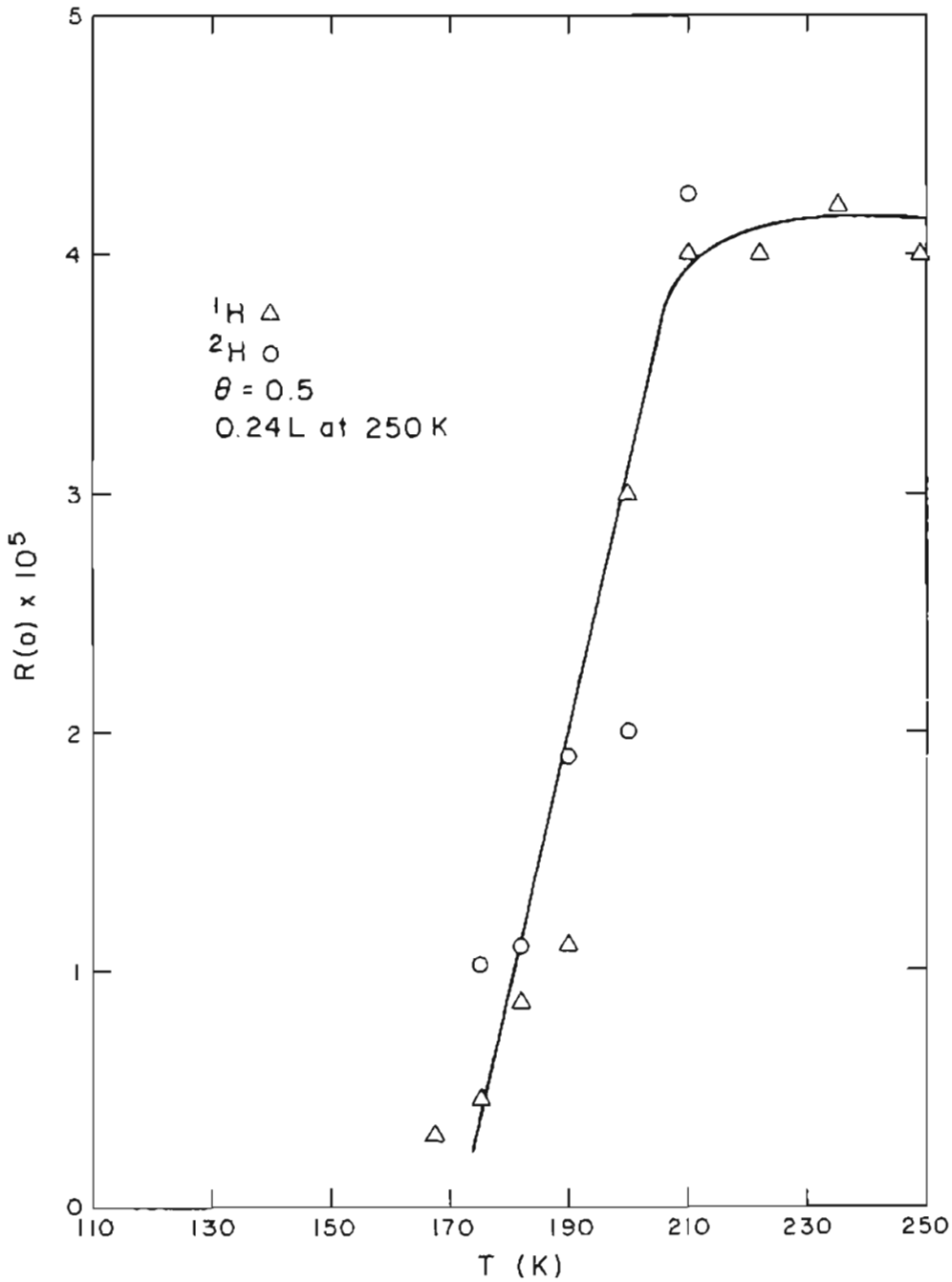

Fig. 8. Plot of noise power temperature dependence of H/W(111) at $\theta = 0.5$ with an initial dose of 0.24L at 250K. Data from Fig.18 of reference [6].

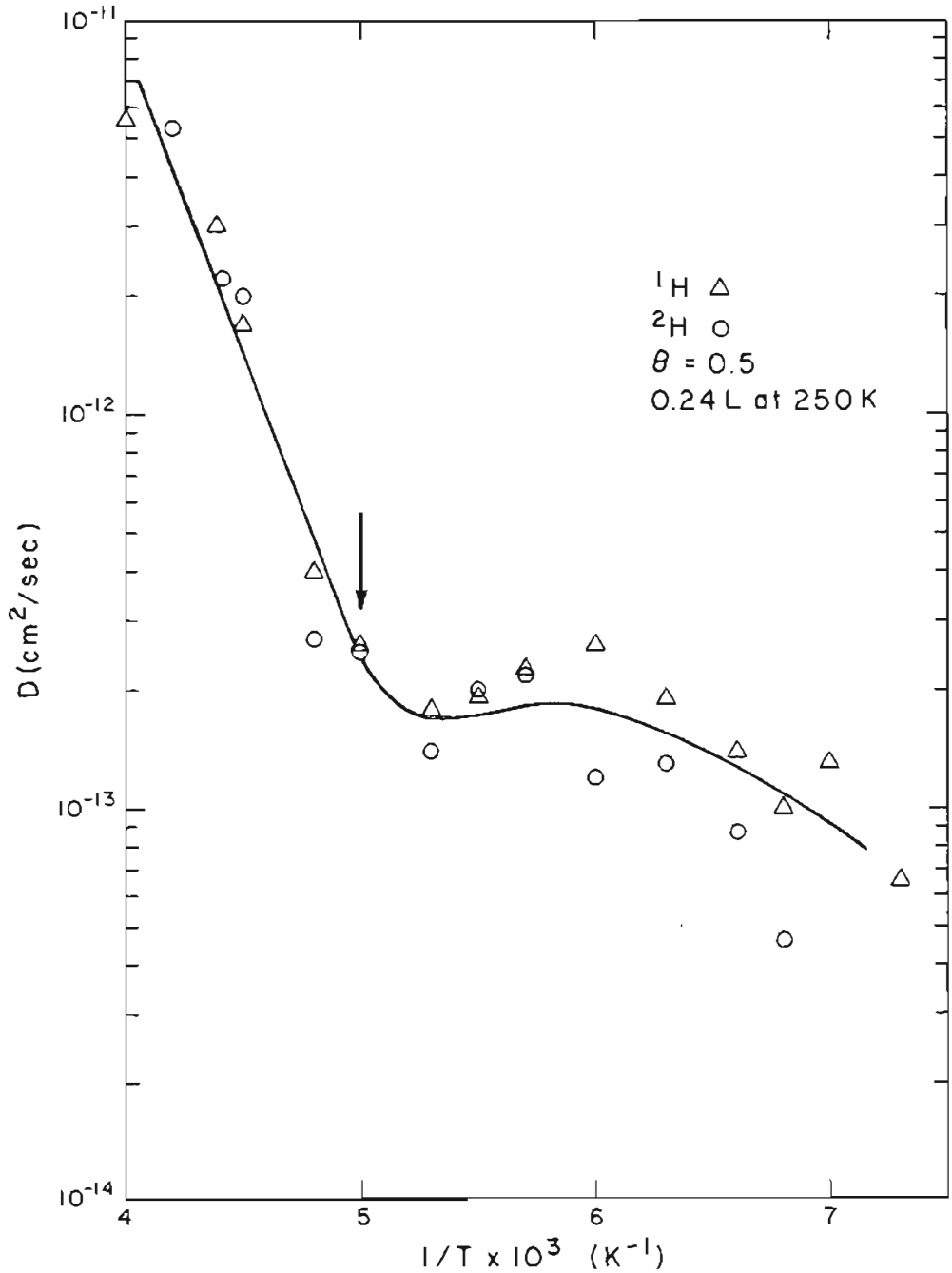

Fig. 9. Arrhenius plot of diffusivity for H/W(111) at $\theta = 0.5$. Data from Fig.16 of reference [6].

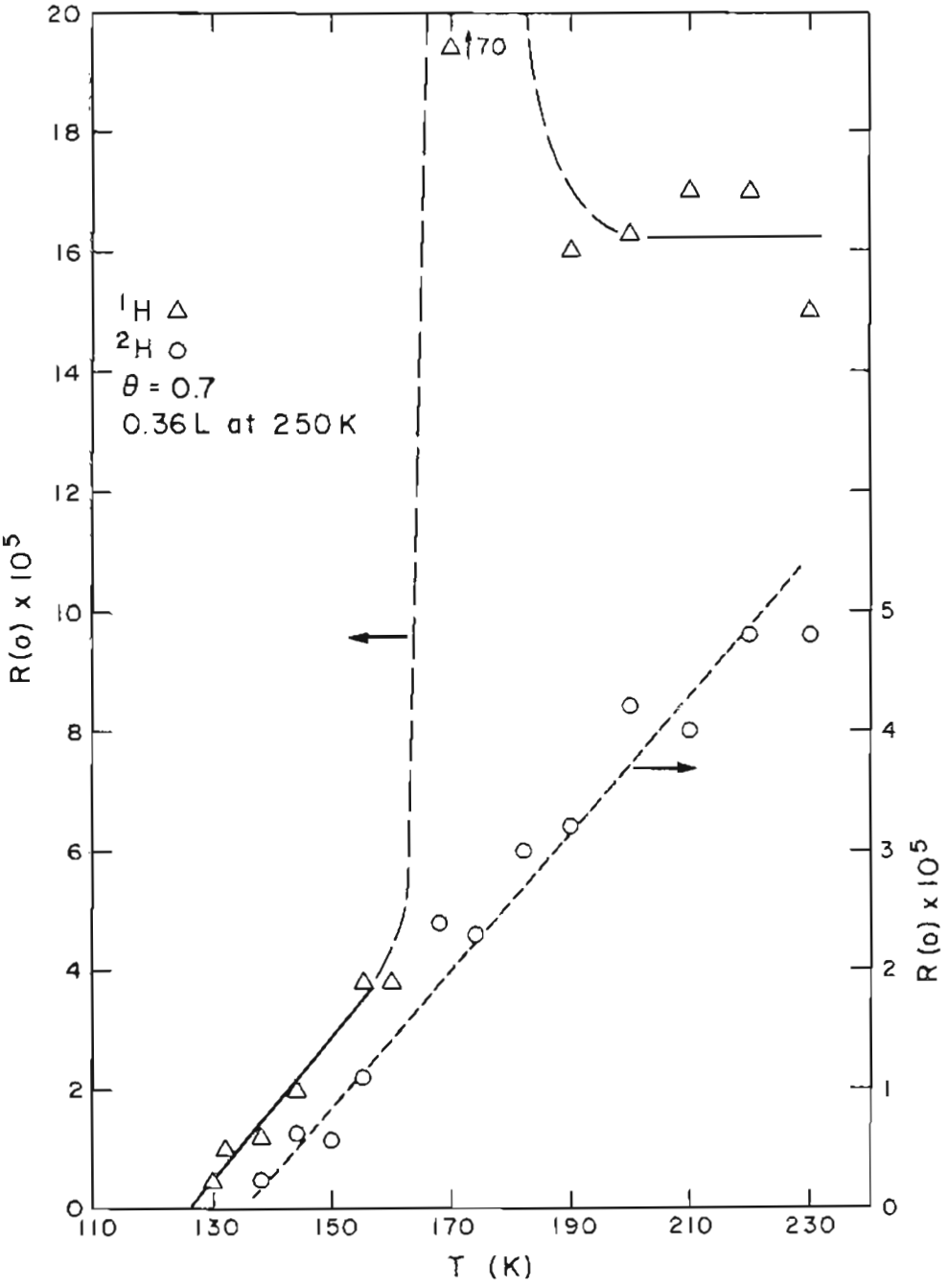

Fig. 10. Plot of noise power temperature dependence of H/W(111) at $\theta = 0.7$. Data from Fig.19 of reference [6].

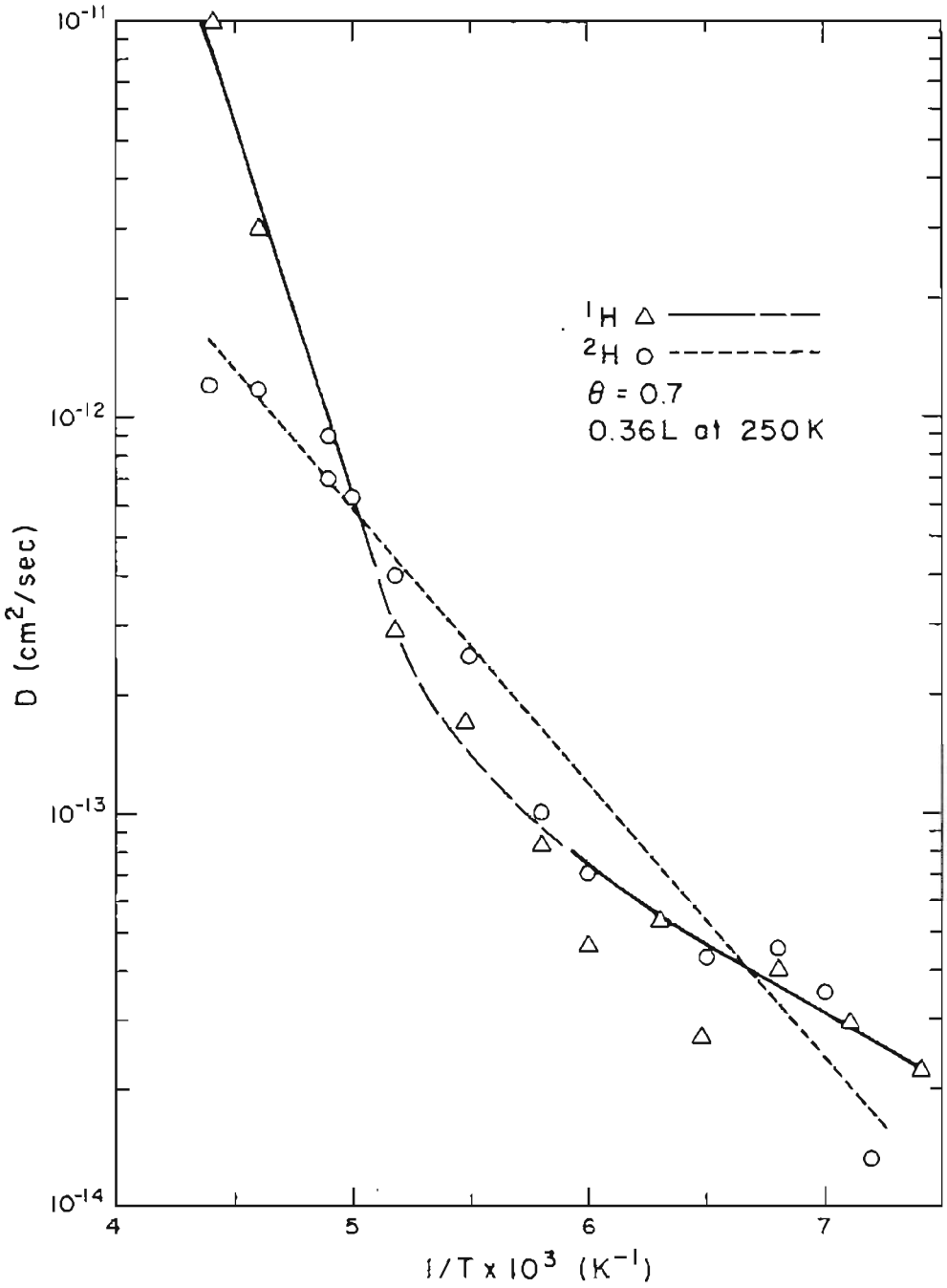

Fig. 11. Arrhenius plot of diffusivity for H/W(111) at $\theta = 0.7$. Data from Fig.17 of reference [6].

D. Summary.

The temperature dependence of field emission flicker noise induced by diffusive adatom motion in the thermally activated regime has been shown to be sensitive to the onset of nonideal behavior in terms of both the isothermal compressibility and diffusivity for the K/W(112), Xe/W(110), and H/W(111) systems. A simple model of the temperature dependence of the isothermal compressibility is found useful for detecting a phase transition by measurement of the total noise power. The autocorrelation or spectral density of the field emission current fluctuations indicate the onset of ad-ad interactions via nonlinear Arrhenius plots of surface diffusivity $D(T)$. This latter relationship provides an estimate of the K/W(112) diffusion coefficient in the low coverage limit, $E_D = 0.20\,eV$, similar to values derived from field emission shadowing experiments. The present study has yielded several previously unidentified phase changes whose transition temperature is confirmed by the agreement between κ_T and $D(T)$. Although the analysis of the entire phase diagram and associated diffusive motion requires a more general theory, the relatively simple method presented here using field emission noise measurements has elucidated at least a portion of it without requiring additional variables that must be obtained by other experimental methods. Data analysis of H/W(111) measurements at $\theta = 0.7$ indicate a possible isotope effect with respect to $\kappa(T)$ and $D(T)$ properties of ^1H and ^2H in the thermally activated diffusion regime. The origin of this effect remains to be explained. It is concluded that field emission noise measurements provide a useful insight to the statistical thermodynamics of incipient nonideal behavior for a number of chemically dissimilar, two dimensional adsorbate systems.

E. Chapter III references.

[1] R. Gomer, "Current Fluctuations from Small Regions of Adsorbate Covered Field Emitters. A Method for Determining Diffusion Coefficients on Single Crystal Planes." *Surface Sci.* **38** *(1973) 373.*

[2] G. Mazenko, J.R. Banavar, and R. Gomer, "Diffusion Coefficients and the Time Autocorrelation Function of Density Fluctuations." *Surface Sci.* **107**

[3] M. Gesley and L.W. Swanson, "Spectral Analysis of Adsorbate Induced Field Emission Flicker (1/f) Noise - Canonical Ensemble." Submitted to *Phys. Rev.*

[4] B. Bell, R. Gomer, and H. Reiss, "Concentration Fluctuations in Adsorbed Layers." *Surface Sci.* **55** *(1976) 494.*

[5] J.-R. Chen and R. Gomer, "Mobility of Oxygen on the (110) Plane of Tungsten." *Surface Sci.* **79** *(1979) 413.*

[6] C. Dharmadhikari and R. Gomer, "Diffusion of Hydrogen and Deuterium on the (111) Plane of Tungsten." *Surface Sci.* **143** *(1984) 223.*

[7] M. Tringides and R. Gomer, "A Monte Carlo Study of Oxygen Diffusion of the (110) Plane of Tungsten." *Surface Sci.*, **145** *(1984) 121.*

[8] L.E. Reichl, *"A Modern Course in Statistical Physics", (Univ. Texas, 1980).*

[9] S.M. Breitling and H. Eyring, *"Liquid Metals", chpt.5,* ed. S. Beer, *(Marcel Dekker, 1972).*

[10] H.B. Callen, *"Thermodynamics" (Wiley and Sons, New York 1960).*

[11] M.H. Cohen and D. Turnbull, "Molecular Transport in Liquids and Gases." *J.Chem. Phys.* **31** *(1959) 1164.*

[12] R. DiFoggio and R. Gomer, "Diffusion of Hydrogen and Deuterium on the (110) Plane of Tungsten." *Phys. Rev.* **25** *(1982) 3490.*

[13] D.A. Reed and G. Ehrlich, "Surface Diffusion, Atomic Jump Rates and Thermodynamics." *Surface Sci.* **102** *(1981) 588.*

[14] M. Gesley and L.W. Swanson, "Nature of Diffusion Coefficients and Their Relation to Field Emission Noise." *Surface Sci.* In press.

[15] E.M. Lifshitz and L.P. Pitaevskii, " *Statistical Physics* " *3rd ed. part 1 (Pergamon Press, Oxford 1980).*

[16] S. Chandrasekhar, "Stochastic Problems in Physics and Astronomy." *Rev. Mod. Physics* **15** *(1943) 1.*

[17] J. Topping, "On the Mutual Potential Energy of a Network of Doubles." *Proc. Roy. Soc.* **A114** *(1927) 67.*

[18] J. Beben, Ch. Kleint, and R. Meclewski, "Activation Energy of Field Emission Flicker Noise Power Due to Adsorbed Potassium on Tungsten." *Surface Sci.* **93** *(1980) 33.*

[19] L. Schmidt and R. Gomer, "Adsorption of Potassium on Tungsten." *J. Chem. Phys.* **42** *(1965) 3573.*

[20] R. Meclewski, "Measurement of the Surface Diffusion Activation Energy of Potassium on Tungsten." *Acta Phys. Polon.* **A37** *(1970) 41.*

[21] J.-R. Chen and R. Gomer, "Mobility and Two-Dimensional Compressibility of Xe on the (110) Plane of Tungsten." *Surface Sci.* **94** *(1980) 456.*

IV. Field Emission Flicker Noise - Grand Canonical Ensemble.

We shall not cease from exploration
And the end of all our exploring
Will be to arrive where we started
And know the place for the first time.
T.S Eliot *FourQuartets*

A. Introduction.

Many flicker $1/f$ noise theories work within a canonical ensemble such as chapter I, where it was assumed that the total number of adatoms on a single (hkl) plane is kept constant. The grand canonical ensemble (GCE) has received relatively little attention. Here this means the total adatom number is allowed to fluctuate about a mean value. The present chapter provides the first divergence free spectral density function for equilibrium fluctuations within this ensemble. The theory will be used to explain experimental measurements of the noise spectrum of a tungsten thermal field emitter [1]. This is the only experimental study that exists with which a comparison can be made. Although not all aspects of the theory can be tested in detail it is shown that almost every characteristic of the experimental spectra can be explained. Furthermore the analysis extracts new information from this data by specifying precise relationships between probe and net plane geometries, the diffusion

coefficient, and the spectral density function. The theory is not only formally complete; and by this I mean all significant consequences are derived from a few basic postulates, are consistent with them, and the resulting formulas calculable; but it is also possible to measure every physical variable that appears in the theory. While the primary interest is with the relation of surface density fluctuations to field emission noise the model is applicable to any diffusive system linearly related to the observed experimental variable and characterized by a GCE. Thus it is possible to imagine experiments involving, e.g. an Auger microprobe to which this analysis might be applied given the appropriate system. The noise analysis introduces a new method for studying equilibrium mass transport properties of thermal field emitters in the temperature range $\sim$ 800 - 1300K, which is not readily accessible by other methods. Diffusion studies involving field ion microscopy typically operate at temperatures between 250-400K whereas macroscopic nonequilibrium tip blunting and build up experiments run from $\sim$ 1500 - 2500K. These methods measure respectively diffusion activation energy and defect vacancy formation energetics. Both of these properties are derived by applying the analysis presented in this chapter to the measured noise spectra. The good agreement with the values found by the other methods provides a strong argument in support of the theory. The nature of the noise spectrum is explained by including boundary, adatom lifetime, and geometrical effects.

This chapter incorporates several aspects of two previous spectral analyses of diffusion models within a GCE. To my knowledge these are the only two papers that evaluate such systems. Voss and Clarke (VC) studied temperature induced resistance fluctuations. Temperature fluctuations are formally equivalent to the present problem as both are based on a diffusion mechanism [2]. VC suggested a very useful approximation of a double space integration of the two point frequency correlation

$C(|\vec{x}_1 - \vec{x}_2|, \omega)$ that yields a proportionality between the noise spectrum, the point-frequency correlation function, and the number of correlated volumes $N_c(\omega)$, $S(\omega) \propto N_c^{-1}(\omega)\, C(x=0, \omega)$. The correlated volume is essentially defined as the r.m.s distance a fluctuation will diffuse during time ω^{-1}. The result is important because $C(x=0, \omega)$ is calculable and hence an approximate expression can be given for $S(\omega)$ itself, which is the experimentally accessible function. VC's suggestion is verified in section E where an explicit derivation is provided based on Fourier decomposition of the fluctuating probe current $i(t)$.

An outstanding problem concerning divergent normalization of the total noise power found by VC for $d < 3$ dimensions is solved. This problem actually occurs for $d \leq 3$ and is shown to be the result of two factors. One is by their omission of a fluctuation lifetime τ, which must appear in the diffusion equation. The necessity of including this term is required for equilibrium to be maintained. This is proved in section C by calculating a balance equation involving the rate of creation, the average lifetime of a fluctuation, and $< (\delta N)^2 >$. The second source of the problem comes, somewhat surprisingly, from the correlated volume construction used to approximate the double space integration of $C(|\vec{x}_1 - \vec{x}_2|, \omega)$. Analysis of the k-space correlation $C(\vec{k}, \omega)$ requires the imposition of an upper bound on the magnitude of physically allowable $\vec{k}$-vectors. Equivalently a lower limit must exist on the minimum length scale over which a fluctuation can be uncorrelated with itself at a given frequency. Otherwise an infinite spatial subdivision takes place that would lead to the unphysical situation of an individual fluctuation being distinguished from itself. This leads to a novel method of measuring the resolution of the field emission microscope from the noise spectrum.

While VC considered the effect of probe spatial averaging on $S(\omega)$, whose influence is contained in the number of correlated volumes $N_c(\omega)$, boundary effects due to sample geometry were not included. These enter through the term $C(x=0, \omega)$. Bliek has attempted a calculation of this function [3]; however several problems exist with his analysis, all of which are corrected here. The most important is that $C(x=0, \omega)$ is incorrectly identified as being $S(\omega)$ itself, thereby ignoring probe averaging effects altogether. The complementary parts of the theory excluded by Voss and Clarke are incorporated in the present work. Section D proves that, contrary to Bliek's claim, a multidimensional version of Carson's theorem can be stated and applied to a bounded region in a manner similar to the case of infinite sample size. This avoids Bliek's ad hoc construction of $C(x=0, \omega)$, which is also based on an incorrect formulation of the bounded fundamental solution to the diffusion equation. In spite of these difficulties Bliek's general conclusion that $S(\omega) \propto \omega^{-1}$ occurs when the thickness of the sample is small compared to its other dimensions is, with some qualifications concerning probe geometry, still true. A divergent low frequency noise power is also found in Bliek's study. He attempted to solve this problem by arbitrarily introducing a low frequency correlation term, but this factor has no direct physical significance. Again I show the the problem arises from omission of the fluctuation lifetime τ factor. Bliek's principal contribution to the present work is the suggestion Carson's theorem is related to the analysis of Langevin-type diffusion equations.

The chapter begins with the field emission autocorrelation function derived in chapter I. Evaluation of the two point time delayed covariance of the density $< \delta n(\vec{x}_1, t)\, \delta n(\vec{x}_2, 0) >$ marks the departure from the canonical ensemble theory. The fluctuation dynamics are given in section B by a stochastic diffusion equation of the Langevin-type. The solution to this equation is developed in terms of convolution

products that provide a compact formulation convenient for Fourier analysis. The contribution of the inhomogeneous source term requires evaluation of the statistics of Poisson impulses, which is carried out in section C. Using a calculation method developed by Rice [4] proofs are given for the first and second order statistics of the impulse functions. The spectral density is constructed from the multidimensional version of Carson's theorem and the results of the previous sections are then combined to give the integral equation for the spectrum of field emission current fluctuations. The double space integration of $C(\ |\vec{x}_1 - \vec{x}_2|\ , \omega)$ is then approximated using the correlated volume construction in section E, which reduces the problem to a calculation of $C(\ x=0\ , \omega)$. The explicit form of $C^{\infty}(\ x=0\ , \omega)$ is given, which is the point-frequency correlation excluding boundary effects. Several methods are proposed for extracting the diffusion coefficient D from it. The influence of the net plane boundary is contained in $C(\ \vec{x}=0,\ \omega)$ and this is evaluated in section F.

The development of $S(\omega)$ including boundary and lifetime effects is completed in section G and yields the first equilibrium diffusivity analysis of a thermal field emitter noise measurement. The reader who wishes to see how the theory is applied in practice may go directly to this section. Knowledge of the characteristics of $S(\omega)$ provides the most direct method of determining the surface diffusion coefficient and reveals probe and net plane geometry effects, particularly those due to thermal field buildup, i.e. growth of net planes due to a combination of electric field stress and thermal diffusivity of the atoms that tends to displace them from their initial equilibrium positions. Also the defect formation activation energy is derived. Besides revealing the energetics for both defect adatom formation and diffusion the theory also presents a new method for measuring the resolution of the field emission microscope. This has potential practical application as it means the virtual source size can be obtained,

which is an important variable in the development of finely focused charged particle beams. The section concludes with a discussion of the optimum probe-sample geometry for $S(\omega) \propto \omega^{-1}$ over the widest frequency band allowable by the diffusion model. Section H provides a general summary of the chapter.

B. Stochastic diffusion equation.

The field emission autocorrelation function is given by Eq.(I.11) as

$$R(t) = C_{FN} \int\int < \delta n(\vec{r}_1, t)\, \delta n(\vec{r}_2, 0) > d\vec{r}_1\, d\vec{r}_2. \qquad \text{(IV.1)}$$

Eq.(1) is where the present work diverges from the canonical ensemble theory of Chapter I. The present chapter reinterprets this equation in two ways. First, integration extends over a probed volume $V_p = A_p\, l_z$, where the volume encloses the surface by addition of a depth l_z on the order of several lattice constants of the substrate. Second, a defect vacancy-adatom creation-recombination mechanism is invoked that results from surface free energy minimization. The fluctuation in local density $\delta n(\vec{r}, t)$ then occurs through a combination of both diffusive motion and finite adatom lifetime effects.

For later reference it is noted that Eq.(1) can be written

$$R(t)/C_{FN} = \int\int < n(\vec{r}_1, t)\, n(\vec{r}_2, 0) > d\vec{r}_1\, d\vec{r}_2 - < N >^2. \qquad \text{(IV.2)}$$

Results on Poisson impulses in section C will clarify the need for this equation.

The situation in one dimension is considered first to lay necessary groundwork for extension to three dimensions. If a single adatom is created at $\mathbf{x}_j \in [0,L_x]$ at time $\mathbf{t}_j$ then the local one dimensional density $n_j(x,t)$ must satisfy,

$$\left[\frac{\partial}{\partial t} - D\,\frac{\partial^2}{\partial x^2} + \tau^{-1}\right] n_j(x,t) = \delta(x-\mathbf{x}_j)\,\delta(t-\mathbf{t}_j). \qquad \text{(IV.3)}$$

The necessity of including the average lifetime τ to maintain equilibrium will be shown in later sections. This point has not been addressed in any other fluctuation theory I am presently aware of. The use of a bold variable, e.g. $\mathbf{x}_j$, denotes a random variable, whose statistics will be clarified as the discussion progresses. The solution to Eq.(3) is

$$n_j(x,t) = e^{-(t-\mathbf{t}_j)/\tau}\; n_j^o(x,t), \qquad \text{(IV.4)}$$

where $n_j^o(x,t)$ solves

$$\left[\frac{\partial}{\partial t} - D\,\frac{\partial^2}{\partial x^2}\right] n_j^o(x,t) = \delta(x-\mathbf{x}_j)\,\delta(t-\mathbf{t}_j). \qquad \text{(IV.5)}$$

The bounded fundamental solution to Eq.(5) is

$$n_j^o(x,t) = \frac{1}{\sqrt{4\pi D(t-\mathbf{t}_j)}} \sum_{n=-\infty}^{\infty} \left\{ e^{\frac{-(x-\mathbf{x}_j+2nL_x)^2}{4D(t-\mathbf{t}_j)}} \pm e^{\frac{-(x+\mathbf{x}_j+2nL_x)^2}{4D(t-\mathbf{t}_j)}} \right\}, \qquad \text{(IV.6)}$$

where $+(-)$ represents reflecting (absorbing) boundaries. To retain clarity only reflecting boundaries are initially considered. The question of whether absorbing boundaries modify the noise characteristics is addressed in sections C and D.

That τ does act as an average lifetime follows from

$$p_j(t) = \int n_j(x,t)\,dx, \qquad \text{(IV.7)}$$

which is the probability that the particle created at $(\mathbf{x}_j,\mathbf{t}_j)$ still exists at time t.

Evaluating the integral for either a bounded or unbounded interval leads to

$$p_j(\ t\ ) = e^{-(t-\mathrm{t}_j)/\tau}. \tag{IV.8}$$

Eq.(8) expresses conservation of particle number.

It is further assumed that adatom creation, occurring by the defect vacancy mechanism, is a random process whereby Poisson statistics govern the number of events in a given time interval. The density $n(x,t)$ then solves,

$$\left(\frac{\partial}{\partial t} - D\frac{\partial^2}{\partial x^2} + \tau^{-1}\right) n(x,t) = \sum_{j=-\infty}^{\infty} \left[\,\delta(x-\mathrm{x}_j)+\delta(x+\mathrm{x}_j)\,\right]\delta(t-\mathrm{t}_j), \tag{IV.9}$$

where the t_j are uniformly distributed in time and uncorrelated with the x_j, which themselves are uniformly distributed in $[\,0, L_x\,]$. The presence of the second source term on the right side of Eq.(9) will be useful in writing a compact solution convenient for subsequent Fourier analysis, but otherwise does not affect the validity of the fundamental solution. The index j is to be understood as a label only and not as being representative of any particular ordering of the random variables.

The solution to Eq.(9) is now of the form

$$n(x,t) = \sum_{j=-\infty}^{\infty} n_j(x,t). \tag{IV.10}$$

By defining the double convolution of two functions $f(x,t)$ and $g(x,t)$ as

$$f^{**}g = \int_{-\infty}^{\infty} dv \int_{-\infty}^{\infty} dw\, f(v,w)\, g(x-v,t-w),$$

Eq.(10) becomes

$$n(x,t) = \mathrm{Z}_+(x,t)^{**}e^{-t/\tau}\, G(x,t) \qquad \left(\,0 \le x \le L_x\,,\ t \ge \tau\,\right), \tag{IV.11}$$

where

$$\mathbf{Z}_+(x,t) = \sum_{j=-\infty}^{\infty} \left[\delta(x-\mathbf{x}_j)+\delta(x+\mathbf{x}_j)\right] \delta(t-\mathbf{t}_j) \qquad \left(\mid x \mid \leq L_x \right) \text{(IV.12)}$$

and

$$G(x,t) = (4\pi Dt)^{-1/2} \sum_{n=-\infty}^{\infty} e^{-(x-2nL_x)^2/4Dt}. \qquad \text{(IV.13)}$$

Note that the domain of definition for Eqs.(11) and (12) is restricted. This also carries through into the three dimensional formulation and is important when calculating several of the convolution products below. Ignoring these restrictions can lead to divergences in otherwise apparently well behaved expressions. From an abstract viewpoint Eq.(11) is composed of periodic functions of x via Eq.(6). For a derivation that reflects this aspect see, e.g. reference [6]. However from a physical or probabilistic standpoint the fluctuations must be restricted to the interval $[0, L_x]$. Interestingly there appears to be only one derivation of Eq.(6), for the case of absorbing boundaries, which assumes this probabilistic viewpoint [7].

Derivation of Eq.(11).

$$\mathbf{Z}_+(x,t) ** e^{-t/\tau} G(x,t) = \int_{-\infty}^{\infty} dv \int_{-\infty}^{t} dw\, e^{-(t-w)/\tau}\, G(x-v,t-w)\, \mathbf{Z}_+(v,w)$$

$$= \int dv \int dw \left\{ e^{-(t-w)/\tau} \left[4\pi D(t-w)\right]^{-1/2} \sum_{n=-\infty}^{\infty} e^{-(x-v-2nL_x)^2/4D(t-w)} \right\}$$

$$\times \left\{ \sum_{j=-\infty}^{\infty} \delta(w-\mathbf{t}_j) \left[\delta(v-\mathbf{x}_j) + \delta(v+\mathbf{x}_j) \right] \right\}$$

$$= \sum_{j=-\infty}^{\infty} e^{-(t-\mathbf{t}_j)/\tau} \left[4\pi D(t-\mathbf{t}_j) \right]^{-1/2} \sum_{n=-\infty}^{\infty} \left\{ e^{\frac{-(x-\mathbf{x}_j-2nL_x)^2}{4D(t-\mathbf{t}_j)}} + e^{\frac{-(x+\mathbf{x}_j-2nL_x)^2}{4D(t-\mathbf{t}_j)}} \right\}$$

$$= \sum_{j=-\infty}^{\infty} e^{-(t-\mathbf{t}_j)/\tau}\, n_j^o(x,t) = \sum_{j=-\infty}^{\infty} n_j(x,t) = n(x,t). \qquad Q.E.D.$$

Eq.(13) is reducible to

$$G(x,t) = f(x) * F(x,t) \tag{IV.14}$$

where

$$f(x) = \sum_{m=-\infty}^{\infty} \delta(x-2mL_z) \tag{IV.15}$$

and

$$F(x,t) = (4\pi Dt)^{-1/2} \; e^{-x^2/4Dt}. \tag{IV.16}$$

All statistical information resides in $\mathbf{Z}_+(x,t)$ as $G(x,t)$ is a deterministic function.

Derivation of Eq.(14)

$$f(x) * F(x,t) = \int_{-\infty}^{\infty} dv \left[\sum_{m=-\infty}^{\infty} \delta(v-2mL_z) \right] \times \left[(4\pi Dt)^{-1/2} e^{-(x-v)^2/4Dt} \right]$$

$$= (4\pi Dt)^{-1/2} \sum_{m=-\infty}^{\infty} e^{-(x-2mL_z)^2/4Dt} = G(x,t). \qquad Q.E.D.$$

Using Eq.(14), (11) can be written

$$n(x,t) = \mathbf{Z}_+(x,t) ** e^{-t/\tau} \left[f(x) * F(x,t) \right]. \tag{IV.17}$$

By defining

$$\mathbf{Z}_*(x,t) \equiv \mathbf{Z}_+(x,t) * f(x) = \sum_{m=-\infty}^{\infty} \mathbf{Z}_+(x-2mL_z, t) \tag{IV.18}$$

Eq.(17) becomes

$$n(x,t) = \mathbf{Z}_*(x,t) ** e^{-t/\tau} F(x,t). \tag{IV.19}$$

Note that Eq.(19), which is the bounded fundamental solution to Eq.(9), is cast in a

form involving the unbounded solution $F(x,t)$. This will substantially reduce the complexity of later Fourier analysis.

Derivation of Eq.(19)

$$\mathbf{Z}_*(x,t)^{**}e^{-t/\tau}F(x,t) = \int_{-\infty}^{t} dw \int_{-\infty}^{\infty} \mathbf{Z}_*(v,w)\, e^{-(t-w)/\tau} F(x-v,t-w)\, dv$$

$$= \int\int \left\{ \sum_m \mathbf{Z}_+(v-2mL_x,w) \right\} \times \left\{ e^{-(t-w)/\tau} \left[4\pi D(t-w) \right]^{-1/2} e^{\frac{-(x-v)^2}{4D(t-w)}} \right\} dv\, dw$$

$$= \int \left\{ \sum_m \sum_j \left[\delta(v-2mL_x-\mathbf{x}_j) + \delta(v-2mL_x+\mathbf{x}_j) \right] \delta(w-\mathbf{t}_j) \right\}$$

$$\times \left\{ \frac{1}{\sqrt{4\pi D(t-w)}}\, e^{-(t-w)/\tau}\, e^{\frac{-(x-v)^2}{4D(t-w)}} \right\}$$

$$= \sum_{m,j} e^{-(t-\mathbf{t}_j)/\tau} \left[4\pi D(t-\mathbf{t}_j) \right]^{-1/2} \left\{ e^{\frac{-(x-2mL_x+x_i)^2}{4D(t-\mathbf{t}_j)}} + e^{\frac{-(x-2mL_x-x_i)^2}{4D(t-\mathbf{t}_j)}} \right\}$$

$$= \sum_j e^{-(t-\mathbf{t}_j)/\tau} n_j^o(x,t) = n(x,t). \qquad Q.E.D.$$

The multidimensional formulation of the above equations is now developed. Assuming a cartesian coordinate system, the three dimensional solution of the diffusion equation

$$\left(\frac{\partial}{\partial t} - D\nabla^2 + \tau^{-1} \right) n_j(\vec{x},t) = \delta(\vec{x}-\vec{\mathbf{x}}_j)\,\delta(t-\mathbf{t}_j) \qquad \text{(IV.20)}$$

is

$$n_j(\vec{x},t) = e^{-(t-\mathbf{t}_j)/\tau} \prod_{i=1}^{3} n_j^o(x_i,t) = \prod_{i=1}^{3} n_j(x_i,t), \qquad \text{(IV.21)}$$

where $n_j^o(x_i,t)$ is given by Eq.(6).

The multidimensional version of Eq.(9) is then

$$\left(\frac{\partial}{\partial t} - D\nabla^2 + \tau^{-1} \right) n(\vec{x},t) = \mathbf{Z}_+(\vec{x},t), \qquad \text{(IV.22)}$$

where

$$\mathbf{Z}_+(\vec{x},t) \equiv \sum_{j=-\infty}^{\infty} \delta(t-\mathrm{t}_j) \prod_{i=1}^{3} \Big[\delta(x_i - \mathbf{x}_{ji}) + \delta(x_i + \mathbf{x}_{ji}) \Big], \tag{IV.23}$$

and

$$n(\vec{x},t) = \sum_{j=-\infty}^{\infty} n_j(\vec{x},t). \tag{IV.24}$$

Eq.(24) can then be expressed as

$$n(\vec{x},t) = \mathbf{Z}_+(\vec{x},t) \;** \; G(\vec{x},t)\, e^{-t/\tau}, \tag{IV.25}$$

where

$$G(\vec{x},t) = \prod_{i=1}^{3} G(x_i,t) \tag{IV.26}$$

and $G(x_i,t)$ is given by Eq.(13).

Derivation of Eq.(25)

$$\mathbf{Z}_+(\vec{x},t) \;** \; e^{-t/\tau} G(\vec{x},t) =$$

$$\int_{-\infty}^{t} dT \prod_{i=1}^{3} \int_{-L_i}^{L_i} dw_i \sum_{j=-\infty}^{\infty} \delta(T-\mathrm{t}_j) \Big[\delta(w_i - \mathbf{x}_{ji}) + \delta(w_i + \mathbf{x}_{ji}) \Big] e^{-(t-T)/\tau}$$

$$\times \Big[4\pi D(t-T) \Big]^{-1/2} \sum_{n_i=-\infty}^{\infty} e^{\frac{-(x_i - w_i - 2n_i L_i)^2}{4D(t-T)}}$$

$$= \sum_j e^{-(t-\mathrm{t}_j)/\tau} \prod_{i=1}^{3} \sum_{n_i} \Big[4\pi D(t-\mathrm{t}_j) \Big]^{-1/2} \left\{ e^{\frac{-(x_i - \mathbf{x}_{ji})}{4D(t-\mathrm{t}_j)}} + e^{\frac{-(x_i + \mathbf{x}_{ji})}{4D(t-\mathrm{t}_j)}} \right\}$$

$$= \sum_j e^{-(t-\mathrm{t}_j)/\tau} \prod_{i=1}^{3} n_j^o(x_i,t) = \sum_j n_j(\vec{x},t) = n(\vec{x},t). \qquad Q.E.D.$$

Eq.(26) is of the form

$$G(\vec{x},t) = f(\vec{x}) * F(\vec{x},t), \tag{IV.27}$$

where

$$f(\vec{x}) \equiv \sum_{|\vec{n}|=-\infty}^{\infty} \delta(\vec{x}-2\vec{L}_m), \tag{IV.28}$$

$\vec{L}_m \equiv (n_x L_x, n_y L_y, n_z L_z)$ with (L_x, L_y, L_z) being the dimensions of the bounding surface volume, and

$$F(\vec{x},t) \equiv (4\pi Dt)^{-3/2}\, e^{-|\vec{x}|^2/4Dt}. \tag{IV.29}$$

Derivation of Eq.(27)

$$f(\vec{x}) * F(\vec{x},t) = (4\pi Dt)^{-3/2} \prod_{i=1}^{3} \sum_{n_i=-\infty}^{\infty} \int_{-\infty}^{\infty} dv_i\ \delta(v_i - 2n_i L_i)\ e^{-(x_i-v_i)^2/4Dt}$$
$$= (4\pi Dt)^{-3/2} \prod_{i=1}^{3} \sum_{n_i=-\infty}^{\infty} e^{-(x_i-2nL_i)^2/4Dt} = G(\vec{x},t). \qquad Q.E.D.$$

Combining Eqs.(25) and (27) yields

$$n(\vec{x},t) = \mathbf{Z}_*(\vec{x},t) \;**\; e^{-t/\tau} F(\vec{x},t), \tag{IV.30}$$

where

$$\mathbf{Z}_*(\vec{x},t) \equiv \mathbf{Z}_+(\vec{x},t) * f(\vec{x}) = \sum_{|\vec{n}|=-\infty}^{\infty} \mathbf{Z}_+(\vec{x}-2\vec{L}_m). \tag{IV.31}$$

Derivation of Eq.(31)

$$\mathbf{Z}_+(\vec{x},t) * f(\vec{x}) =$$
$$\left\{ \sum_{j=-\infty}^{\infty} \delta(t-\mathbf{t}_j) \prod_{i=1}^{3} \left[\delta(x_i - \mathbf{x}_{ji}) + \delta(x_i + \mathbf{x}_{ji}) \right] \right\} * \left\{ \prod_{i=1}^{3} \sum_{n_i=-\infty}^{\infty} \delta(x_i - 2n_i L_i) \right\}$$
$$= \sum_j \left[\delta(t-\mathbf{t}_j) \prod_{i=1}^{3} \sum_{n_i=-\infty}^{\infty} \delta(x_i - \mathbf{x}_{ji} - 2n_i L_i) + \delta(x_i + \mathbf{x}_{ji} - 2n_i L_i) \right]$$
$$= \sum_{|\vec{n}|} \mathbf{Z}_+(\vec{x}-2\vec{L}_m) = \mathbf{Z}_*(\vec{x},t) \qquad Q.E.D.$$

Derivation of Eq.(30)

$$\mathbf{Z}_*(\vec{x},t) \;** e^{-t/\tau}F(\vec{x},t) = \sum_{|\vec{n}|=-\infty}^{\infty} \mathbf{Z}_+(\vec{x}-2\vec{L}_m) \;** e^{-t/\tau}(4\pi Dt)^{-3/2}\, e^{-|\vec{x}|^2/4Dt}$$

$$= \sum_{|\vec{n}|}\sum_{j} \delta(t-\mathbf{t}_j)\prod_{i=1}^{3}\left[\delta(x_i-\mathbf{x}_{ji}-2n_iL_i)+\delta(x_i+\mathbf{x}_{ji}-2n_iL_i)\right] \;** e^{-t/\tau}(4\pi Dt)^{-3/2}\prod_{i=1}^{3} e^{-x_i^2/4Dt}$$

$$= \sum_{|\vec{n}|}\sum_{j}\int dT \prod_{i=1}^{3}\int dw_i\, \delta(T-\mathbf{t}_j)\left[\,\delta(w_i-\mathbf{x}_{ji}-2nL_i)+\delta(w_i+\mathbf{x}_{ji}-2n_iL_i)\right]$$

$$\times\, e^{-(t-T)/\tau}\left[4\pi D(t-T)\right]^{-3/2}\, e^{-(x_i-w_i)^2/4Dt}$$

$$= \sum_{|\vec{n}|}\sum_{j} e^{-(t-\mathbf{t}_j)/\tau}\left[4\pi D(t-\mathbf{t}_j)\right]^{-3/2}\prod_{i=1}^{3}\left\{e^{\frac{-(x_i-\mathbf{x}_{ji}-2n_iL_i)^2}{4D(t-\mathbf{t}_j)}}+e^{\frac{-(x_i+\mathbf{x}_{ji}-2n_iL_i)^2}{4D(t-\mathbf{t}_j)}}\right\}$$

$$= \sum_{j} e^{-(t-\mathbf{t}_j)/\tau}\prod_{i=1}^{3} n_j^o(x_i,t) = n(\vec{x},t). \qquad Q.E.D.$$

1. Summary of section B.

A model has been postulated for describing density fluctuations in a grand canonical ensemble. The density fluctuations obey the stochastic differential equation

$$\left(\frac{\partial}{\partial t} - D\nabla^2 + \tau^{-1}\right) n(\,\vec{x},t\,) = \mathbf{Z}_+(\,\vec{x},t\,), \tag{IV.22}$$

where $\mathbf{Z}_+(\vec{x},t)$ is an infinite sum of Poisson impulses. The solution to this equation is compactly written

$$n(\vec{x},t) = \mathbf{Z}_*(\vec{x},t) \;** e^{-t/\tau}F(\vec{x},t), \tag{IV.30}$$

where $\mathbf{Z}_*(\vec{x},t)$ is a second set of Poisson impulses. The form of Eq.(30) will be useful in the subsequent Fourier analysis where the spectral density function is derived. Before proceeding to this it is necessary to develop further the statistics of Poisson impulses, which is done in the following section. Finally it is noted that, in contrast to Eq.(30), Bliek's proposed fundamental solution [3] is not correct as the boundary conditions are not satisfied.

C. Statistics of Poisson impulses.

A combination of defect adatom creation, diffusion, and annihilation is postulated as a physical mechanism for thermal field emission noise. The present stochastic analysis, based on a Langevin-type diffusion equation, places surface density fluctuations in a grand canonical ensemble. Specifically the total number of net excess adatoms is allowed to fluctuate about a steady state value. The stochastic assumption is embodied in the sum of Poisson impulses $\mathbf{Z}_+(\vec{r},t)$, Eq.(23), which is composed of uncorrelated and uniformly distributed random variables $\mathbf{x}_j$ and $\mathbf{t}_j$. The uniformity and uncorrelatedness of their distributions is an assumed property of the adatom creation process.

The purpose of this section is to derive the first and second order statistics of $\mathbf{Z}_+(\vec{r},t)$. The goal, as developed in the following section, is to calculate the spectral density from Eq.(2). The calculational method used in the present section is similar to Rice's proof of Campbell's theorem [4].

The statistics of a one dimensional point process consisting of Poisson distributed impulses are calculated first and then the results are extended to the multidimensional cases involving $\mathbf{Z}_*(\vec{r}\,,\,t\,)$ and $\mathbf{Z}_+(\vec{r}\,,\,t\,)$. The technique is to first consider $\mathbf{k}$ events, e.g. $\mathbf{t}_k$, in an interval $[\,-T/2,\ T/2\,]$ and averaged with respect to the uniformly distributed $\mathbf{t}_k$. The resultant quantity is then averaged with respect to the random variable $\mathbf{k}$, which by assumption has a Poisson distribution

$$p(\,\mathbf{k}\,) = \frac{(\lambda\, T)^k}{k!}\, e^{-\lambda T}\,. \tag{IV.32}$$

The term $p(\mathbf{k})$ is the probability k events occur at a rate λ in the interval of

duration T. Later the interval is extended over the entire time axis. This is a standard method of Fourier analysis, however in the case of the $\mathbf{x}_j$ the interval will be taken as the volume V_p, which will in general remain finite.

Given exactly **k** events occur in $[-T/2,\ T/2]$ then define

$$\mathbf{Z}_k(t) = \sum_{j=1}^{\mathbf{k}} \delta(t - \mathbf{t}_k) \tag{IV.33}$$

and average Eq.(33) with respect to the uniformly distributed $\mathbf{t}_k$'s,

$$<\mathbf{Z}_k(t)>_{t_i} = <\sum_{j=1}^{\mathbf{k}} \delta(t-\mathbf{t}_k)> = \sum_{j=1}^{\mathbf{k}} \left[\frac{1}{T} \int_{-T/2}^{T/2} \delta(t-\mathbf{t}_k)\, d\mathbf{t}_k \right] = \frac{\mathbf{k}}{T}. \tag{IV.34}$$

Eq.(34) is now averaged with respect to the random variable **k**

$$<\mathbf{Z}(t)> = << \mathbf{Z}_k(t) >_{t_i}>_k = \frac{<\mathbf{k}>}{T}.$$

It follows from the Poisson distribution, Eq.(32), that

$$<\mathbf{k}> = \sum_{k=0}^{\infty} k\ \frac{(\lambda T)^k}{k!}\ e^{-\lambda T} = \lambda T.$$

Therefore

$$<\mathbf{Z}(t)> = \lambda, \tag{IV.35}$$

which is just a special case of Campbell's theorem. Papoulis has proved Eq.(35) by another method [8].

To calculate the autocorrelation $R_{zz}(t_1,t_2) \equiv <\mathbf{Z}(t_1)\ \mathbf{Z}(t_2)>$ one starts by assuming **k** events occur in the time interval $[-T/2,\ T/2]$. Then it follows that

$$<\mathbf{Z}_k(t_1)\ \mathbf{Z}_k(t_2)>_{t_i} = <\left[\sum_{j=1}^{k} \delta(\ t_1 - \mathbf{t}_j\ )\right]\left[\sum_{m=1}^{k} \delta(\ t_2 - \mathbf{t}_m\ )\right]>_{t_i}$$

$$= \mathbf{k} < \delta(t_1 - \mathbf{t}_j)\,\delta(t_2 - \mathbf{t}_j) >_{t_i} + (\mathbf{k}^2 - \mathbf{k}) < \delta(t_1 - \mathbf{t}_j)\,\delta(t_2 - \mathbf{t}_m) >_{t_i} \qquad (j \neq m)$$

$$= \frac{\mathbf{k}}{T} \int_{-T/2}^{T/2} \delta(t_1 - t)\,\delta(t_2 - t)\,dt + \frac{(\mathbf{k}^2 - \mathbf{k})}{T^2} \int_{-T/2}^{T/2} \int_{-T/2}^{T/2} \delta(t_1 - s)\,\delta(t_2 - w)\,ds\,dw$$

$$= \frac{\mathbf{k}}{T}\,\delta(t_1 - t_2) + \frac{(\mathbf{k}^2 - \mathbf{k})}{T^2},$$

i.e., the autocorrelation is

$$R_{zz}(t_1, t_2) = < \mathbf{Z}(t_1)\ \mathbf{Z}(t_2) >_k = \frac{< \mathbf{k} >}{T}\,\delta(t_1 - t_2) + \frac{< \mathbf{k}^2 - \mathbf{k} >}{T^2}.$$

The second moment of $\mathbf{k}$,

$$< \mathbf{k}^2 > = e^{-\lambda T} \sum_{k=0}^{\infty} k^2 \frac{(\lambda T)^k}{k!} = (\lambda T)^2 + \lambda T,$$

is calculated with Eq.(32) as distribution function, which means

$$< \mathbf{k}^2 - \mathbf{k} > = (\,\lambda T\,)^2.$$

Then the autocorrelation function is

$$R_{zz}(t_1 - t_2) = \lambda\,\delta(t_1 - t_2) + \lambda^2, \tag{IV.36}$$

which is a special case of the second part of Campbell's theorem. R_{zz} is stationary since $R_{zz}(t_1, t_2) = R_{zz}(t_1 - t_2)$. Again an alternate method has been used by Papoulis to prove this result [8].

The arguments are now repeated for the space-time Poisson impulse function

$$\mathbf{Z}_+(\,\vec{x}\,,\,t\,) = \sum_{j=-\infty}^{\infty} \delta\,(t - \mathbf{t}_j) \prod_{i=1}^{3} \left[\,\delta\,(x_i - \mathbf{x}_{ji}) + \delta\,(x_i + \mathbf{x}_{ji})\right]. \tag{IV.23}$$

As before a time interval $[\,-T/2,\ T/2\,]$ is taken in which exactly $\mathbf{k}$ events occur, although now in the volume V_t

$$\mathbf{Z}_{+k}(\vec{x},t) = \sum_{j=1}^{k} \delta(t-\mathbf{t}_j)\left[\delta(\vec{x}-\vec{\mathbf{x}}_j) + \delta(\vec{x}+\vec{\mathbf{x}}_j)\right]$$

Averaging over the uncorrelated $\mathbf{t}_j$ and $\vec{\mathbf{x}}_j$ yields

$$<\mathbf{Z}_{+k}(\vec{x},t)>_{t_j,x_j} = \sum_{j=1}^{k} <\delta(t-\mathbf{t}_j)> \; <\left[\delta(\vec{x}-\vec{\mathbf{x}}_j) + \delta(\vec{x}+\vec{\mathbf{x}}_j)\right]>$$

$$= \frac{\mathbf{k}}{T}\int_{-T/2}^{T/2} \delta(t-\mathbf{t}_j)\, d\mathbf{t}_j \times \frac{1}{V_t}\int_{V_t} d\vec{\mathbf{x}}_j\left[\delta(\vec{x}-\vec{\mathbf{x}}_j) + \delta(\vec{x}+\vec{\mathbf{x}}_j)\right] = \frac{\mathbf{k}}{TV_t}.$$

Note $\int d\vec{\mathbf{x}}_j\, \delta(\vec{x}+\vec{\mathbf{x}}_j)=0$, as this set of impulses lies outside the volume V_t. Then

$$<\mathbf{Z}_{+}(\vec{x},t)>_k = << Z_{+k}(\vec{x},t)>_{x_k,t_k}>_k = \frac{<\mathbf{k}>}{T\,V_t} = \frac{\lambda}{V_t}. \qquad \text{(IV.37)}$$

The two point time delayed correlation is calculated in the same manner as for the simpler case that led to Eq.(36). Starting from its definition as,

$$R_{Z+}(\vec{x}_1,t_1;\vec{x}_2,t_2) \equiv <\mathbf{Z}_{+}(\vec{x}_1,t_1)\,\mathbf{Z}_{+}(\vec{x}_2,t_2)> = << \mathbf{Z}_{+k}(\vec{x}_1,t_1)\,\mathbf{Z}_{+k}(\vec{x}_2,t_2)>_{x_k,t_k}>_k \quad \text{(IV.38)}$$

the first average is calculated by fixing $\mathbf{k}$ events in $[-T/2,\ T/2]$

$$<\mathbf{Z}_{+k}(\vec{x}_1,t_1)\ \mathbf{Z}_{+k}(\vec{x}_2,t_2)>_{x_k,t_k} = <\left\{\sum_{j=1}^{k}\left[\delta(\vec{x}_1-\vec{\mathbf{x}}_j)+\delta(\vec{x}_1+\vec{\mathbf{x}}_j)\right]\delta(t_1-\mathbf{t}_j)\right\}\times$$

$$\left\{\sum_{l=1}^{k}\left[\delta(\vec{x}_2-\vec{\mathbf{x}}_l)+\delta(\vec{x}_2+\vec{\mathbf{x}}_l)\right]\delta(t_2-\mathbf{t}_l)\right]\Big\}>^{2}_{x_k,t_k}$$

$$= \mathbf{k} <\left[\delta(\vec{x}_1-\vec{\mathbf{x}}_j)+\delta(\vec{x}_1+\vec{\mathbf{x}}_j)\right]\times\left[\delta(\vec{x}_1-\vec{\mathbf{x}}_j)+\delta(\vec{x}_2+\vec{\mathbf{x}}_j)\right]>_{x_j}$$

$$\times <\delta(t_1-\mathbf{t}_j)\,\delta(t_2-\mathbf{t}_j)>_{t_j}$$

$$+(\mathbf{k}^2-\mathbf{k})<\delta(\vec{x}_1-\vec{\mathbf{x}}_j)+\delta(\vec{x}_1+\vec{\mathbf{x}}_j)>_{x_j} <\delta(\vec{x}_2-\vec{\mathbf{x}}_l)+\delta(\vec{x}_2+\vec{\mathbf{x}}_l)>_{x_l}$$

$$\times <\delta(t_1-\mathbf{t}_j)>_{t_j}<\delta(t_2-\mathbf{t}_l)>_{t_l} \quad (j\neq l).$$

Recalling $<\delta(\vec{x}+\vec{x}_j)>=0$, then

$$< \mathbf{Z}_{+k}(\vec{x}_1,t_1)\ \mathbf{Z}_{+k}(\vec{x}_2,t_2) >_{x_i,t_i} =$$

$$\mathrm{k}<\delta(\vec{x}_1-\vec{x}_j)\ \delta(\vec{x}_2-\vec{x}_j)>_{x_j}<\delta(t_1-\mathrm{t}_j)\ \delta(t_2-\mathrm{t}_j)>_{t_j}$$

$$+(\mathrm{k}^2-\mathrm{k})<\delta(\vec{x}_1-\vec{x}_j)>^2_{x_j}<\delta(t_1-\mathrm{t}_j)>^2_{t_j}$$

$$=\frac{\mathrm{k}}{V_t T}\ \delta(\vec{x}_1-\vec{x}_2)\ \delta(t_1-t_2)+\frac{(\mathrm{k}^2-\mathrm{k})}{V_t^2 T^2}.$$

With this result Eq.(38) becomes

$$R_{Z_+}(\vec{x}_1-\vec{x}_2,t_1-t_2)=\frac{\lambda}{V_t}\ \delta(\vec{x}_1-\vec{x}_2)\ \delta(t_1-t_2)+\frac{\lambda^2}{V_t^2}, \qquad \text{(IV.39)}$$

by summing over the Poisson distributed $\mathbf{k}$.

The first and second order statistics of $\mathbf{Z}_+(\vec{x},t)$, Eqs.(37) and (39), are checked for consistency by combining them with the fundamental solution

$$n(\vec{x},t)=\mathbf{Z}_+(\vec{x},t)\ **\ e^{-t/\tau}\ G(\vec{x},t). \qquad \text{(IV.25)}$$

The mean value of Eq.(25) is calculated using Eq.(37) and recalling that all statistics reside in $\mathbf{Z}_+(\vec{x},t)$,

$$<n(\vec{x},t)>=<\mathbf{Z}_+(\vec{x},t)>\ **\ e^{-t/\tau}\ G(\vec{x},t). \qquad \text{(IV.40)}$$

Expanding the right hand side of Eq.(40)

$$<\mathbf{Z}_+(\vec{x},t)>\ **\ e^{-t/\tau}\ G(\vec{x},t)=\frac{\lambda}{V_t}\int_0^\infty dT\ e^{-T/\tau}\prod_{i=1}^{3}\int_{-L_i}^{L_i} d\,w_i\ G(w_i,T),$$

where the product form of $G(\vec{x},t)$, Eq.(26), is used. Combining this with Eq.(13) leads to

$$<\mathbf{Z}_+(\vec{x},t)>\ **\ e^{-t/\tau}\ G(\vec{x},t)=$$

$$= \frac{\lambda}{V_l} \int_0^\infty dT\ e^{-T/\tau} \prod_{i=1}^{3} (4\pi D\, T)^{-1/2} \int_{-L_i}^{L_i} d\, w \sum_{n=-\infty}^{\infty} e^{-(w - 2nL_i)^2/4DT}.$$

$$= \frac{8\lambda}{V_l} \int_0^\infty dT\ e^{-T/\tau} \prod_{i=1}^{3} (4\pi D\, T)^{-1/2} \int_{0}^{L_i} d\, w \sum_{n=-\infty}^{\infty} e^{-(w - 2nL_i)^2/4DT}. \qquad \text{(IV.41)}$$

By defining $y = (w - 2nL_i)/4Dt$, Eq.(41) becomes

$$< \mathbf{Z}_+(\vec{r}, t) > ** e^{-t/\tau}\, G(\vec{r}, t) =$$

$$\frac{8\lambda}{V_l} \int_0^\infty dT\ e^{-T/\tau} \prod_{i=1}^{3} \pi^{-1/2} \sum_{n=-\infty}^{\infty} \int_{-2np_i}^{(-2n+1)p_i} e^{-y^2}\, dy, \qquad \text{(IV.42)}$$

where $p_i \equiv L_i/\sqrt{4Dt}$. Performing the T integration converts Eq.(42) to

$$< \mathbf{Z}_+(\vec{r}, t) > ** e^{-t/\tau}\, G(\vec{r}, t) = \frac{8\lambda\tau}{V_l \pi^{3/2}} \prod_{i=1}^{3} \sum_{n=-\infty}^{\infty} \int_{-2np_i}^{(-2n+1)p_i} e^{-y^2}\, dy. \qquad \text{(IV.43)}$$

Now

$$\sum_{n=-\infty}^{\infty} \int_{-2np_i}^{(-2n+1)p_i} e^{-y^2}\, dy = \left\{ \int_0^{p_i} dy + \sum_{n=-1}^{-\infty} \int_{-2np_i}^{(-2n+1)p_i} dy + \sum_{n=1}^{\infty} \int_{-2n}^{(-2n+1)p_i} dy \right\} e^{-y^2}$$

$$= \left\{ \int_0^{p_i} dy + \sum_{n=1}^{\infty} \int_{2np_i}^{(2n+1)p_i} dy - \sum_{n=1}^{\infty} \int_{2np_i}^{(2n-1)p_i} dy \right\} e^{-y^2}$$

$$= \left\{ \int_0^{p_i} dy + \sum_{n=1}^{\infty} \int_{2np_i}^{(2n+1)p_i} dy + \int_{(2n-1)p_i}^{2np_i} dy \right\} e^{-y^2}$$

$$= \int_0^\infty e^{-y^2}\, d\, y = \frac{1}{2}\sqrt{\pi}. \qquad \text{(IV.44)}$$

Combining Eqs.(42) and (44),

$$< \mathbf{Z}_+(\vec{x},t) > \;**\; e^{-t/\tau}\, G(\vec{x},t) = \frac{\lambda\tau}{V_t}. \qquad \text{(IV.45)}$$

Comparing Eqs.(40) and (45) yields

$$< n > = \lambda\tau / V_t, \qquad \text{(IV.46)}$$

which agrees with the definition $< N > = \lambda\tau$. Eq.(46) shows that fluctuations with infinite lifetime in a finite size diffusive system do not lead to an equilibrium state. For a fixed density $< n >$ and rate λ there is a single lifetime τ that will result in equilibrium fluctuations. Until now no fluctuation theory based on the diffusion equation has included τ^{-1} in the diffusion operator, Eq.(3). The present results demonstrate the necessity of including this term.

The statistics of Eq.(39) are now checked by forming the two point density autocorrelation from the fundamental solution, Eq.(25),

$$< n(\vec{x}_1,t_1)\, n(\vec{x}_2,t_2) > =$$

$$< \left[\mathbf{Z}_+(\vec{x}_1,t_1) \;**\; e^{-t_1/\tau}\, G(\vec{x}_1,t_1) \right] \times \left[\mathbf{Z}_+(\vec{x}_2,t_2) \;**\; e^{-t_2/\tau}\, G(\vec{x}_2,t_2) \right] >. \qquad \text{(IV.47)}$$

The right hand side is calculated using Eq.(39),

$$< \mathbf{Z}_+(\vec{x}_1,t_1)\, \mathbf{Z}_+(\vec{x}_2,t_2) > \;**\; e^{-t_1/\tau}\, G(\vec{x}_1,t_1) \;**\; e^{-t_2/\tau}\, G(\vec{x}_2,t_2)$$

$$= \left\{ \frac{\lambda}{V_t}\, \delta(\vec{x}_1-\vec{x}_2)\, \delta(t_1-t_2) + \frac{\lambda^2}{V_t^2} \right\} **\; e^{-t_1/\tau}\, G(\vec{x}_1,t_1) \;**\; e^{-t_2/\tau}\, G(\vec{x}_2,t_2)$$

$$= \frac{\lambda}{V_t} \left[\delta(\vec{x}_1-\vec{x}_2)\, \delta(t_1-t_2) \;**\; e^{-t_1/\tau}\, G(\vec{x}_1,t_1) \right] **\; e^{-t_2/\tau}\, G(\vec{x}_2,t_2)$$

$$+ \frac{\lambda^2}{V_t^2} \left[\int_0^\infty dT\; e^{-T/\tau} \prod_{i=1}^{3} \int_{-L_i}^{L_i} dw_i\; G(w_i,T) \right]^2$$

$$= \frac{\lambda}{V_t} \int_0^\infty \delta(T-t_2)\, e^{-(t_1-T)/\tau} \prod_{i=1}^{3} \int_{-L_i}^{L_i} dw_i\; \delta(x_i-w_i-x_{2i})\; G(w_i,t_1-T)$$

$$** \; e^{-t_2/\tau} \, G(\overline{x}_2, t_2) + \frac{\lambda^2 \tau^2}{V_t^2}$$

$$= \frac{\lambda}{V_t} \left[e^{-(t_1 - t_2)/\tau} \prod_{i=1}^{3} G(x_{1i} - x_{2i}, t_1 - t_2) \right] ** \; e^{-t_2/\tau} \, G(\overline{x}_2, t_2) + < n >^2$$

$$= \frac{\lambda}{V_t} \left[e^{-(t_1 - t_2)/\tau} \, G(\overline{x}_1 - \overline{x}_2, t_1 - t_2) ** \; e^{-t_2/\tau} \, G(\overline{x}_2, t_2) \right] + < n >^2 \quad \text{(IV.48)}$$

Substituting Eq.(48) into Eq.(2) results in

$$R(t_1 - t_2)/C_{FN} = \quad \text{(IV.49)}$$

$$\frac{\lambda}{V_t} \int_{V_t} \int_{V_t} d\overline{x}_1 \, d\overline{x}_2 \, e^{-(t_1 - t_2)/\tau} \, G(\overline{x}_1 - \overline{x}_2, t_1 - t_2) ** \; e^{-t_2/\tau} \, G(\overline{x}_2, t_2) \quad (t_1 \geq t_2)$$

Eq.(49) is the general form of the field emission autocorrelation function in the grand canonical ensemble. It is stationary and hence consistent with the description of equilibrium fluctuations.

The frequency domain analysis will result in a simpler integral equation to be solved for the spectral density function. However the present line of derivation is continued further to demonstrate the consistency of the formalism and develop the total noise power P for the case $V_p = V_t$, which is derived by setting $t_1 = t_2$ in Eq.(49),

$$R(0, V_p = V_t)/C_{FN} =$$

$$\frac{\lambda}{V_t} \int_{V_t} d\overline{x}_2 \left[\int_{V_t} d\overline{x}_1 \, G(\overline{x}_1 - \overline{x}_2, 0) \right] ** \; e^{-t/\tau} \, G(\overline{x}_2, t). \quad \text{(IV.50)}$$

Noting that

$$G(\overline{x}_1 - \overline{x}_2, 0) = \delta(\overline{x}_1 - \overline{x}_2)$$

transforms Eq.(50) to

$$R(0, V_t = V_t)/C_{FN} = \frac{\lambda}{V_t} \int_{V_t} d\overline{x}_2 \left[1 ** \; e^{-t/\tau} \, G(\overline{x}_2, t) \right]$$

$$= \frac{\lambda}{V_t} \int_0^\infty dT \; e^{-T/\tau} \int_{V_t} d\vec{r}_2 \left[\prod_{i=1}^{3} \int_{-L_i}^{L_i} dw_i \; G(w_i, t) \right]$$

$$= \frac{8\lambda\tau}{V_t} \int_{V_t} d\vec{r}_2 \left[\prod_{i=1}^{3} \int_{0}^{L_i} dw_i \; g(w_i, t) \right]. \qquad \text{(IV.51)}$$

Substituting the results of the derivation of Eqs.(43) and (44) into (51) yields

$$R(0, V_p = V_t)/C_{FN} = \lambda\tau. \qquad \text{(IV.52)}$$

Eq.(52) shows the construction involving the Poisson impulse functions is consistent with the physical interpretation of

$$R(0, V_p = V_t) = <(\delta N)^2> = < N >. \qquad \text{(IV.53)}$$

The last equality assumes the adatoms behave ideally in the thermodynamic sense. This holds for a dilute system, i.e. one at low coverage, and is consistent with $\lambda\tau = < N >$. However the relation between R and $<(\delta N)^2>$ in Eq.(53) is a completely general one and suggests an extension of the definition of λ and τ so that

$$\lambda\,\tau \equiv <(\delta N)^2>, \qquad \text{(IV.54)}$$

which allows of the formalism to include fully interacting diffusive systems. This conjecture is tentatively assumed true. Calculation of the statistics depends on $\mathbf{x}_j$ and $\mathbf{t}_j$ being uniformly distributed and mutually uncorrelated. Therefore the conjecture Eq.(54) requires the creation-annihilation process not to be correlated with diffusive fluctuations in a fully interacting system. For this reason one expects that critical fluctuations are excluded in addition to the reasons given in chapter I. Otherwise fully interacting noncritical systems can be incorporated within the domain of the present theory. This procedure has been justified for the canonical ensemble using hydrodynamic fluctuation theory by Mazenko, Banavar, and Gomer [9].

A difference between the canonical and grand canonical ensembles is manifested by comparing Eqs.(I.34) and (53). In the canonical ensemble the noise power $P(A_p = A_t) = 0$, whereas Eq.(53) shows that the noise power is nonzero even when the probed and net plane regions are equal. Physically this is because fluctuations are caused by the creation - recombination mechanism even in the absence of diffusive mass transport into and out of the probed region.

The final question to be discussed in this section is, to what degree will the existence of absorbing as opposed to reflecting boundaries influence the spectral density function itself? For notational simplicity the following discussion is restricted to the one dimensional case, which will sufficiently expose the salient points. The bounded fundamental solution for a single particle with absorbing boundaries in one dimension is denoted $n_j^a(x,t)$. Its specific form is given by Eq.(6). Analogous to the case of reflecting boundaries the general solution is written as a convolution product

$$n^a(x,t) = \mathbf{Z}_-(x,t) \;^{**}\; e^{-t/\tau}\, G(x,t) \tag{IV.55}$$

where

$$\mathbf{Z}_-(x,t) = \sum_j \delta(t - \mathbf{t}_j) \prod_{i=1}^{3} \left[\delta(x_i - \mathbf{x}_{ji}) - \delta(x_i + \mathbf{x}_{ji}) \right]. \tag{IV.56}$$

It is immediately apparent that the Poisson impulse functions $\mathbf{Z}_+$ and $\mathbf{Z}_-$ have identical first and second order statistics, i.e.

$$< \mathbf{Z}_+(x,t) > = < \mathbf{Z}_-(x,t) >$$

and

$$R_{Z_+}(x,t) = R_{Z_-}(x,t).$$

Thus Eq.(55) is equal in the wide sense with the reflecting barrier solution. Therefore

the particular boundary type can only affect the spectral density through λ, τ, or $< n >$. The relationship of these three variables is now considered by calculating the balance equation for the absorbing boundary, which is

$$< N >_{x_k,t_k} = < \int_0^{L_x} n^a(x\,,\,t)\,dx >_{x_k,t_k} \tag{IV.57}$$

$$= < \sum_{j=1}^{k} e^{-(t-t_j)/\tau} \frac{1}{\sqrt{4\pi D(t-t_j)}} \times$$

$$\sum_{n=-\infty}^{\infty} \int_0^{L_x} \left[e^{\frac{-(x-x_j-2nL_x)^2}{4D(t-t_j)}} - e^{\frac{-(x+x_j-2nL_x)^2}{4D(t-t_j)}} \right] dx >_{x_k,t_k}.$$

To solve Eq.(57) the integration is broken up as follows

$$\int_0^{L_x} n^a(x,t)\,dx = \int_0^{\infty} n^a(x,t)\,dx - \sum_{m=1}^{\infty} \int_{(2m-1)L_x}^{(2m+1)L_x} n^a(x,t)\,dx. \tag{IV.58}$$

The second term on the right side of Eq.(58) is a series of integrals, each over a length $2L_x$. To exploit this property note that $n^a(x,t)$ is a periodic function. This can be shown by a several methods. One is to express Eq.(6) in terms of Jacobi theta functions [6]

$$n_j^a(x,t) = \frac{1}{2L_x} \left[\Theta\left(\frac{x-x_j}{2L_x}, \frac{t-t_j}{4L_x^2} \right) - \Theta\left(\frac{x+x_j}{2L_x}, \frac{t-t_j}{4L_x^2} \right) \right]. \tag{IV.59}$$

These functions have period $2L_x$, hence

$$n_j^a(x+2L_x\,,t) = n_j^a(x\,,t) \tag{IV.60}$$

Also they are uniformly convergent in $[0, L_x]$, which allows summation and integration to be exchanged in Eq.(57) [10]. Given $n_j^a(x,t)$ has periodicity $2L_x$ then for all

$m \geq 1$

$$\int_{(2m-1)L_x}^{(2m+1)L_x} n^a(x,t)\,dx = 0 \qquad \text{(IV.61)}$$

and so Eq.(58) reduces to

$$\int_0^{L_x} n^a(x,t)\,dx = \int_0^{\infty} n^a(x,t)\,dx. \qquad \text{(IV.62)}$$

Combining Eqs.(57) and (62) yields

$$< N >_{x_j,t_j} = < \sum_{j=1}^{k} e^{-(t-t_j)/\tau} \left\{ \operatorname{erf}\left(\frac{\mathbf{x}_j}{\sqrt{4D(t-\mathrm{t}_j)}} \right) + \sum_{n=1}^{\infty} \left[\operatorname{erf}\left(\frac{2nL+\mathbf{x}_j}{\sqrt{4D\,(t-\mathrm{t}_j)}} \right) - \operatorname{erf}\left(\frac{2nL-\mathbf{x}_j}{\sqrt{4D(t-\mathrm{t}_j)}} \right) \right] \right\} >_{x_j,t_j}. \qquad \text{(IV.63)}$$

The next step is to average Eq.(63) with respect to t_j. Each of the three terms on the right side of Eq.(63) can be written in the form $\lim_{T\to\infty} \frac{1}{T}\, g(\tau^{-1})$, where

$$g(\tau^{-1}) = \int_0^{\infty} e^{-t\tau^{-1}} \operatorname{erf}\left(\tfrac{1}{2}\sqrt{\beta_n^{\pm}/t} \right) dt \qquad \text{(IV.64)}$$

and $\beta_n^{\pm} = (2nL_x \pm \mathbf{x}_j)^2/D$. The function $g(\tau^{-1})$ is a tabulated Laplace transform [11]

$$g\{\tau^{-1}\} = \tau\left(1 - e^{-\sqrt{\beta_n^{\pm}\tau^{-1}}} \right). \qquad \text{(IV.65)}$$

Combining Eqs.(63) and (65) yields,

$$< N >_{x_k,t_j} =$$

$$\lim_{T\to\infty} \frac{\tau}{T} \sum_{j=1}^{k} < 1 - e^{-x_j/\sqrt{D\tau}} + \sum_{n=1}^{\infty} e^{-2nL_x/\sqrt{D\tau}} \left[e^{x_j/\sqrt{D\tau}} - e^{-x_j/\sqrt{D\tau}} \right] >_{x_j}, \qquad \text{(IV.66)}$$

from which follows

$$<N> = \lambda\tau \; < \; 1 - e^{-x_j/\sqrt{D\tau}} + \sum_{n=1}^{\infty} e^{-2nL_z/\sqrt{D\tau}} \left[\; e^{x_j/\sqrt{D\tau}} - e^{-x_j/\sqrt{D\tau}} \right] \; >_{x_j}, \quad \text{(IV.67)}$$

To complete the evaluation of Eq.(67) the terms above are averaged with respect to the uniformly distributed $\mathbf{x}_j$. These are of the form

$$< e^{\pm \alpha x_j} >_{x_j} = \frac{1}{\pm \alpha L} \left(\; e^{\pm \alpha L} - 1 \right),$$

where $\alpha = 1/\sqrt{D\tau}$. Eq.(67) then reduces to

$$<N> = \lambda\tau \left\{ 1 + (\alpha L)^{-1} \left(e^{-\alpha L} - 1 \right) + (\alpha L)^{-1} \left(e^{\alpha L} + e^{-\alpha L} - 2 \right) \sum_{n=1}^{\infty} e^{-2\alpha L} \right\}. \quad \text{(IV.68)}$$

Noting $\sum_{n=1}^{\infty} x^n = \frac{x}{1-x}$ transforms Eq.(68) to

$$<N> = \lambda\tau \left(\; 1 - \epsilon \; \right), \quad \text{(IV.69)}$$

where

$$\epsilon = \frac{e^{2\alpha L} - 2\, e^{\alpha L} + 1}{\alpha L \left(e^{2\alpha L} - 1 \right)} \quad \text{(IV.70)}$$

Eq.(69) is the desired relation that distinguishes absorbing boundaries from reflecting ones. It relates λ, τ, and $<N>$ in a balance equation, which also involves the diffusion coefficient D and sample geometry L. Several properties of this type of system are revealed by considering its limiting forms. The first limit is

$$\lim_{D\tau \ll L^2} <N> = \lambda\tau,$$

which reduces to the expression found in the case of reflecting boundaries. This is reasonable because here the standard deviation of the Brownian particle

$<x^2>^{1/2} = 2D\tau$ is much smaller than the linear dimension L of the sample. Thus the type of boundary is unimportant as on the average the particle never interacts with it. The boundary type becomes more important in the second limit, which produces a lower bound on $<N>$. For the absorbing boundary a restriction on the maximum value of τ appears

$$\tau \leq \tau_{max} = L^2/2D,$$

because the standard deviation can be no greater than the sample dimension. Therefore

$$0.57\lambda\tau \leq <N> \leq \lambda\tau.$$

The influence of the boundary begins to be felt when $D\tau \approx L^2$. Then there are two possible situations. If $<N>$ is somehow fixed the boundary type affects τ. The following sections show τ influences the noise spectrum in the low frequency band. The more likely situation is that $\lambda\tau$ is fixed, e.g. the systems are at constant temperature. Then the boundary type will determine $<N>$, but otherwise has no affect on the noise spectrum.

1. Summary of section C.

The density fluctuations in the grand canonical ensemble obey the stochastic diffusion equation (22). The solution, Eq.(30), is written as a convolution product involving the Poisson impulse function $\mathbf{Z}_+(\vec{x}, t)$. Section C has been devoted to the calculation of the first and second order statistics of this function. To introduce the calculational method the one dimensional case was considered first. This resulted in special cases of Campbell's theorem, Eqs.(35) and (36). Rice's calculational method

using the Poisson distribution is applied here in a similar fashion to find $< \mathbf{Z}(t) >$, which involves the uniformly distributed $\mathbf{t}_j$. Papoulis has derived these equations by considering the derivative of Poisson increments [8], although this approach is not readily extended to the multidimensional case that is of present interest. Another approach is possible that exploits the uniformity of the individual $\mathbf{t}_j$ and $\mathbf{x}_j$, however Rice's method is chosen as being more concise. The arguments are then repeated for the four dimensional space-time Poisson impulse function, Eq.(23), which results in the mean, Eq.(37), and two point autocorrelation, Eq.(39).

The statistics of $\mathbf{Z}_+(\vec{x}, t)$ were then checked by combining the previous results with the fundamental solution $n(\vec{x}, t)$, Eq.(25). An important consequence of the present system is that a finite lifetime τ is required for equilibrium to be maintained. This point has not been recognized by the two other studies of the grand canonical ensemble, [2,3]. The influence τ has on the spectral density is discussed in the following sections.

Investigation of the two point density autocorrelation, Eq.(47), shows that it is stationary, Eq.(49), and hence consistent with the equilibrium condition. Eq.(49) is also the general expression for the field emission autocorrelation function. Unfortunately its structure does not readily lend itself to further detailed study at this time. Fourier analysis will reduce the degree of complexity by converting the convolution operation to multiplication. However the special case of the total noise power with a probed region equal to the total net plane was evaluated. It was shown that the construction of the Poisson impulses is consistent with the physical interpretation of the noise power being proportional to $< N >$, which is true for a thermodynamically ideal system. An extension of the definition $\lambda\tau = < N >$ to $\lambda\tau = < (\delta N)^2 >$ is therefore suggested, which encompasses fully interacting systems.

It is also noted that the noise power does not approach zero as the probed region equals the net plane, contrary to the canonical ensemble case. This is because fluctuations occur not only by diffusive mass transport into and out of the probed region, but also by the creation-recombination mechanism of defect vacancy-adatom formation.

Finally the question of the affect of the boundary type was discussed, i.e. whether there are important differences between reflecting and absorbing barriers. It is argued that this can only influence the solutions to the spectral density through the rate of creation λ, the average particle lifetime τ, and the average number of adatoms on the net plane $< N >$. This argument is based on the balance equation (69), which relates these terms to sample geometry and the diffusion coefficient. Overall the type of boundary is relatively unimportant as only τ can actually influence the frequency dependence of the spectrum and this occurs in the low frequency band as shown in the next section.

D. The multidimensional version of Carson's theorem.

The multidimensional version of Carson's theorem [8,12,13] is required for the spectral analysis of the field emission fluctuations. To begin it will be useful to define $C(\vec{x}_1 - \vec{x}_2, t_1 - t_2) \equiv < n(\vec{x}_1, t_1)\, n(\vec{x}_2, t_2) >$, appearing in Eq.(47). The definition

$$R_{Z,n}(\vec{x}_1, t_1; \vec{x}_2, t_2) \equiv < Z_*(\vec{x}_1, t_1)\, n(\vec{x}_2, t_2) >, \qquad \text{(IV.71)}$$

combined with Eq.(30) becomes

$$R_{Z,n}(\vec{x}_1, t_1; \vec{x}_2, t_2) = R_{Z,}(\vec{x}_1, t_1; \vec{x}_2, t_2) \;** F_\tau(\vec{x}_2, t_2), \qquad \text{(IV.72)}$$

where

$$F_\tau(\vec{x}, t) \equiv e^{-t/\tau} F(\vec{x}, t). \tag{IV.73}$$

Then

$$C(\vec{x}_1 - \vec{x}_2, t_1 - t_2) = R_{Z.n}(\vec{x}_1 - \vec{x}_2, t_1 - t_2) \;** F_\tau(\vec{x}_1, t_1). \tag{IV.74}$$

That Eq.(74) can be written as a stationary function follows from the derivation of Eq.(48) and

$$R_{Z.}(\vec{x}, t) = R_{Z_s}(\vec{x}, t) * f(\vec{x}) + \lambda^2/V_t^2, \tag{IV.75}$$

where

$$R_{Z_s}(\vec{x}, t) \equiv R_{Z_+}(\vec{x}, t) - \lambda^2/V_t^2. \tag{IV.76}$$

Proof of Eq. (75)

$$R_{Z.}(\vec{x}_1, t_1; \vec{x}_2, t_2) = \left\langle \left[\mathbf{Z}_+(\vec{x}_1, t_1) * f(\vec{x}_1) \right] \times \left[\mathbf{Z}_+(\vec{x}_2, t_2) * f(\vec{x}) \right] \right\rangle$$
$$= R_{Z_+}(\vec{x}_1 - \vec{x}_2, t_1 - t_2) ** f(\vec{x}_1) f(\vec{x}_2)$$
$$= \frac{\lambda}{V_t} \delta(t_1 - t_2) \sum \int \delta(\vec{s} - 2\vec{L}_m)\, \delta(\vec{x}_1 - \vec{x}_2 - s - 2\vec{L}_n)\, ds + \lambda^2/V_t^2$$
$$= R_{Z_s}(\vec{x}_1 - \vec{x}_2, t_1 - t_2) * f(\vec{x}_2) + \lambda^2/V_t^2. \qquad Q.E.D.$$

Using the coordinate transformation $(\vec{x}_1, t_1) \rightarrow (\vec{\xi} + \vec{x}, \eta + t)$ and $(\vec{x}_2, t_2) \rightarrow (\vec{\xi}, \eta)$, Eq.(72) is transformed to

$$R_{Z_s n}(\vec{x}, t) = R_{Z_s}(\vec{x}, t) ** F_\tau(\vec{x}, t) \tag{IV.77}$$

and Eq.(74) becomes

$$C(\vec{x}, t) = R_{Z.n}(\vec{x}, t) ** F_\tau(\vec{x}, t), \tag{IV.78}$$

The following convention will be used for Fourier transformations

$$F(s) = \int_{-\infty}^{\infty} F(v)\, e^{-isv}\, dv$$

$$F(v) = \frac{1}{2\pi} \int_{-\infty}^{\infty} F(s)\, e^{isv}\, ds.$$

Application of the Wiener-Khinchin theorem (see chapter I, appendix A) to the two point time delayed correlation $C(\vec{x}, t)$ and Fourier transformation of Eq.(72) leads respectively to

$$C(\vec{k}, \omega) = 2 \int_{-\infty}^{\infty} \int_{-\infty}^{\infty} C(\vec{x}, t)\, e^{-i(\vec{k}\cdot\vec{x}+\omega t)}\, d\vec{x}\, dt. \qquad \text{(IV.79)}$$

and

$$R_{Z,n}(\vec{k}, \omega) = R_{Z_s}(\vec{k}, \omega)\, F_r^*(\vec{k}, \omega), \qquad \text{(IV.80)}$$

and F_r^* denotes complex conjugation. Combining Eqs.(77), (79), and (80) results in

$$C(\vec{k}, \omega) = 2\, R_{Z_s}(\vec{k}, \omega)\, |\, F_r(\vec{k}, \omega)\,|^2. \qquad \text{(IV.81)}$$

Fourier transformation of Eqs.(39) and (75) in conjunction with Eq.(81) yields

$$C(\vec{k}, \omega) = 2 \left[\frac{\lambda f(\vec{k})}{V_t} + \frac{(2\pi)^4 \lambda^2}{V_t^2}\, \delta(\vec{k})\, \delta(\omega) \right] |\, F_r(\vec{k}, \omega)\,|^2. \qquad \text{(IV.82)}$$

Eq.(82) is the four dimensional space-time extension of Carson's theorem and refutes Bliek's claim that the theorem cannot be applied to systems of finite size. The second term on the right side of Eq.(82) will later be shown to cancel the constant factor $< (\delta N)^2 >$ appearing in $R(t)$ and has no affect on the spectral density itself.

Lighthill proves that there exists a unique Fourier series representation of any periodic generalized function, which converges to the function, whose coefficients can be determined, and which can be differentiated term by term [14]. Therefore the Fourier series expansion of Eq.(28), given by

$$f(\vec{x}) = \prod_{i=1}^{3} \sum_{n_i=-\infty}^{\infty} C_{\vec{n}}\, e^{i2\pi n_i z_i / L_i}$$

is well defined. Operating on this equation and Eq.(28) with $\int dx_i\, e^{-i2\pi n_i x_i / L_i}$ and then equating the two expressions yields

$$C_{\vec{n}} = 1/L_1 L_2 L_3.$$

Thus

$$f(\vec{x}) = \prod_{i=1}^{3} \frac{1}{L_i} \sum_{n_i=-\infty}^{\infty} e^{2\pi i n_i x_i / L_i}.$$

Fourier transformation of Eq.(28) then produces

$$f(\vec{k}) = \prod_{i=1}^{3} \frac{\pi}{L_i} \sum_{n_i=-\infty}^{\infty} \delta\left(k_i - \frac{\pi n_i}{L_i} \right). \tag{IV.83}$$

This result is a variant of a three dimensional Poisson summation formula from which the quantization condition

$$k_i = n\,\pi / L_i \tag{IV.84}$$

is obtained. This differs from Bliek's study by a factor of 2, which can be traced to an algebraic error in his proposed fundamental solution.

From Eq.(82) the two point frequency correlation is immediately obtained

$$C(\vec{x},\omega) = \frac{2\lambda}{(2\pi)^3 V_t}\, F_r^*(\vec{x},\omega) * \left[f(\vec{x}) * F_r(\vec{x},\omega) \right] \tag{IV.85}$$

$$+ \frac{4\pi\lambda^2}{V_t^2} \left| F_r(k=0,\omega) \right|^2 \delta(\omega).$$

The spectral density of the field emission fluctuations is then

$$S(\omega)/C_{FN} = \int \int C(\vec{x}_1 - \vec{x}_2 , \omega)\, d\vec{x}_1\, d\vec{x}_2 \qquad \text{(IV.86)}$$

where $C(\vec{x}_1 - \vec{x}, \omega)$ is given by Eq.(85). Precise calculation of this expression has eluded me, however section E (uncorrelated volumes) provides an approximation method for solving it, which is directed through k-space analysis. An important point not realized by Bliek is that

$$C(x=0,\omega) = \frac{1}{(2\pi)^3} \int C(\vec{k},\omega)\, d\vec{k}$$

gives the point-frequency correlation of the process, but is not the true spectral density, e.g. as given by Eq.(86). $C(x=0, \omega)$ does not include the probe averaging effect, represented by the double spatial integration, which is characteristic of any noise theory based on a diffusion process. This aspect of the problem has been recognized by VC.

Finally, a note on the general structure of Eqs.(82) and (86). In the one dimensional version of Carson's theorem the power per unit frequency, i.e. the spectral density, is partitioned among the individual pulses due to their uncorrelatedness. Hence it is possible to write $S(\omega)$ as a product of a rate times the spectrum of an individual pulse. In the case of a stochastic field comparison of Eqs.(82) and (86) reveals that there is a partioning of energy in k-space only. In analogy with the one dimensional version the modes here are uncorrelated and hence there is no energy exchange between them. I believe this is due to the linearity of the formulation. It is well known, e.g. in turbulence theories, that nonlinearity in the Navier-Stokes equations leads to energy cascades in k-space, which represent energy transfer from larger to smaller eddies. A further exposition of this subject is beyond the scope of the present work, except to note that in real space fluctuations decay with a spatial dependence

due to the diffusive nature of the process and therefore one would not expect Eq.(86) to exhibit such a partioning of the energy.

1. Summary of section D.

The $\vec{k}$ -correlated spectrum $C(\vec{k}, \omega)$, Eq.(82), has been derived. It is the extension of Carson's theorem to four dimensions and reflects the finite size of the system by the k-space quantization condition $k_i = n\,\pi/L_i$, Eq.(84). This function will be used in section F to calculate the point frequency correlation function $C(\,x\,=0,\,\omega) = \frac{1}{(2\,\pi)^3}\int C(\vec{k},\omega)\,d\,\vec{k}$. This is one of two major pieces upon which the noise spectrum $S(\omega)$ is constructed. The next section provides the bridge between $C(\,x\,=0,\omega\,)$ and $S(\omega)$.

E. The correlated volume concept.

The fluctuation theory of the present chapter is now to the point where an integral equation for $S(\omega)$ has been formulated, Eq.(86). This section presents an approximation method for its solution. The result of the construction is a relation between $S(\omega)$ and the point-frequency correlation $C(\, x=0, \omega\,)$. This relation is first used to derive the spectrum excluding boundary effects $S^{\infty}(\omega)$. The fluctuation lifetime τ is shown to be an important factor in removing an apparent divergence in the noise power integral that appears in VC's theory. The correlated volume construction is also shown to be part of this problem. The section concludes by discussing a method, which determines the diffusion coefficient D by measuring $C^{\infty}(\, x=0\,,\, \omega\,)$.

To begin, the autocorrelation Eq.(2) is rewritten

$$R(t)/C_{FN} = \int_{V_p}\int_{V_p} C(\,\vec{r}_1 - \vec{r}_2,\, t\,)\, d\vec{r}_1\, d\vec{r}_2 - <N_p>^2. \qquad \text{(IV.87)}$$

Applying the Wiener-Khinchin theorem to Eq.(87) yields

$$S_o(\omega) = \int_{V_p}\int_{V_p} C(\,\vec{r}_1 - \vec{r}_2,\, \omega\,)\, d\vec{r}_1\, d\vec{r}_2, \qquad \text{(IV.88)}$$

where $S_o(\omega) \equiv S(\omega)/C_{FN} - 4\pi <N_p>^2 \delta(\omega)$ and a factor of 2 is absorbed in $C(\,\vec{r},\, \omega\,)$, see Eqs.(79),(81), and (82). It is shown below that there exists a length Λ_r and a frequency ω_o, such that $C\left(\,|\,\vec{r}_1 - \vec{r}_2\,| < \Lambda_r,\, \omega < \omega_o\,\right) \approx C(\, x=0\,,\omega\,)$, i.e. the two point frequency correlation $C(\vec{x},\, \omega\,)$ is independent of $\vec{x}$. Assuming this to be the case Eq.(88) reduces to

$$S_c(\,\omega\,) = V_p^2\, C(\, x=0,\, \omega\,), \qquad \text{(IV.89)}$$

where the notation $S_c(\omega)$ indicates the condition $|\vec{r}| < \Lambda_r$ is satisfied.

The next step is to couple the correlated spectrum $S_c(\omega)$ to $S_o(\omega)$. Then using Eq.(89) a relation between $S_o(\omega)$ and $C(x=0, \omega)$ will be given. As $C(x=0, \omega)$ can be calculated the method then provides an expression for $S_o(\omega)$ itself, which is the experimentally accessible function.

To begin the probe current $i_p(t)$, which is a fluctuating random variable, is expanded as a Fourier series in the interval $|t| \leq T/2$

$$i_p(t) = \sum_{n=-\infty}^{\infty} a(\omega_n)\, e^{i\omega_n t}, \tag{IV.90}$$

where $\omega_n = 2\pi n/T$ and the statistics of $a(\omega_n)$ are left unspecified.

The probed region V_p is divided into N_c subvolumes v_k so $N_c\, v_k = V_p$. Then the total current emitted from V_p is

$$i_p(t) = \sum_{k=1}^{N_c} i_k(t), \tag{IV.91}$$

where

$$i_k(t) = \sum_{n=-\infty}^{\infty} a_k(\omega_n)\, e^{i(\omega_n T + \alpha_k)}. \tag{IV.92}$$

The α_k are uniformly distributed over the interval $[0, 2\pi]$ and are uncorrelated with a_k, i.e. $< f(a_k)\, g(\alpha_k) > = < f(a_k) >< g(\alpha_k) >$ for two functions f and g.

The spectral density is defined as (see appendix A, chapter I)

$$S(\omega) = \lim_{T\to\infty} 2T < a(\omega_n)\, a^*(\omega_n) >. \tag{IV.93}$$

The following relation is obtained by combining Eqs.(90) and (92)

$$\mathbf{a}(\omega_n) = \sum_{k=1}^{N_c(\omega)} \mathbf{a}_k(\omega_n)\, e^{i\alpha_k}. \tag{IV.94}$$

Substituting Eq.(94) into (93) gives

$$S(\omega) = N_c(\omega)\; S_k(\omega), \tag{IV.95}$$

where $S_k(\omega) \equiv \lim_{T\to\infty} 2T < \mathbf{a}_k(\omega_n)\, \mathbf{a}_k^*(\omega_n) >$ and the cross terms of the summation, Eq.(94), drop out of Eq.(95) because $< e^{i(\alpha_i - \alpha_j)} > = 0$ for $j \neq k$.

If the fluctuations were correlated over the entire volume V_p then $\alpha_k = \alpha_j$ for all k and j. The correlated spectrum $S_c(\omega) = S(\omega, \alpha_k = \alpha_j, k \neq j)$ is

$$S_c(\omega) = N_c^2(\omega)\, S_k(\omega), \tag{IV.96}$$

where Eqs.(93) and (94) are again used.

The desired result of the correlated volume construction is then derived by combining Eqs.(89), (95), and (96)

$$S_o(\omega) \approx \frac{V_p^2\; C(x=0,\omega)}{N_c(\omega)}, \tag{IV.97}$$

which allows the spectral density to be calculated from the point-frequency correlation

$$C(|\vec{x}|=0, \omega) = \frac{1}{(2\pi)^3} \int d\vec{k}\;\; C(\vec{k}, \omega) \tag{IV.98}$$

and knowledge of $N_c = V_p / v_k$.

The above derivation shows that a correlation length Λ_r exists corresponding to the distance over which the fluctuating current $\mathbf{i}_k(t)$ from the subvolume v_k has a constant phase, Eq.(92). The nature of Λ_r is further developed by considering the first term on the right side of Eq.(82)

$$C_o(\vec{k},\omega) \equiv \frac{2\lambda f(\vec{k})}{V_t} \mid F_r(\vec{k},\omega) \mid^2. \tag{IV.99}$$

At present the influence of boundaries is ignored so that Eq.(99) reduces to

$$C_o^{\infty}(\vec{k},\omega) = 2\lambda V_t^{-1} \mid F_r(\vec{k},\omega) \mid^2. \tag{IV.100}$$

Fourier transformation of Eqs.(29) and (73) converts Eq.(100) to

$$C_o^{\infty}(\vec{k},\omega) = 2\lambda V_t^{-1} \left(\frac{1}{\omega^2 + (\chi + D\,k^2)^2} \right), \tag{IV.101}$$

where $\chi \equiv \tau^{-1}$ and $k^2 = k_x^2 + k_y^2 + k_z^2$. Then by partial fraction expansion

$$\frac{1}{\omega_D^2 + (k^2 + \chi_D)^2} = \frac{A}{k^2 + z_+} + \frac{B}{k^2 + z_-}, \tag{IV.102}$$

where $\chi_D \equiv \chi/D$, $\omega_D \equiv \omega/D$, $z_{\pm} \equiv \chi_D \pm i\,\omega_D$, and $A = -B = i/2\omega_D$.

The two point frequency correlation can be expressed as

$$C_o^{\infty}(\vec{x},\omega) = \frac{2}{(2\pi)^2 x} \int_0^{\infty} C_o^{\infty}(k,\omega)\, k \sin kx \; dk, \tag{IV.103}$$

and $x \equiv \mid \vec{x} \mid$. Combining Eqs.(101-103) leads to

$$C_o^{\infty}(\vec{x},\omega) = \frac{4\lambda A}{(2\pi)^2 V_t D^2 x} \left[\int_0^{\infty} \frac{k \sin kx}{k^2 + z_+} dk - \int_0^{\infty} \frac{k \sin kx}{k^2 + z_-} dk \right]. \tag{IV.104}$$

The integrals are standard Fourier sine transforms

$$\int \frac{k \sin kx}{k^2 + w_{\pm}^2} dk = \frac{\pi}{2} e^{-w_{\pm} x}, \tag{IV.105}$$

where $w_{\pm} = z_{\pm}^{1/2} = (\chi_D \pm i\,\omega_n)^{1/2}$, which is multiple-valued. Let

$$z_{\pm} = r\, e^{i\theta_{\pm}}, \quad r = \mid z \mid, \quad \text{and} \quad \theta_{\pm} = Arctan(\pm \omega\tau).$$

Then $w_{\pm} = r^{1/2}\, e^{i\,\theta_{\pm}/2}$ ($r > 0$, $-\pi < \theta_{\pm} < \pi$), where the principal branch has been used. Because $\omega,\, \tau \geq 0$ the restriction is really ($0 \leq \theta_{+} < \pi/2$) and ($-\pi/2 < \theta_{-} \leq 0$). Define $w_{\pm} = u_{\pm} + i\, v_{\pm} = \rho\, e^{i\,\phi_{\pm}}$. Then $\rho = (\chi_D^2 + \omega_D^2)^{1/4}$ and $\phi_{\pm} = \theta_{\pm}/2$. Also

$$u \equiv u_{+} = \rho \cos\phi_{+} = \rho \cos(-\phi_{-}) = \rho \cos\phi_{-} = u_{-}$$

$$v \equiv v_{+} = \rho \sin\phi_{+} = -\rho \sin(-\phi_{-}) = -v_{-},$$

which implies

$$w_{\pm} = u \pm i\, v.$$

Using the above notation and Eq.(105) converts Eq.(104) to

$$C_o^{\infty}(\vec{x}, \omega) = \left(\frac{\lambda}{2\,\pi\, V_t\, D\, \omega} \right) e^{-u\,x}\, \frac{\sin(v\,x)}{x}. \qquad \text{(IV.106)}$$

Note that

$$u = 2^{1/2}\, \Lambda^{-1} \left[1 + (1/\omega\tau)^2 \right]^{1/4} \cos\left(\frac{1}{2} Arctan\, \omega\tau \right)$$

$$v = 2^{1/2}\, \Lambda^{-1} \left[1 + (1/\omega\tau)^2 \right]^{1/4} \sin\left(\frac{1}{2} Arctan\, \omega\tau \right),$$

where $\Lambda \equiv \sqrt{2\,D/\omega}$ is the correlation length defined by VC. Inspection of Eq.(106) suggests modifying this definition of correlation (decay) length to

$$\Lambda_r \equiv u^{-1} = \frac{\Lambda}{2^{1/2} \left[1 + (1/\omega\tau)^2 \right]^{1/4} \cos\left(\frac{1}{2}\, Arctan\, \omega\tau \right)}. \qquad \text{(IV.107)}$$

Noting $\lim_{\omega\tau \gg 1} u = v$ implies

$$\lim_{\omega\tau \gg 1} \Lambda_r = \Lambda. \qquad \text{(IV.108)}$$

Then Eq.(106) reduces to

$$\lim_{\omega\tau\gg 1} C_o^{\infty}(\vec{x},\omega) = \left(\frac{\lambda}{2\pi V_t D}\right) e^{-x/\Lambda}\,\frac{\sin(x/\Lambda)}{\omega x}, \qquad \text{(IV.109)}$$

which can also be written

$$\lim_{\omega\tau\gg 1} C_o^{\infty}(\vec{x},\omega) = \left(\frac{\lambda}{2^{3/2}\pi V_t D^{3/2}\omega^{1/2}}\right) e^{-x/\Lambda}\,\frac{\sin(x/\Lambda)}{(x/\Lambda)}.$$

This latter expression is, up to a constant factor, equal to Eq.(5.9) obtained by VC.

The other limit case is

$$\lim_{\omega\tau\ll 1} \Lambda_\tau = \sqrt{D\tau}, \qquad \text{(IV.110)}$$

which sets the upper bound on the correlation length when the lifetime or measurement frequency is very small and boundary effects are insignificant. In this limit the correlation length Λ_τ is equal to the standard deviation of the particle displacement. Even without an explicit calculation of $C_o(x,\omega)$ the limit to a correlated fluctuation in any single direction must be the sample dimension L_i if the boundary effect is included. Λ_τ is the decay length for $C_o^{\infty}(\vec{x},\omega)$ and Fig.12 graphs its variation with frequency.

The influence of the correlation length on the noise spectrum itself is demonstrated by first considering the point-frequency correlation using the limit of Eq.(106)

$$C_o^{\infty}(x=0,\omega) = \left(\frac{\lambda}{2\pi V_t D^{3/2}\omega^{1/2}}\right)\left[1+(1/\omega\tau)^2\right]^{1/4}\sin\left(\frac{1}{2}\,Arctan\,\omega\tau\right). \qquad \text{(IV.111)}$$

The long lifetime limit of Eq.(111) is

$$\lim_{\omega\tau\gg 1} C_o^{\infty}(x=0,\omega) = \frac{\lambda}{2^{3/2}\pi V_t D^{3/2}\omega^{1/2}} = \left(\frac{\lambda}{4\pi V_t D^2}\right)\Lambda\,, \qquad \text{(IV.112)}$$

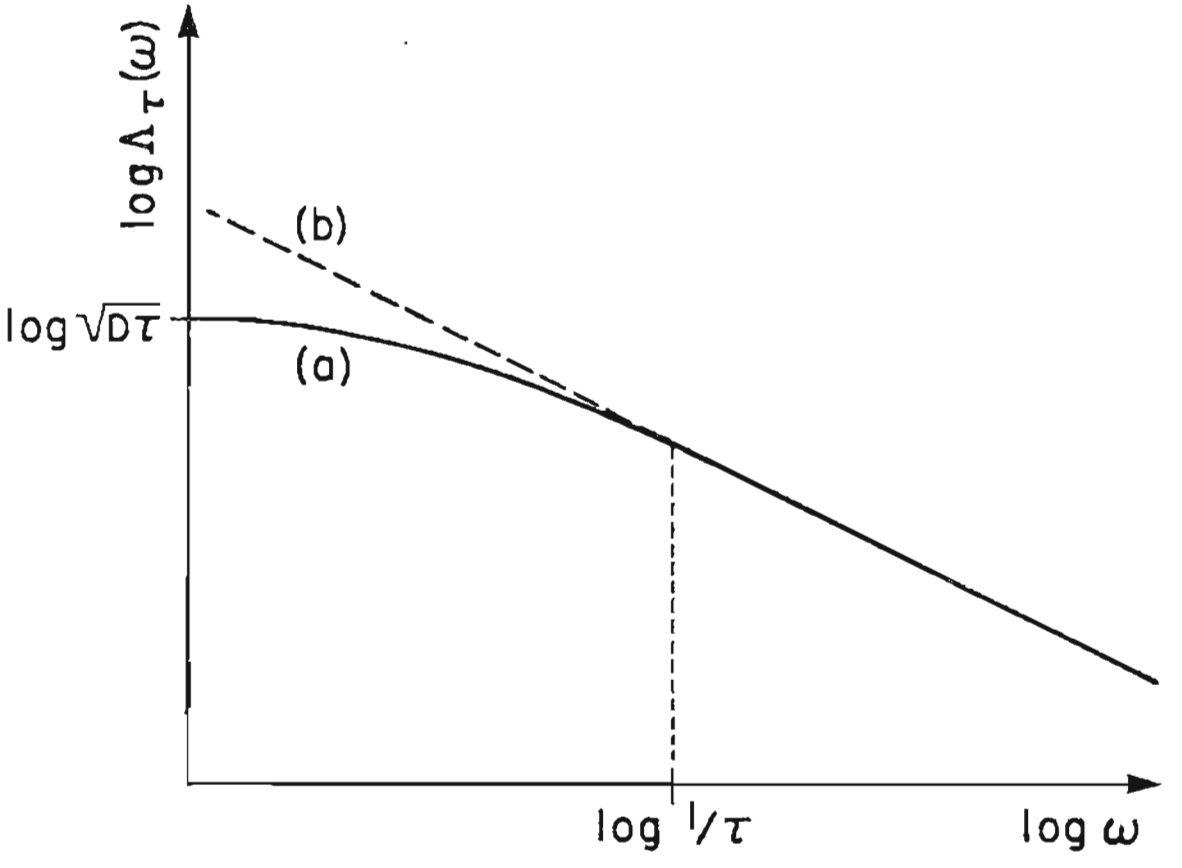

Fig. 12. Curve (a) is the correlation length $\Lambda_\tau(\omega)$. Curve (b) graphs $\Lambda = \sqrt{2D/\omega}$.

The short lifetime limit of Eq.(111) is

$$\lim_{\omega\tau \ll 1} C_o^{\infty}(x=0,\omega) = \frac{\lambda \tau^{1/2}}{4\pi V_t D^{3/2}} = \left(\frac{\lambda}{4\pi V_t D^2}\right) \Lambda_\tau \qquad \text{(IV.113)}$$

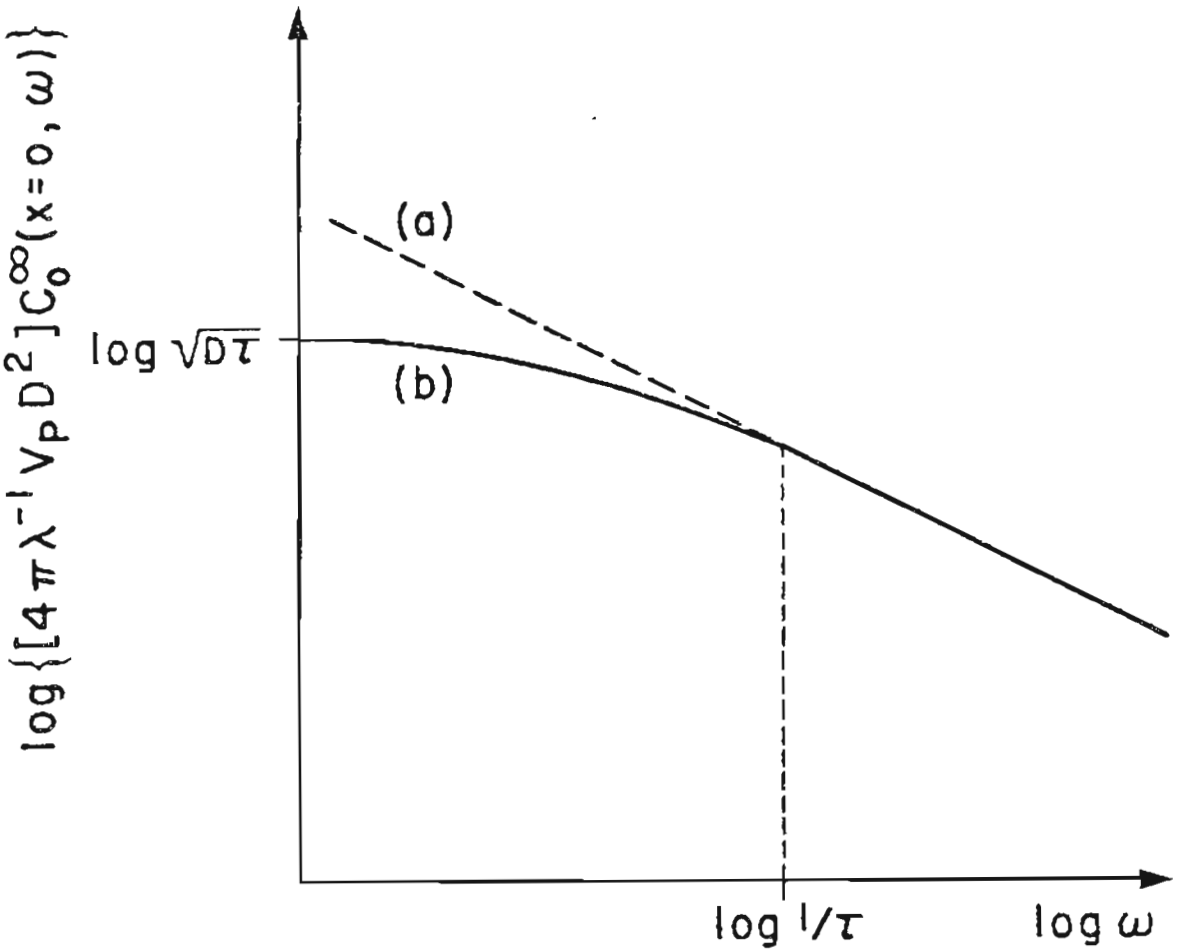

Fig. 13. Log-log graph of the frequency dependent two point spectral density C_o^{∞} excluding boundary effects. Curve (a) is $\Lambda = \sqrt{2D/\omega}$. Curve (b) is $C_o^{\infty}(x=0, \omega)$.

Fig.13 shows how the lifetime τ modifies C_o^{∞} from having an overall $\omega^{-1/2}$ behavior to one with a flat low frequency characteristic. This effect is carried over to the noise spectrum itself. To demonstrate this and also clarify the nature of $N_c(\omega) = l_1 l_2 l_3 / v_t$, where l_i is a linear dimension of the probed region V_p, four cases

are delimited that relate Λ_τ to V_p. A similar argument has been given previously by VC. It is important to recognize that this discussion relates correlation length to probe geometry and not to dimensions of the sample itself. In this section boundary effects are ignored as is the case throughout the study by VC. Including this effect influences $C(x=0,\omega)$ as shown in the following sections.

Assuming $l_3<l_2<l_1$ then three reference frequencies are defined $\omega_i \equiv 2D/l_i^2$ such that:

a) if $\omega_3 < \omega$ then $\Lambda_\tau(\omega) < l_3$ and

$$N_c \approx V_p/\Lambda_\tau^3, \tag{IV.114a}$$

b) if $\omega_2 < \omega < \omega_3$ then $l_3 < \Lambda_\tau(\omega) < l_2$ and

$$N_c \approx l_1 l_2/\Lambda_\tau^2. \tag{IV.114.b}$$

c) if $\omega_1 < \omega < \omega_2$ then $l_2 < \Lambda_\tau(\omega) < l_1$ and

$$N_c \approx l_1/\Lambda_\tau. \tag{IV.114c}$$

d) if $\omega < \omega_1$ then $l_1 = \Lambda_\tau(\omega)$ and

$$N_c \approx 1. \tag{IV.114.d}$$

Fig.14 graphs the spectral density $S_o^\infty(\omega) = V_p^2\, C_o^\infty(x=0,\omega)/N_c(\omega)$, which is produced by combining Eqs.(111-114). Note $\lim_{\omega<1/\tau} S(\omega) = constant$ whereas when $\omega > 1/\tau$ the graph is identical to Fig.7 of VC.

Two problems posed by VC can now be answered. The first is the theoretical justification of the spatial correlation exhibited by the function $C_o^\infty(\,|\vec{x}|,\omega\,)$. The derivation makes it apparent that it is simply due to the

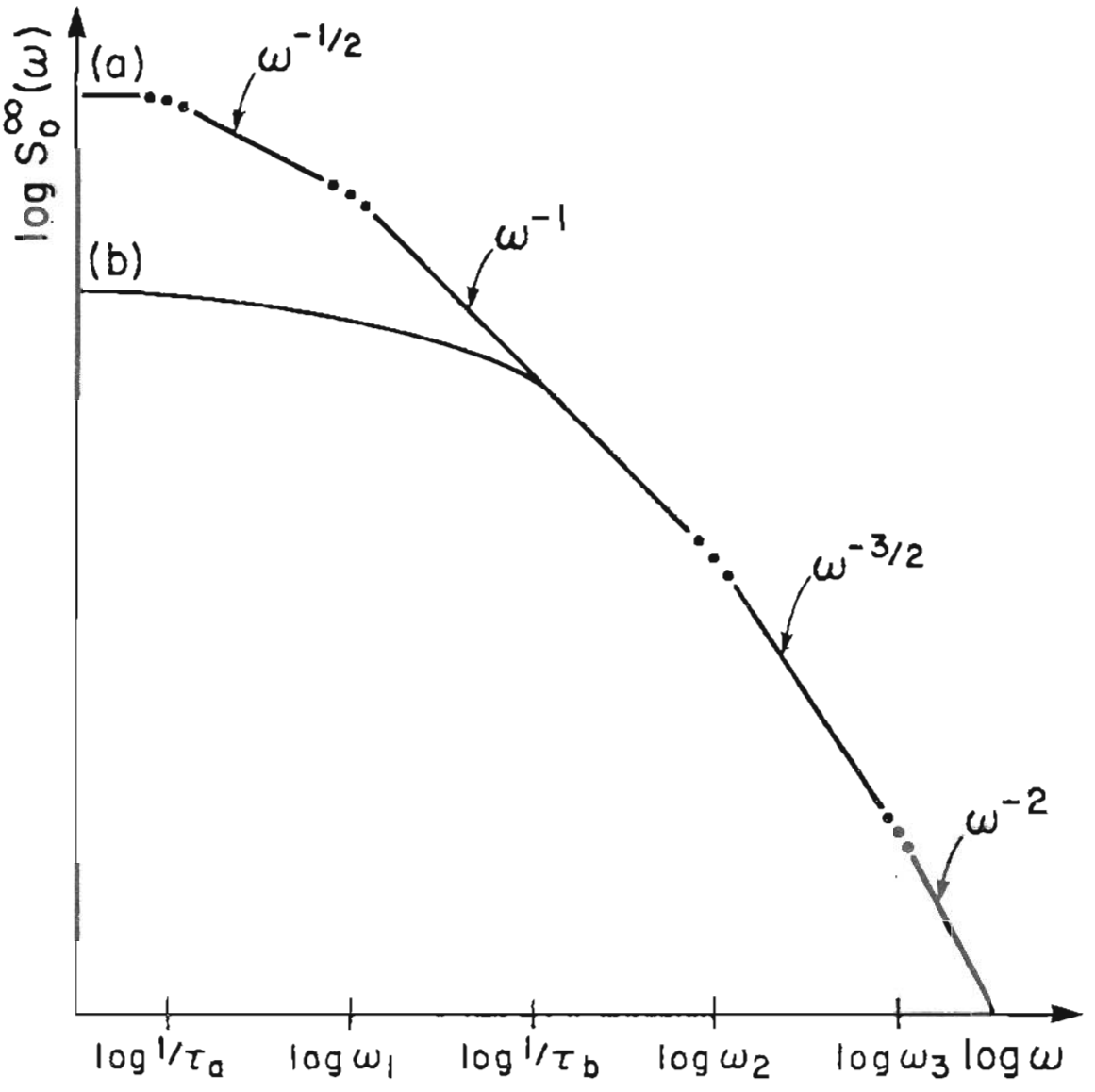

Fig. 14. Graph of $S_o^\infty(\omega)$ using the limit forms of $N_c(\omega)$ discussed in the text, $\omega_i = 2D/l_i^2$. Curve (a) is for a lifetime $1/\tau_a < \omega_1$. Curve (b) corresponds to lifetime $\omega_1 < 1/\tau_b < \omega_2$.

diffusive motion of the fluctuation, in this case the adatom density. The second more serious problem is with an apparent divergence in the total noise power normalization for $d \leq 3$ dimensions. This occurs at three different points in the analysis. Two of these are due to neglect of the finite lifetime factor τ. VC actually state the normalization divergence problem occurs for $d < 3$. Fig.14 shows this occurs for $d = 3$ also. To see this note $\omega_1 = 2D/l_1^2$. Now $l_3 < l_2 < l_1$. Assume l_3 and l_2 are fixed at some nonzero value and let $l_1 \rightarrow \infty$. If $\tau \rightarrow \infty$, as in their analysis, then the graph of S_o^∞ corresponds to an infinitely long probe region with rectangular cross section that has $\lim_{\omega \rightarrow 0} S^\infty(\omega) = 1/\omega$. This is a $d = 3$ system, which yields a divergent noise power in the low frequency band $P_\infty \sim \int_0^{\omega_2} \frac{d\omega}{\omega}$. The presence of the factor τ imposes a lower limit, $1/\tau$, on the $1/\omega$ portion of $S(\omega)$ and removes the normalization problem here.

Let us now consider the part of the problem encountered by VC. Assuming the system is two dimensional, k-space Fourier transformation of Eq.(101) yields the corresponding two point spectrum, which is

$$C_o^\infty(\vec{r}, \omega) = \frac{2\lambda A_l^{-1}}{(2\pi)^2} \int_0^{2\pi} d\theta \int_0^\infty dk\ k\ e^{i k r \cos\theta} \frac{1}{\omega^2 + (\chi + D k^2)^2}, \qquad \text{(IV.115)}$$

which reduces to

$$C_o^\infty(\vec{r}, \omega) = \frac{2\lambda A_l^{-1}}{2\pi} \int_0^\infty \frac{J_o(k r)\, k\, dk}{\omega^2 + (\chi + D k^2)^2}, \qquad \text{(IV.116)}$$

where J_o is the zero order Bessel function. Combining Eq.(116) with the spatially correlated noise power, defined as

$$P_c(\vec{r}) \equiv \int_0^\infty C_o^\infty(\vec{r}, \omega)\, d\omega,$$

yields

$$P_c(\vec{r}) = \frac{\lambda A_l^{-1}}{D} \int_0^\infty \frac{k\, J_o(k\,r)}{\chi_D + k^2} dk = \frac{\lambda A_l^{-1}}{D} K_o(r/\tau D), \qquad \text{(IV.117)}$$

where K_o is the zero order modified Bessel function. Eq.(117) shows that a finite value for τ is necessary for a well behaved noise power since $\lim_{x \to 0} K_o(x) \sim -\log x$. This is the second place where τ is critical in preventing the divergent normalization. However there is a third cause for the problem, which surprisingly lies hidden in the correlated volume construction. To see this first define $x \equiv r/\tau D$ in Eq.(117). The correlated volume construction produces the proportionality

$$\lim_{\omega < 1/\tau} S_o^\infty(\omega) \sim C_o^\infty(x = 0, \omega). \qquad \text{(IV.118)}$$

The total noise power

$$P_o^\infty(\omega) = \int_0^\infty S_o^\infty(\omega)\, d\omega \qquad \text{(IV.119)}$$

combined with Eq.(118) then yields

$$P_o^\infty(\omega) \sim \lim_{r \to 0} P_c(r). \qquad \text{(IV.120)}$$

But by Eq.(117) this also leads to an infinity. The correlated volume construction requires a lower length scale cutoff because the $r = 0$ limit of Eq.(117) implies

$$P_c(x = 0) \sim \int_0^\infty \frac{k\, dk}{\chi + D\, k^2}. \qquad \text{(IV.121)}$$

The presence of $\chi \equiv 1/\tau$ prevents the integrand from diverging in the $k = 0$ limit but the upper integration limit still produces a divergent integral. The concluding proof that the normalization problem is partially an artifact of the correlated volume construction is shown by recalling

$$S_o^\infty(\omega) \sim \int C_o^\infty(\vec{r}, \omega)\, d\vec{r}$$

and hence for two dimensions

$$P_o^\infty(\omega) \sim \int_0^{r_o} d\,r\; r \int_0^\infty C_o^\infty(\vec{r}, \omega)\, d\,\omega,$$

which with Eq.(117) becomes

$$P_o^\infty(\omega) \sim \int_0^{r_o} d\,r\; r\; K_o(r/\tau D) \sim \textit{constant.}$$

Therefore the true noise power for a two dimensional system is finite and proves the apparent normalization problem stated by VC is due to assuming an infinite lifetime for the fluctuations and to the correlated volume construction, which must include a lower length cutoff when discussing $C(\vec{k} < \omega)$, i.e. a lower limit must be placed on the size of an individual correlated volume. This is physically reasonable as a single fluctuation must have some spatial extent even if this is just an atomic diameter. To consider a volume of spatial extent smaller than this is to say that a single atom is not correlated with itself! This defect in the initial construction of the correlated volume theory is subtle as it does not reveal itself in Fig.14. The next section shows that an upper bound in k-space modifies the high frequency portion of $C_o(x = 0, \omega)$.

The structure of the correlation length and the two point spectral density also suggests several novel methods for extracting the diffusion coefficient and determining τ. Define the fractional correlated noise power as the ratio

$$P_c(x,\omega) \equiv \lim_{\omega\tau\gg 1} \frac{C_o^{\infty}(x,\omega)}{C_o^{\infty}(x=0,\omega)}. \tag{IV.122}$$

Substituting Eqs.(109) and (112) into (122) results in

$$P_c(x,\omega) = e^{-x/\Lambda}\,\frac{\sin(x/\Lambda)}{(x/\Lambda)}. \tag{IV.123}$$

Now consider an experiment with two probes separated by a distance x detecting the flicker noise. To simplify the discussion the probes are assumed to have negligible area. Then the two point power spectrum is proportional to $P_c(x,\omega)$ and obtained by simply multiplying the two signals and passing the output through a spectrum analyzer.

One possibility is to monitor a narrow frequency band centered at $\omega_o > 1/\tau$ and plot $P_c = P_c(x,\omega_o)$, as indicated in Fig.15 and note the point $P_c(x_o,\omega_o) \approx 0$. From this data the diffusion coefficient is obtained since here

$$D = \frac{x_0^2\,\omega_o}{2\pi^2}. \tag{IV.124}$$

This depends on the assumption that x_o is greater than the resolution of the field electron microscope $\sim$20 Å . Assuming $D \sim 10^{-12}\,cm^2/sec$ and $x_o \sim$100 Å then $\omega_o \sim 20\,Hz$.

A check on this data can then be made by plotting $x_o = x_o(\omega^{-1/2})$ as in Fig.16. Here the diffusion coefficient is found from the slope since

$$\frac{d\,x_o}{d\,\omega^{-1/2}} = 2^{1/2}\pi D. \tag{IV.125}$$

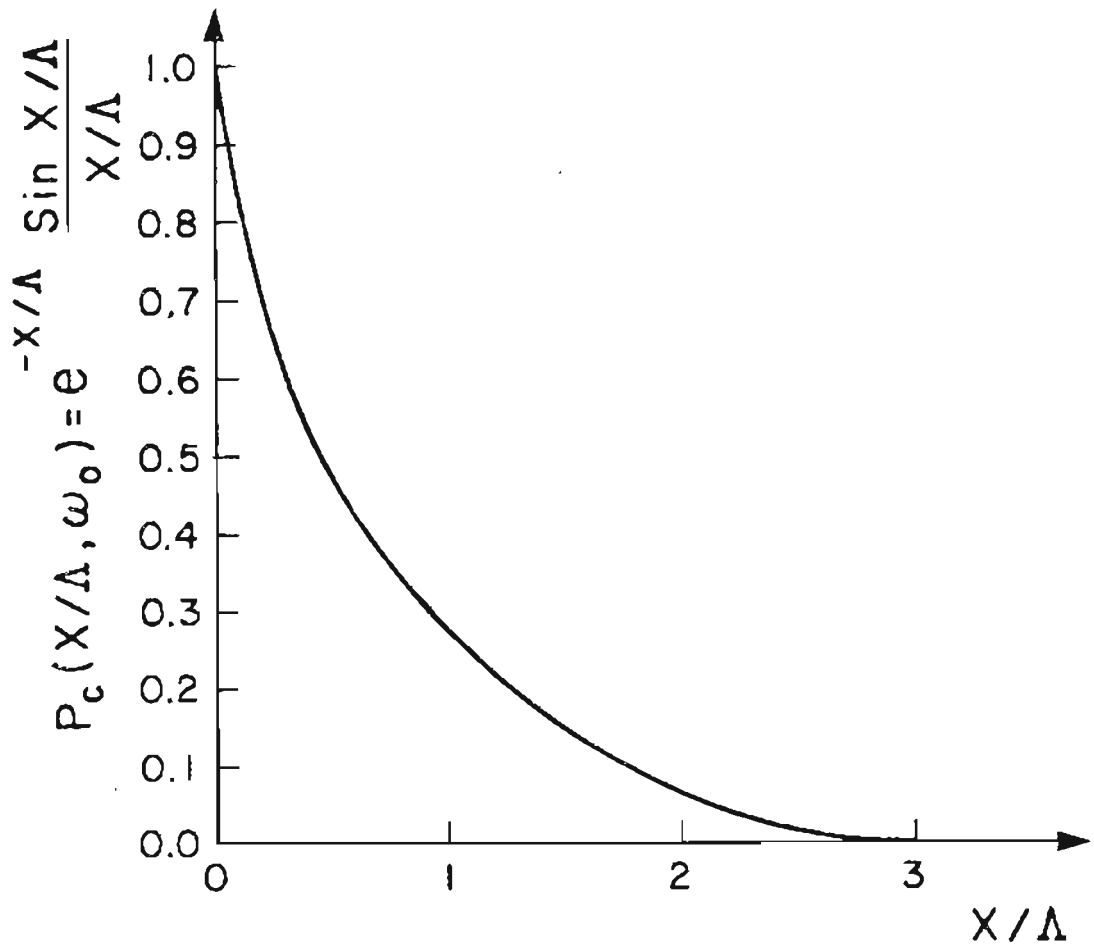

Fig. 15. Graph of the fractional correlated noise power defined by Eq.(123).

Deviation from linearity marks the onset of the finite lifetime effect, see Fig. 12.

Now assume $x = x_f$ is fixed and monitor $P_c = P_c(x_f, \omega)$. Then measure the frequency ω_f such that $P_c(x_f, \omega_f) = 0$. The diffusion coefficient is again obtained via Eq.(117) with x_f replacing x_o.

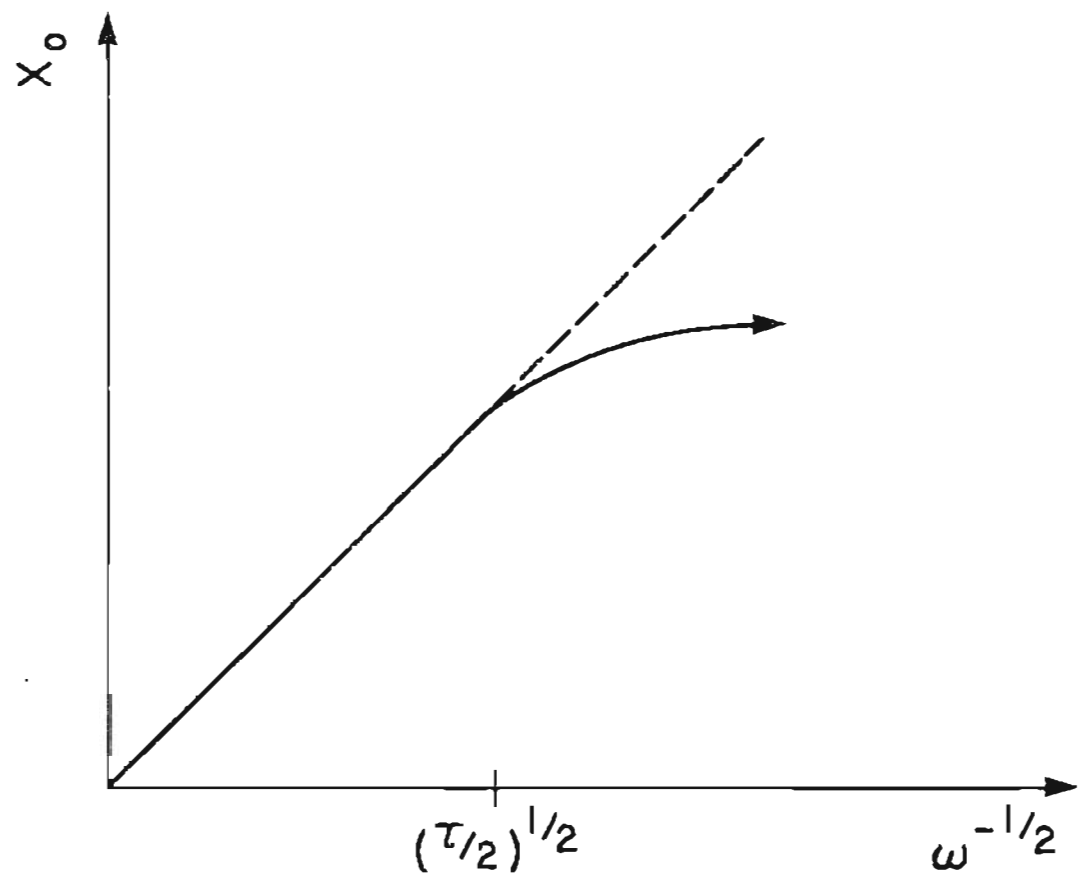

Fig. 16. Graph of probe separation x_o versus $\omega^{-1/2}$.

1. Summary of section E.

The principal goal of this section was to develop an approximation to the double spatial integration in Eq.(88). This was carried out by Fourier analysis of the fluctuating probe current $i_p(t)$ and by separately considering the individual current contributions $i_k(t)$, which correspond to a portion of the probe volume V_p. The number of these volumes is $N_c(\omega) = V_p/v_k$. From this decomposition a relation between the experimentally observable noise spectrum $S_o(\omega)$ and the calculable point-frequency correlation function $C(x=0, \omega)$ is obtained, Eq.(97). The proportionality $S_o(\omega) \propto N_c^{-1}(\omega)\, C(x=0, \omega)$ has been previously stated by VC. The present derivation gives rise to a correlation length Λ_τ that measures the distance over which the current fluctuations are in phase. The nature of this term is further developed by showing that it is the decay length appearing in $C(x=0, \omega)$, Eq.(106). The influence of the finite fluctuation lifetime τ on Λ_τ is given in Fig.12, which shows $\lim_{\omega < 1/\tau} \Lambda_\tau = constant$. The factor τ has a similar affect on the point frequency excluding boundary effects $C_o^\infty(x=0, \omega)$, Fig.13. Fig.14 is a graph of the corresponding spectrum $S_o^\infty(\omega)$. The fluctuation lifetime produces a constant $S_o^\infty(\omega)$ for $\omega < 1/\tau$. The various changes in slope of $S_o^\infty(\omega)$ are the result of the probe spatial averaging of the diffusive random field.

An outstanding problem of equilibrium fluctuation theory for a grand canonical ensemble posed by Voss and Clarke has been solved. This concerns an apparent divergence in the normalization to the total noise power of the spectral density $S(\omega)$. This problem is shown to exist for $d \leq 3$ dimensions as posed by these authors, although it was recognized by them as occurring only for $d < 3$. This problem is manifested in

three places. The first is related to the $d=3$ construction of $S_o^\infty(\omega)$, see Fig.14 and text, where the problem originates by not accounting for the τ factor. Including this term has already been shown to be a necessary condition for the maintenance of equilibrium, section C.

For $d<3$ the problem disappears from the Fig.14 construction even when the appropriate length scale limits are taken, which makes the origin of the problem more obscure. The k-space correlation function $C_o^\infty(\vec{k},\omega)$ is used to analyze the situation. The problem is twofold when considering the $\vec{k}$-space integration of Eq.(115). One part of the divergence is removed by including τ in the formulation. The second cause of the divergence is due to the correlated volume approximation itself. The problem is resolved by placing an upper bound on the magnitude of the $\vec{k}$-vector. This means a lower length scale in real space exists, which introduces in a natural way the resolution limit of the detector.

This section concludes by showing how a measure of the point-frequency correlation $C_o^\infty(x=0,\omega)$ can yield the diffusion coefficient D and the lifetime factor τ. The next step in the development is to include the sample boundary effect in $C_o(x=0,\omega)$. This aspect of the theory was not considered by VC and is addressed in the next section.

F. The point-frequency correlation $C(x=0,\omega)$

The point frequency correlation $C(x=0,\omega)$ for a bounded volume must be developed before the nature of the spectral density $S(\omega)$ including finite lifetime, probe spatial averaging, and sample geometry can be discussed. Then using Eq.(97) and the correlated volume approximation $S(\omega)$ can be constructed.

The probe spatial averaging over the detected volume V_p, which influences $N_c(\omega)$, was the only point where geometrical effects were considered by VC. On the other hand Bliek included sample geometry in his calculation of $C(x=0,\omega)$. However he erroneously identified this last function as the spectrum $S(\omega)$ and was also beset by a divergent low frequency noise power, although not of the same origin as VC's. This forced him into postulating the existence of "low frequency correlations" that do not have any direct physical interpretation. In the present section it is again shown that the problem is solved by including a finite fluctuation lifetime. Bliek also used an erroneous fundamental solution, which introduces several algebraic problems and necessitates an ad hoc derivation of $C(x=0,\omega)$. Therefore, until now, no complete spectral analysis for this ensemble has been given.

To derive $C(x=0,\omega)$ Eq.(82) is rewritten using Eq.(99) as

$$C(\vec{k},\omega) = C_0(\vec{k},\omega) + C_1(\vec{k},\omega), \tag{IV.126}$$

where

$$C_1(\vec{k},\omega) = \frac{2\lambda^2(2\pi)^4}{V_t^2} \mid F_\tau(\vec{k},\omega)\mid^2 \delta(\vec{k})\,\delta(\omega). \tag{IV.127}$$

That $C_1(\vec{k},\omega)$ has no influence on the spectral analysis can be proven by calculating its contribution to the total noise power with the help of Eq.(97)

$$P_1 = \frac{V_p^2}{(2\pi)^4}\int_0^\infty d\omega\, N_c^{-1}(\omega) \int C_1(\vec{k},\omega)\, d\vec{k}. \tag{IV.128}$$

From Eq.(101)

$$\mid F_\tau(\vec{k},\omega)\mid^2 = \frac{1}{\omega^2 + (\chi + D k^2)^2}, \tag{IV.129}$$

which by combining with Eqs.(127), (128), and the definition $\lambda\tau = <N>$ leads to

$$P_1 = 2<N_p>^2. \tag{IV.130}$$

Evaluating the noise power, $P = \int^\infty S(\omega)\, d\omega$, using Eq.(88) yields $P = P_0 + P_1$ where

$$P_1 = \frac{V_p^2}{(2\pi)^4} \int_0^\infty d\omega\, N_c^{-1}(\omega) \int C_1(\vec{k}, \omega)\, d\vec{k}. \qquad \text{(IV.128)}$$

From Eq.(101)

$$|F_r(\vec{k}, \omega)|^2 = \frac{1}{\omega^2 + (\chi + D k^2)^2}, \qquad \text{(IV.129)}$$

which by combining with Eqs.(127), (128), and the definition $\lambda\tau = <N>$ leads to

$$P_1 = 2 <N_p>^2. \qquad \text{(IV.130)}$$

Evaluating the noise power, $P = \int_0^\infty S(\omega)\, d\omega$, using Eq.(88) yields $P = P_o - P_1$, where

$P_o = \int_0^\infty d\omega \int\int C_o(\vec{r}_1 - \vec{r}_2, \omega)\, d\vec{r}_1\, d\vec{r}_2$. Therefore

$$S(\omega)/C_{FN} \approx \frac{V_p^2}{N_c(\omega)} \int C_o(\vec{k}, \omega) \frac{d\vec{k}}{(2\pi)^3}. \qquad \text{(IV.131)}$$

This completes the proof that $C_1(\vec{k}, \omega)$ has no influence on $S(\omega)$.

By combining Eqs.(83), (99), and (129) the term $C_o(\vec{k}, \omega)$ is rewritten

$$C_o(\vec{k}, \omega) = \frac{2\pi^3\lambda}{V_t^2} \frac{1}{\omega^2 + (\chi + D k^2)^2} \prod_{i=1}^{3} \sum_{n_i=-\infty}^{\infty} \delta\Big(k_i - \frac{\pi n_i}{L_i}\Big). \qquad \text{(IV.132)}$$

Eqs.(131) and (132) then result in

$S(\omega)/C_{FN} \approx$

$$\frac{\lambda V_p^2}{4 V_t^2 N_c(\omega)\omega^2} \sum_{n_1, n_2, n_3=-\infty}^{\infty} \frac{1}{1 + \Big[\frac{1}{\omega\tau} + \frac{D\pi^2}{\omega}\Big(\frac{n_1^2}{L_1^2} + \frac{n_2^2}{L_2^2} + \frac{n_3^2}{L_3^2}\Big)\Big]^2}. \qquad \text{(IV.133)}$$

The goal now is to approximate the Eq.(133) summation by an integral for various

ranges of frequency ω.

As a consistency check and to make contact with the results of the previous section it is noted that Eq.(133) yields

$$\lim_{\omega > 1/\tau} S(\omega)/C_{FN} =$$

$$\frac{\lambda V_p^2}{4 V_l^2 N_c(\omega)\omega^2} \sum_{n_1 n_2 n_3 = -\infty}^{\infty} \frac{1}{1 + \left[\frac{D\pi^2}{\omega} \left(\frac{n_1^2}{L_1^2} + \frac{n_2^2}{L_2^2} + \frac{n_3^2}{L_3^2} \right) \right]^2}. \qquad \text{(IV.134)}$$

Assuming $L_3 < L_2 < L_1$ the summation can be approximated by a three dimensional k-space integration for the limiting form

$$\lim_{\omega > \Omega_3} \lim_{\omega > 1/\tau} S(\omega)/C_{FN} \approx \frac{\lambda V_p^2}{4\pi^3 V_l N_c(\omega)\omega^2} \int_0^{2\pi} d\phi \int_0^{\pi} d\theta \sin\theta \int_0^{\infty} \frac{dk\ k^2}{1 + \frac{D^2 k^4}{\omega^2}}$$

$$= \left(\frac{\lambda V_p^2}{2^{3/2} \pi V_l N_c(\omega) D^{3/2}} \right) \omega^{-1/2}, \qquad \text{(IV.135)}$$

where $d\vec{k} = \pi^3 V_l^{-1} d\vec{n}$ and $\Omega_i \equiv \pi^2 D / L_i^2$. The right side of Eq.(135) is also obtained by combining Eqs.(97) and (112), which involves $\lim_{\omega > 1/\tau} S_o^{\infty}(\omega)$. That Eq.(135) can be derived by two methods is because in both cases fluctuations do not have sufficient time to diffuse to the boundary. For $\lim_{\omega > 1/\tau} S_o^{\infty}(\omega)$ this is simply because the bounded fundamental solution to the diffusion equation has not been used. And for $\lim_{\omega > 1/\tau} S(\omega)$ given in Eq.(135) the other limit there is equivalent to assuming $\Lambda < L_3$, i.e. the correlation length is smaller than the smallest sample dimension. Again this effectively means the boundaries are not "felt" at this frequency.

The consequences of keeping τ finite are now investigated while still assuming $\omega > \Omega_3$. Later this restriction is relaxed. In this case Eq.(133) becomes

$$\lim_{\omega > \Omega_3} S(\omega)/C_{FN} \approx \frac{\lambda V_p^2}{\pi^2 V_t N_c(\omega) \omega^2} \int_0^\infty \frac{k^2 \, d\, k}{1 + \left[\frac{1}{\omega\tau} + \frac{D\, k^2}{\omega} \right]^2}. \qquad \text{(IV.136)}$$

By partial fraction expansion

$$\frac{1}{1 + \left[\frac{1}{\omega\tau} + \frac{D\, k^2}{\omega} \right]^2} = \frac{i}{2} \left[\frac{1}{D\, \omega^{-1} k^2 + q_+} - \frac{1}{D\, \omega^{-1} k^2 + q_-} \right], \qquad \text{(IV.137)}$$

where $q_\pm \equiv \frac{1}{\omega\tau} \pm i$. Combining Eqs.(136) and (137)

$$\lim_{\omega > \Omega_3} S(\omega)/C_{FN} \approx$$

$$\left(\frac{\lambda V_p^2}{\pi^2 V_t N_c(\omega) \omega^2} \right) \frac{i}{2} \left\{ \lim_{a \to \infty} \int_0^a \frac{k^2\, dk}{q_+ + D\, \omega^{-1} k^2} - \int_0^a \frac{k^2\, dk}{q_- + D\, \omega^{-1} k^2} \right\}. \qquad \text{(IV.138)}$$

Evaluating the integrals leads to

$$\lim_{\omega > \Omega_3} S(\omega)/C_{FN} = \frac{\lambda V_p^2 \, r^{1/2} \sin(\theta/2)}{2\pi V_t N_c(\omega) D^{3/2} \omega^{1/2}}. \qquad \text{(IV.139)}$$

Eq.(139) is checked by taking

$$\lim_{\omega > \frac{1}{\tau}} \lim_{\omega > \Omega_3} S(\omega)/C_{FN} = \frac{\lambda V_p^2}{2^{3/2} \pi V_t N_c(\omega) D^{3/2} \omega^{1/2}},$$

which is again Eq.(135) as it should be. In the short time limit the frequency dependence of Eq.(139) reduces to

$$\lim_{\omega < \frac{1}{\tau}} \lim_{\omega > \Omega_3} S(\omega)/C_{FN} = \frac{\lambda V_p^2 \tau^{1/2}}{4\pi V_t N_c(\omega) D^{3/2}}. \qquad \text{(IV.140)}$$

Eq.(140) shows that the presence of a finite lifetime τ results in a flat low frequency spectrum. The above arguments also demonstrate the consistency of the partial fraction expansion and the approximation method, which replaces the summation by integration.

The next case to be dealt with is

$$\Omega_2 < \omega < \Omega_3.$$

Here the n_3 summation is negligible with respect to the other terms and is replaced by a δ-function, which gives

$$S(\omega)/C_{FN} = \frac{\lambda V_p^2}{2\pi V_t N_c(\omega)\omega^2 L_3} \int_0^\infty \frac{k\ dk}{1 + \left[\frac{1}{\omega\tau} + D\,\omega^{-1}k^2\right]^2}. \qquad \text{(IV.141)}$$

Substituting Eq.(137) into (141) yields

$$S(\omega)/C_{FN} =$$

$$\frac{\lambda V_p^2}{2\pi V_t N_c(\omega) L_3 \omega^2} \left\{ \frac{i}{2} \lim_{a\to\infty} \int_0^a \frac{k\ dk}{q_+ + D\,\omega^{-1}k^2} - \int_0^a \frac{k\ dk}{q_- + D\,\omega^{-1}k^2} \right\}. \qquad \text{(IV.142)}$$

Evaluating the integrals converts Eq.(142) to

$$S(\omega)/C_{FN} = \frac{\lambda V_p^2\ Arctan\,(\omega\tau)}{4\pi V_t N_c(\omega) D L_3 \omega}. \qquad \text{(IV.143)}$$

The limit forms of Eq.(143) are

$$\lim_{\omega > \frac{1}{\tau}} S(\omega)/C_{FN} = \left\{ \frac{\lambda V_p^2}{2^{5/2}\pi V_t N_c(\omega) L_3 D} \right\} \omega^{-1} \qquad \text{(IV.144)}$$

and

$$\lim_{\omega < \frac{1}{\tau}} S(\omega)/C_{FN} = \left(\frac{\lambda \tau V_p^2}{4 \pi N_c(\omega) V_t L_3 D} \right). \qquad \text{(IV.145)}$$

The results assume $\Omega_2 < \omega < \Omega_3$ with Eq.(145) applicable only if $\Omega_2 < \frac{1}{\tau} < \Omega_3$. The finite lifetime τ again flattens the spectrum at low frequencies.

The next case is

$$\Omega_1 < \omega < \Omega_2.$$

Here Eq.(133) reduces to

$$S(\omega)/C_{FN} = \left(\frac{\lambda V_p^2}{4 \pi N_c(\omega) V_t L_3 L_2 \omega^2} \right) \int_0^\infty \frac{dk}{1 + \left[\frac{1}{\omega \tau} + \frac{D k^2}{\omega} \right]^2}. \qquad \text{(IV.146)}$$

The partial fraction expansion, Eq.(137), converts Eq.(146) to

$$S(\omega)/C_{FN} = \left(\frac{\lambda V_p^2}{4 \pi V_t N_c(\omega) L_2 L_3 \omega^2} \right)$$

$$\left(\frac{i}{2} \lim_{a \to \infty} \int_0^a \frac{dk}{q_+ + D \omega^{-1} k^2} - \int_0^a \frac{dk}{q_- + D \omega^{-1} k^2} \right). \qquad \text{(IV.147)}$$

Evaluating the integrals results in

$$S(\omega)/C_{FN} = \frac{\lambda V_p^2}{8 N_c(\omega) V_t L_2 L_3 D^{1/2} \omega^{3/2}} \left(\frac{\sin \frac{\theta}{2}}{r^{1/2}} \right). \qquad \text{(IV.148)}$$

The limiting forms of Eq.(148) are

$$\lim_{\omega > \frac{1}{\tau}} S(\omega)/C_{FN} = \left(\frac{\lambda V_p^2}{2^{7/2} N_c(\omega) V_t L_2 L_3 D^{1/2}} \right) \omega^{-3/2} \qquad \text{(IV.149)}$$

and

$$\lim_{\omega < \frac{1}{\tau}} S(\omega)/C_{FN} = \frac{\lambda V_p^2 \tau^{3/2}}{16 N_c(\omega) V_t L_2 L_3 D^{1/2}}. \qquad \text{(IV.150)}$$

Again the presence of τ produces a flat low frequency spectrum, Eq.(150), for the case $\Omega_1 < \omega < \Omega_2$.

The next case is

$$\omega < \Omega_1.$$

Here Eq.(133) reduces to

$$S(\omega)/C_{FN} = \frac{\lambda V_p^2}{4 V_t^2 N_c(\omega) \omega^2} \left[\frac{1}{1 + \left(1/\omega\tau \right)^2} \right]. \qquad \text{(IV.151)}$$

The limiting forms of Eq.(151) are

$$\lim_{\omega > \frac{1}{\tau}} S(\omega)/C_{FN} = \left(\frac{\lambda V_p^2}{4 V_t^2 N_c(\omega)} \right) \omega^{-2} \qquad \text{(IV.152)}$$

and

$$\lim_{\omega < \frac{1}{\tau}} S(\omega)/C_{FN} = \frac{\lambda \tau^2 V_p^2}{4 V_t^2 N_c(\omega)}. \qquad \text{(IV.153)}$$

The final question that needs answering before putting together all of the results is, what influence does imposing an upper limit in k-space have on $S(\omega)$? This effect will be important at high frequencies where small length scales are involved. Recall the existence of this limit arose from the correlated volume construction, whose origin requires that an individual fluctuation be correlated with itself. Let this upper limit be defined as $k_o \equiv \pi/\delta$. In this case Eq.(133) becomes

$$S(\omega)/C_{FN} =$$

$$\frac{\lambda V_p^2}{4 V_t^2 N_c(\omega)\omega^2} \sum_{|n_i| \le L_i/\delta} \frac{1}{1 + \left[\frac{1}{\omega\tau} + \frac{D\pi^2}{\omega}\left(\frac{n_1^2}{L_1^2} + \frac{n_2^2}{L_2^2} + \frac{n_3^2}{L_3^2} \right) \right]^2}. \quad \text{(IV.154)}$$

Again the summation is approximated by a k-space integration. As the affect of τ on the spectrum is now well documented and because only high frequencies are influenced by the k-space limit, $\omega > \frac{1}{\tau}$ is assumed. Carrying out the integration yields

$$S(\omega)/C_{FN} = \frac{\lambda V_p^2}{2^{3/2}\pi^2 V_t N_c(\omega) D^{3/2}\omega^{1/2}}$$

$$\left[\frac{1}{2}\log\left(\frac{x^2 - 2^{1/2}x + 1}{x^2 + 2^{1/2}x + 1} \right) + \tan^{-1}\left(\frac{2^{1/2}x}{1 - x^2} \right) \right], \quad \text{(IV.155)}$$

where $x = \frac{\pi}{\delta}\sqrt{D/\omega}$. The high frequency limit of Eq.(155) is

$$\lim_{\Omega_4 < \omega} S(\omega)/C_{FN} = \left(\frac{\pi\lambda V_p^2}{3 N_c(\omega) V_t \delta^3} \right) \omega^{-2}, \quad \text{(IV.156)}$$

where $\Omega_4 \equiv \pi D^2/\delta$. The low frequency limit of Eq.(155) is

$$\lim_{\omega < \Omega_4} S(\omega)/C_{FN} = \frac{\lambda V_p^2 \delta}{\pi^3 V_t N_c(\omega) D^2}. \quad \text{(IV.157)}$$

1. Summary of section F.

Table 1. Limit cases of $C_o(\, x=0\,,\, \omega\,)$

	$\omega < 1/\tau$		$\omega > 1/\tau$	
$\omega < \Omega_1$	$\left(\frac{\lambda \tau^2}{4 V_t^2} \right)$	(IV.153)	$\left(\frac{\lambda}{4 V_t^2} \right) \omega^{-2}$	(IV.152)
$\Omega_1 < \omega < \Omega_2$	$\left(\frac{\lambda \tau^{3/2}}{16 V_t L_2 L_3 D^{1/2}} \right)$	(IV.150)	$\left(\frac{\lambda}{2^{7/2} V_t L_2 L_3 D^{1/2}} \right) \omega^{-3/2}$	(IV.149)
$\Omega_2 < \omega < \Omega_3$	$\left(\frac{\lambda \tau}{4 \pi V_t L_3 D} \right)$	(IV.145)	$\left(\frac{\lambda}{2^{5/2} \pi V_t L_3 D} \right) \omega^{-1}$	(IV.144)
$\Omega_3 < \omega < \Omega_4$	$\left(\frac{\lambda \tau^{1/2}}{4 \pi V_t D^{3/2}} \right)$	(IV.140)	$\left(\frac{\lambda}{2^{3/2} \pi V_t D^{3/2}} \right) \omega^{-1/2}$	(IV.135)
	$\omega < \Omega_4$		$\omega > \Omega_4$	
	$\left(\frac{\lambda \delta}{\pi^3 V_t D^2} \right)$	(IV.157)	$\left(\frac{\lambda \pi}{3 V_t \delta^3} \right) \omega^{-2}$	(IV.156)

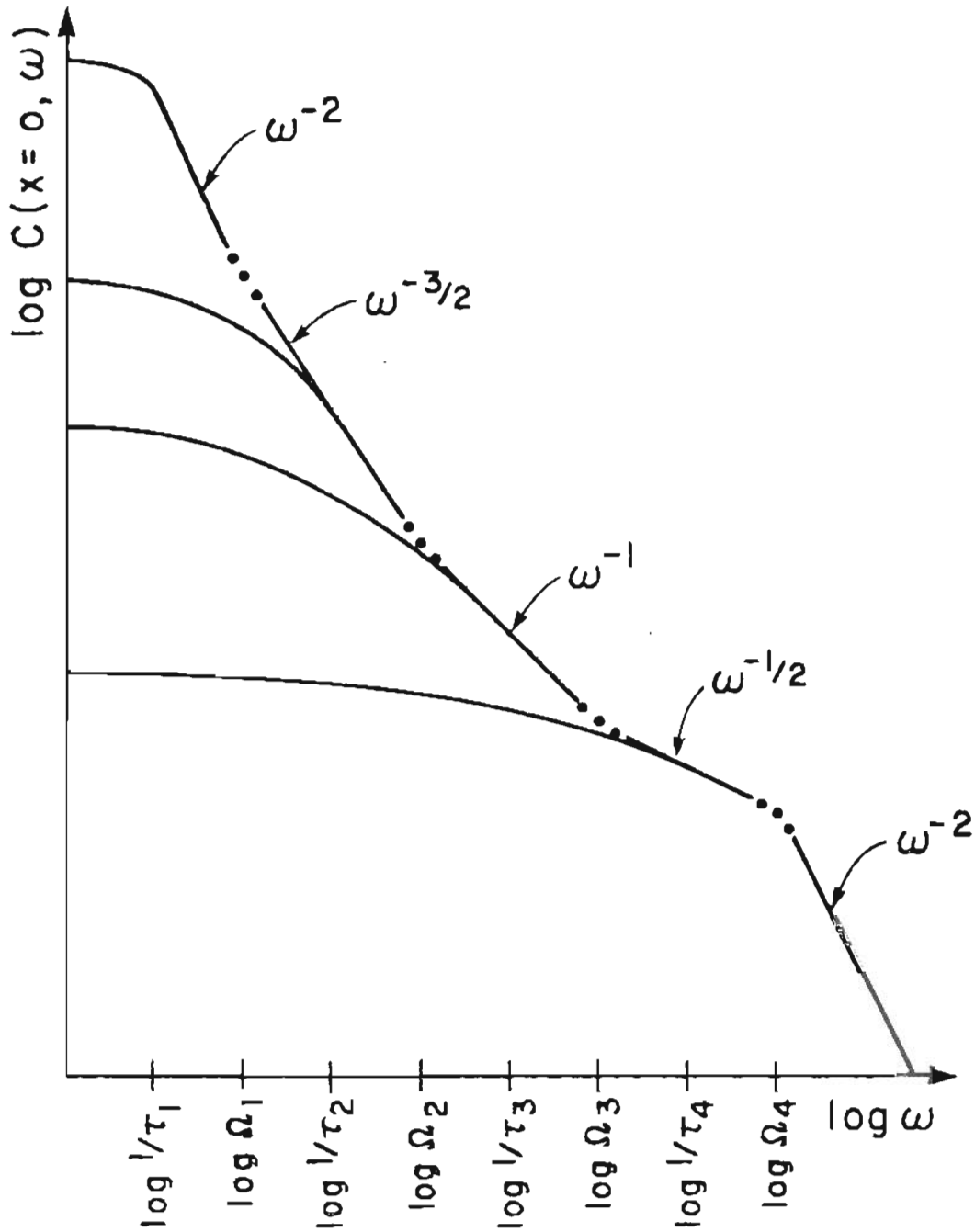

Fig.17. Graph of the point-frequency correlation function $C(\ x=0\,,\omega)$. See table 1 for a summary of the various limit cases. $\Omega_i \equiv \pi^2 D/L_i^2$ and $L_4 \equiv \delta$. To show the finite lifetime effect various values of τ are given.

The limiting forms of the point-frequency correlation $C(\,x=0\,,\,\omega\,)$, which include the boundary effects due to finite sample size are summarized in Table 1 where Eq.(97) has been used, $S(\omega) = V_p^2\, C(x=0,\omega)/N_c(\omega)$. The results show that if $\omega < 1/\tau$ then $C(\,x=0\,,\,\omega\,)$ is constant, which proves that the finite fluctuation lifetime τ removes, in every case, a divergent $\lim_{\omega\to 0} S(\omega)$. These results are graphed in Fig.17, which is, to within scale factors, similar to that given by Bliek; except he has not provided the correct low frequency functional dependence of $C(\,x=0\,,\,\omega\,)$ and has erroneously identified this function with $S(\omega)$ itself.

This section essentially completes the mathematical analysis required for formulation of the diffusive theory of equilibrium fluctuations in the GCE. The following section synthesizes these results in graphical form to produce the spectral density function $S(\omega)$ in a form that can be compared to the experimental data. Various characteristics of $S(\omega)$ are discussed along with the physical interpretation of the pertinent variables.

G. The spectral density function $S(\omega)$.

We have finally reached the point where the noise spectrum $S(\omega)$ itself can be discussed. The principal relation is Eq.(131), which is rewritten as

$$S(\omega) \approx V_p^2 \, C_o(x=0,\omega) \, N_c^{-1}(\omega). \qquad \text{(IV.158)}$$

The point-frequency correlation $C_o(x=0,\omega)$ was evaluated in the previous section and found to contain the geometrical effects due to the sample itself. Its functional form is graphed in Fig.17. The other major factor that influences $S(\omega)$ is the frequency-dependent number of correlated volumes $N_c(\omega)$. It represents the spatial averaging of the probe as shown in section E. For clarity its properties, given by Eqs.(114a-d), are reproduced in Table 2.

Table 2. The correlated volume number $N_c(\omega)$, $\omega_i \equiv 2D/l_i^2$

$\omega_3 < \omega$	$N_c^{-1} \approx (2D/\omega)^{3/2}/V_p$
$\omega_2 < \omega < \omega_3$	$N_c^{-1} \approx (2D/\omega)/l_1 l_2$
$\omega_1 < \omega < \omega_2$	$N_c^{-1} \approx (2D/\omega)^{1/2}/l_1$
$\omega < \omega_1$	$N_c^{-1} \approx 1$

Each frequency band is delimited by combination of the sets of characteristic frequencies $\{\Omega_i \equiv \pi^2 D/L_i^2\}$ and $\{\omega_i \equiv 2D/l_i^2\}$ associated with the various limit forms

of $C_o(x=0,\omega)$ and $N_c(\omega)$ given in tables 1 and 2. These sets are themselves defined in terms of the probe (l_1, l_2, l_3) and net plane (L_1, L_2, L_3) geometries and the resolution of the detector $\delta \equiv L_4$, which in the present case is the field emission microscope. Therefore particular sets $\{\Omega_i\}$ and $\{\omega_i\}$ determine $S(\omega)$ to within scale factors, one each for the ordinate and frequency abscissa. As a test of the theory thermal field electron noise data is analyzed [1]. These measurements provide the experimental $S(\omega)$ and the probe area A_p. This latter variable is derived from the Fowler-Nordheim (FN) equation. The theoretical $S(\omega)$ is fit to the experimental noise spectrum by setting the characteristic frequencies $\{\Omega_i\}$ and $\{\omega_i\}$ so that $dS(\omega)/d\omega$ is matched over the entire frequency range. Knowledge of A_p then automatically determines $\{l_i\}$. Once the $S(\omega)$ curves are fit the $\{\Omega_i\}$ and $\{\omega_i\}$, which correspond to changes in $dS(\omega)/d\omega$, are equated to the measured frequencies. From this comparison the diffusion coefficient is obtained from every Ω_i and ω_i appearing in $S(\omega)$ over the measured frequency band. The minimum resolvable length δ is also obtained given Ω_4 can be identified. The finite lifetime τ is found by identifying the frequency $\omega = 1/\tau$ where $dS(\omega)/d\omega = 0$.

Before proceeding to the data analysis additional remarks are required concerning the adatom creation rate λ. A standard free energy minimization argument is followed [15] to explain the Schottky-type lattice defect mechanism as depicted in Fig.18. It is assumed that the defect energetics are temperature independent and the eigenfrequencies of the lattice vibrations do not change significantly.

Given there exists m defect adatoms and M equilibrium sites then the system entropy is

$$S = k\left[\log \frac{M!}{(M-m)!\,m!}\right]. \qquad \text{(IV.159)}$$

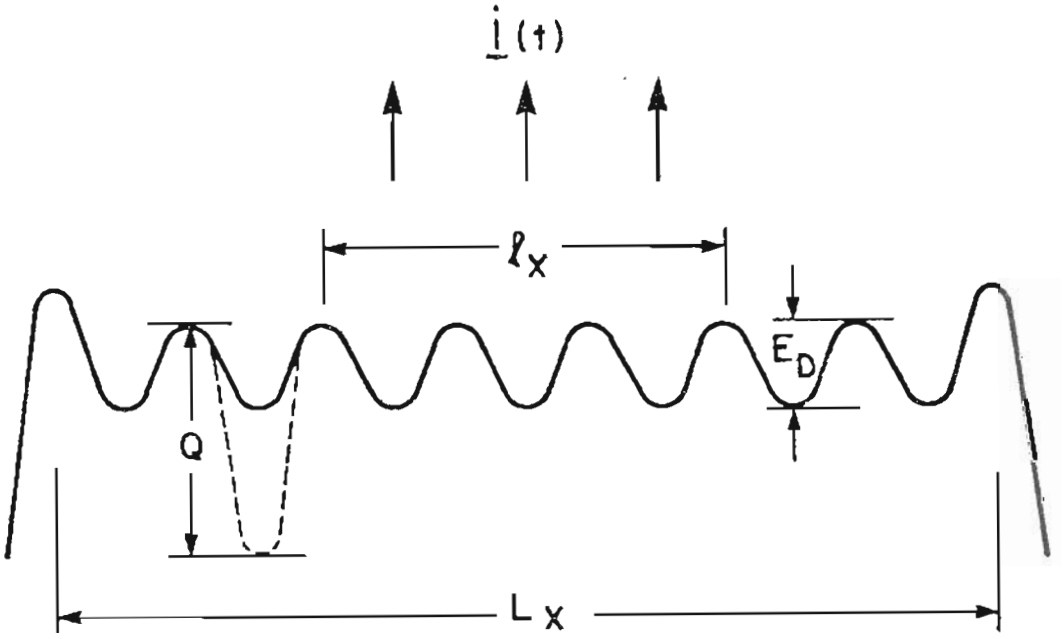

Fig.18. Diagram of relevant parameters involved in the diffusion model. The defect adatom vacancy formation energy Q and the diffusion activation energy E_D are specified along with a linear dimension of the net plane L_x and probed region l_x from which the fluctuating current $\mathrm{i}(t)$ is collected.

The work required for diffusion of an atom reversibly far removed from the lattice site is E_D so the internal energy is

$$U = m\, E_D \tag{IV.160}$$

and the Helmholtz free energy is

$$A = U - T\, S. \tag{IV.161}$$

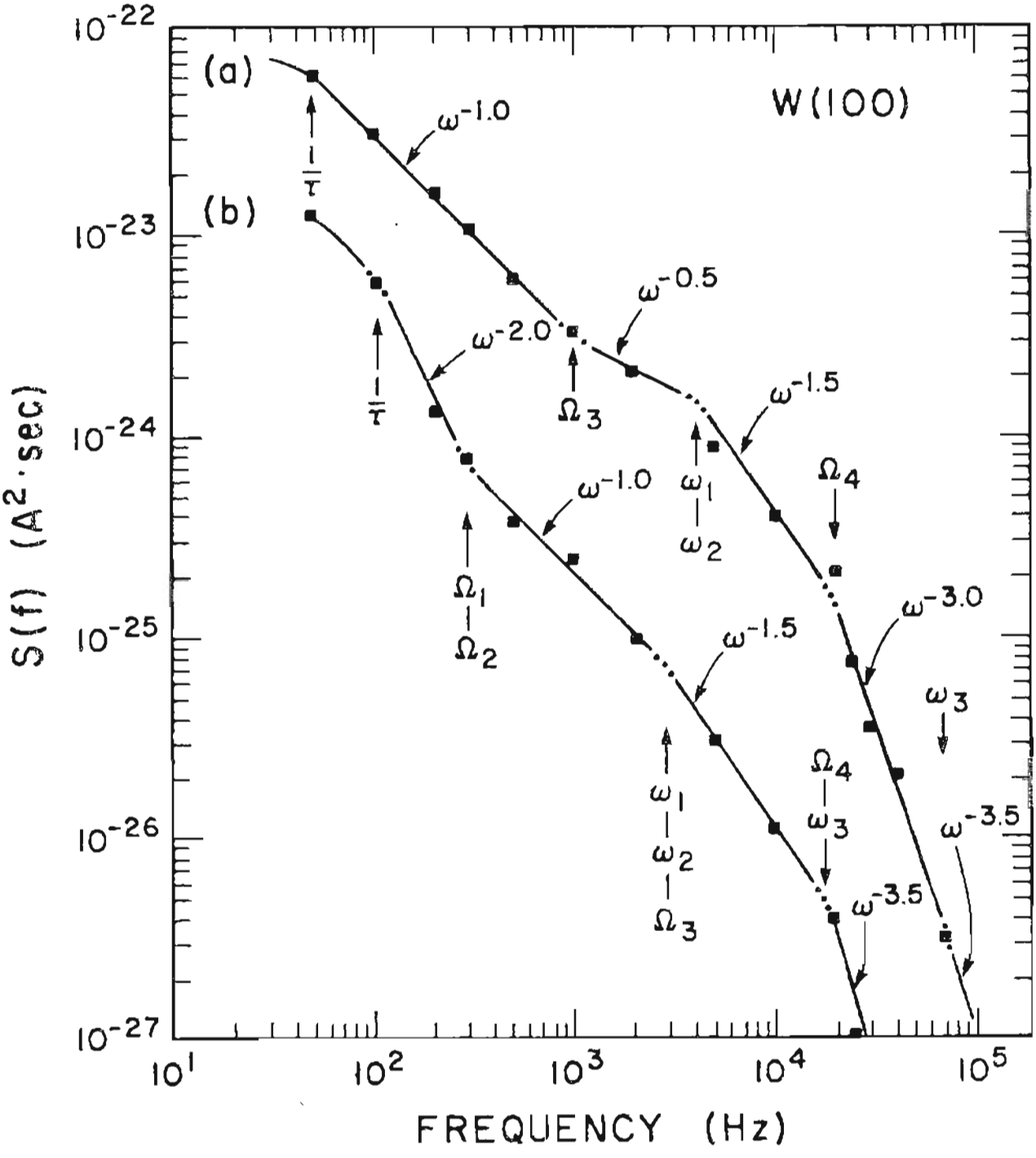

Fig.19. Graph of the variation of the spectral density function $S(f)$ with frequency. Curve (a) is at $905K$ and curve (b) is at $1318K$. The sets of characteristic frequencies $\{\Omega_i\}$ and $\{\omega_i\}$ define the range over which $dS(\omega)/d\omega$ has the indicated slopes. The solid squares correspond to the experimental measurements of ref.[1].

$$(\partial A / \partial m)_T = 0. \qquad \text{(IV.162)}$$

This condition coupled with Eqs.(159-161) yields

$$\lambda = \lambda_o \, e^{-Q/kT}, \qquad \text{(IV.163)}$$

where $\lambda = m\,\nu$, ν is the average vibrational frequency of the atom at a lattice site, $\lambda_o = \nu N$, and it is assumed that $m \ll M$.

1. Graphical Analysis.

Having completed the discussion concerning the general procedure for curve fitting and the rate λ it is now possible to proceed to specific cases corresponding to different orientations of $W(hkl)$ planes from which thermal field electron emission noise spectra were measured [1].

i) W(100).

Referring first to curve (a) of Fig.19, which is $S(\omega)$ measured at $905K$, the characteristic frequencies that provide the best fit to the measured $S(\omega)$ are

$$\Omega_3 = 10^3\,Hz,\ \Omega_4 = 2{\times}10^4\,Hz,\ 1/\tau = 50\,Hz$$

$$\omega_1 = \omega_2 = 4{\times}10^3\,Hz,\ \omega_3 = 7{\times}10^4\,Hz.$$

Fig.20 shows that there is no field induced buildup at $905K$. It is therefore possible to use the measured FN area as the probe area $A_p = 1400$ Å ^{2}. Curve (a) shows $\omega_1 = \omega_2$ and thus $l_1 = l_2 = 37$ Å and $l_3 = 9$ Å is obtained from the ratio ω_3/ω_1. The diffusion coefficient is then found from $D = \omega_i l_i^2/2$ to be $D(905K) = 2.8{\times}10^{-10}\,cm^2/sec$.

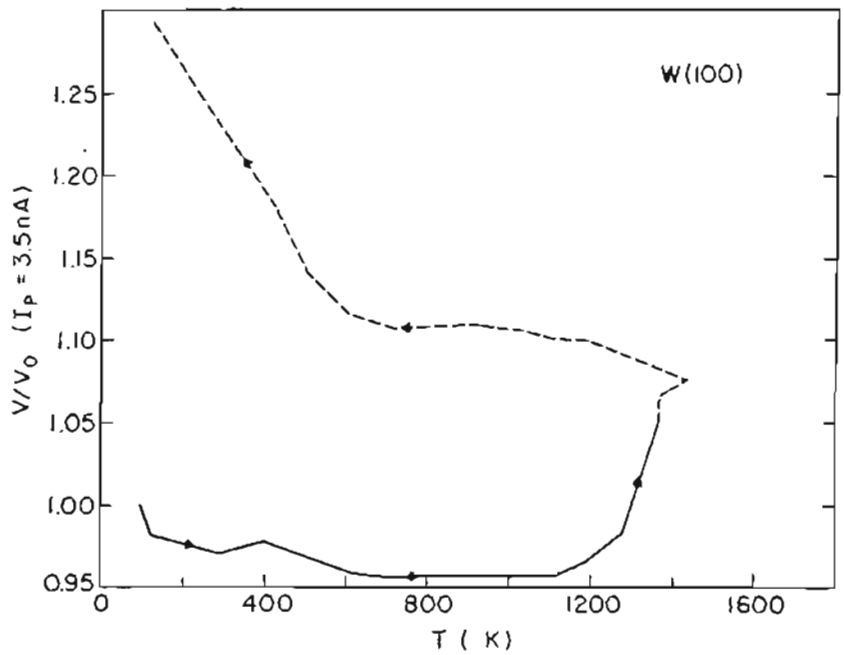

Fig.20. Curve shows the variation of the voltage ratio required to maintain a constant probe current i_p emitted from a W(100) plane. Dashed line is due to thermal field buildup of the surface. The graph is a reproduction of Fig.1 of ref.[1].

Using $\Omega_4 = \pi^2 D / \delta^2$ the minimum length $\delta = 37$ Å , which gives the resolution of the field emission microscope for this case. This value can be compared with the resolution limit derived by Gomer who calculated it by considering the electron momentum distribution transverse to the normal emission direction [16]. The expression assumes a Fermi-Dirac distribution at $0K$ and is given by

$$\delta = 2.62\times10^{-4}\,\beta\,(r_t/k\,\alpha\,\phi^{1/2})^{1/2} \quad cm, \qquad \text{(IV.164)}$$

where β is the beam angular compression factor due to local demagnification of the emitted electrons caused by electrostatic shielding of the emitter shank. It is calculated from $\beta = \sqrt{A_p/A_g}$, A_g is the geometrical or "apparent" area determined from the emitter apex radius r_t and the angle subtended by the probe hole in the anode. r_t is found from the slope of the FN plot, which also yields the field factor $k = V/Fr_t \approx 5$. This term represents the reduction of the surface electric field F for a given applied voltage V that is also caused by emitter-shank shielding. The term $\alpha \equiv (1-y)^{1/2}$ with $y = 3.8\times10^{-4}F^{1/2}/\phi$ is the result of the image force reduction of the field F, which appears in the FN equation [16]. A value of $\alpha = 0.8$ is assumed throughout as this corresponds to fields $F = 0.1-0.5\ V/\text{Å}$ and $\phi = 4.52\ eV$. The latter value is the average work function of tungsten [17]. Using the measured $r_t = 610$ Å and $\phi(100) = 4.62\,eV$ yields $\delta = 58$ Å , which is in reasonable agreement with the value obtained from the noise theory. The length $L_3 = \sqrt{\pi^2 D/\Omega_3}$ is calculated to be $L_3 = 166$ Å . While $l_3 = 9$ Å appears to be a reasonable value for the depth of the probed region, here and in the following cases, L_3 consistently is larger than one might first expect. However this systematic overestimation results from the resolution limit of the microscope. The smallest resolvable length scale is $L_4 = \delta$ and by definition $L_3 > \delta$. Therefore a sample dimension can be estimated only if the detector can resolve that particular length. That this is a reasonable conclusion is partly corroborated by calculating the correlation length $\Lambda(\Omega_3) = \sqrt{2D/\Omega_3}$, which yields $\Lambda(\Omega_3) = 75$ Å $< L_3$. This says that the noise at Ω_3 is not influenced by increasing the sample depth beyond 75 Å . The net plane area A_t was not measured and cannot be evaluated here as Ω_1 and Ω_2 do not appear in Fig.19. Typically

$L_1, L_2 \gg \delta$ is true and so the net plane area estimate will be accurate given these characteristic frequencies appear in the measured $S(\omega)$.

Next consider curve (b) of Fig.19, which corresponds to thermal field emission at $1318K$. The characteristic frequencies are

$$1/\tau = 10^2\,Hz,\ \Omega_1 = \Omega_2 = 300\,Hz,\ \omega_1 = \omega_2 = \Omega_3 = 3\times10^3\,Hz,\ \Omega_4 = 1.4\times10^4\,Hz.$$

First note that $\omega_i(1318K) \leq \omega_i(905K)$. Since $dD/dT > 0$ and $\omega_i = 2D/l_i^2$ this result implies $dl_i/dT \geq 0$, i.e. the probed volume has increased with temperature. This is caused by an increase in the net plane area due to the buildup process, which in turn increases the beam angular compression factor β. Because the average emitter apex radius r_t remains unchanged the apparent area A_g is constant and the local demagnification is directly related to A_p only [1]. Evidence for the thermal field buildup of the net plane is given in Fig.20. An irreversible change occurs at $1350K$, but note that by $1318K$ the voltage ratio required to keep the probe current constant has increased significantly. This reflects a corresponding increase in the net plane area.

Therefore the low temperature estimate $A_p = 1400$ Å cannot be used as the case at $905K$. Instead the probed area is estimated as follows.

Because the net plane radius is proportional to the applied voltage the V/V_o curve shown in Fig.20 allows a linear dimension of the probed region to be approximated by

$$l_i(T)/l_o = e^{b(T-T_o)} \qquad \text{(IV.165)}$$

in the interval $1100K \leq T \leq 1350K$. This is also based on the assumption that the apparent area A_g is constant over this temperature range, which is true for the case

discussed here. To find the empirical constant b other boundary conditions are required for Eq.(165). This necessitates using Swanson's data from a different emitter, labeled "C" in his study [1]. The reason for this is that the FN area A_p corresponding to emitter "C" has been given for both the low temperature and built up W(100) planes. This sets the initial and final values of $l_i(1350K)/l_o(1100K)$ in Eq.(165), which were measured as $A_p(1100K) = 1500$ Å^2 and $A_p(1350K) = 2.37\times10^6$ Å^2 . These values yield $l_1(1350K) = 1.5\times10^3$ Å and $l_1(1100K) = 39$ Å and then $b = 1.46\times10^{-2}\ (K^{-1})$.

The interpolated value for the W(100), $A_p(1318K)$ can now be found for emitter "A", which corresponds to the measured $S(\omega)$ plotted in Fig.19. For this emitter $l_o = 37$ Å and hence $l_1 = l_2 = 892$ Å . The diffusion coefficient then directly follows, $D(1318K) = 1.2\times10^{-7}\ cm^2/sec$. From the values for $D(905K)$ and $D(1318K)$ the corresponding activation energy is $E_D = 1.5\ eV$.

The activation energy for vacancy formation Q is found by first noting from Fig.19 that at $f = 1\ KHz$ $S(f) \propto f^{-1}$ in the range $905K \leq T \leq 1318K$. Define $d\ln S(\omega)/d\,1/T = -E_m/k$. Then from Eq.(144), $S(\omega) \propto \lambda/A_t\, D\ \omega$, from which follows

$$E_m = Q - E_D - 2bk(T - T_o)^2, \qquad \text{(IV.166)}$$

where the buildup energetics of A_t are given by Eq.(165). The $S(\omega, T)$ data of Fig.19 yields $E_m = 0.66\ eV$ therefore the defect adatom vacancy formation activation energy is $Q = 2.6\ eV$.

Finally from Ω_4 the resolution for the W(100) plane at $1318K$ is $\delta = 920$ Å . Eq.(164) predicts $\delta = 1322$ Å . These large values are caused by large beam angular compression due to W(100) net plane buildup.

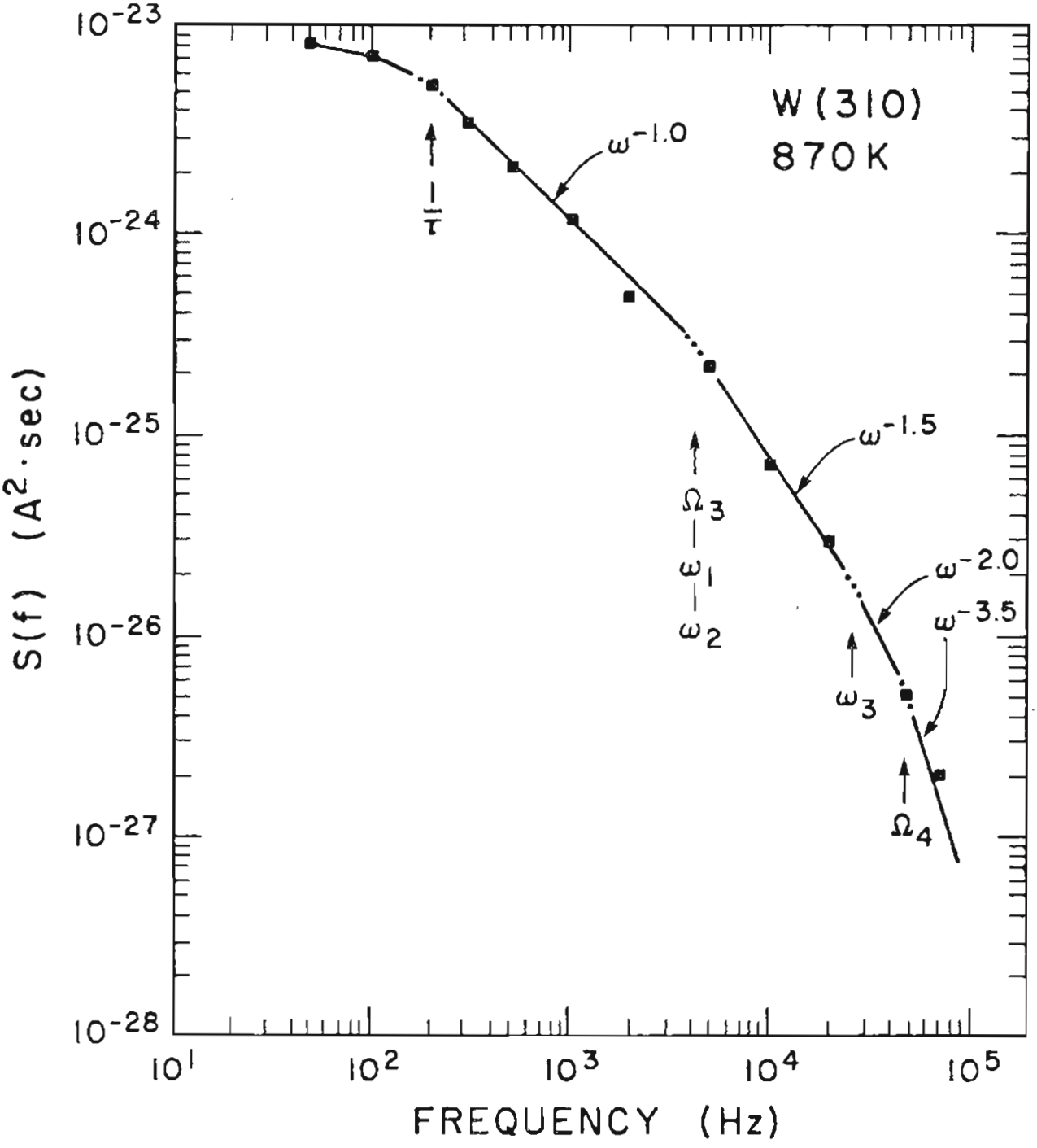

Fig.21. Graph of the variation of the spectral density function $S(f)$ with frequency for W(310) at $870K$. The solid squares correspond to the experimental data of ref.[1].

ii) W(310).

Fig.21 graphs the thermal field noise spectrum $S(\omega)$ from reference [1] measurements along with the predicted $S(\omega)$ and the sets of characteristic frequencies $\{\Omega_i\}$ and $\{\omega_i\}$ used for the curve fitting, which are

$$1/\tau = 200\,Hz,\ \omega_1 = \omega_2 = \Omega_3 = 4{\times}10^3\,Hz,\ \omega_3 = 2.6{\times}10^4\,Hz,\ \Omega_4 = 5{\times}10^4\,Hz.$$

The probe area $A_p = 1900$ Å^2, was measured, which implies $l_1 = l_2 = 44$ Å , and with ω_3/ω_1 yields $l_3 = 17$ Å . The resolution given by Ω_4 is $\delta = 27$ Å while Eq.(164) gives $\delta = 49$ Å , using $\beta = 1.83$, $\phi = 4.52\,eV$, and $r_t = 896$ Å . The diffusion coefficient is then determined to be $D(870K) = 3.8{\times}10^{-10}\,cm^2/sec$.

Fig.22 graphs the measured noise data for W(310) at $1318K$ along with the theoretical $S(\omega)$ and the corresponding sets $\{\Omega_i\}$ and $\{\omega_i\}$, which are

$$1/\tau = 10^2\,Hz,\ \Omega_3 = 4{\times}10^2\,Hz,\ \omega_1 = \omega_2 = 7{\times}10^3\,Hz,\ \omega_3 = \Omega_4 = 10^4\,Hz.$$

As with the W(100) plane the (310) exhibits thermal field facetting above $1000K$, which becomes irreversible above $1400K$, as shown in Fig.23.

A complication with the (310) plane not found with the (100) orientation appears when comparing Figs.(20) and (23). From the FN measurements the (310) is known to increase its surface area with increasing temperature, yet the voltage ratio shown in Fig.23 actually decreases during the buildup process. Thus while the (100) buildup process is directly related to the electric field reduction, as shown by the increase in the voltage ratio V/V_o, the process is masked for the (310). There are two reasons that might explain this behavior. The emitter used to produce the (310) data depicted in Figs.(20) and (23) had a (100) on-axis orientation, which results in off-axis emission from the (310). Also other low index planes are building up at a greater rate than this surface. This could cause an increase in the local field above the (310) plane by placing it at the edge of two larger low index planes. As $A_p(1318K)$ cannot be determined by

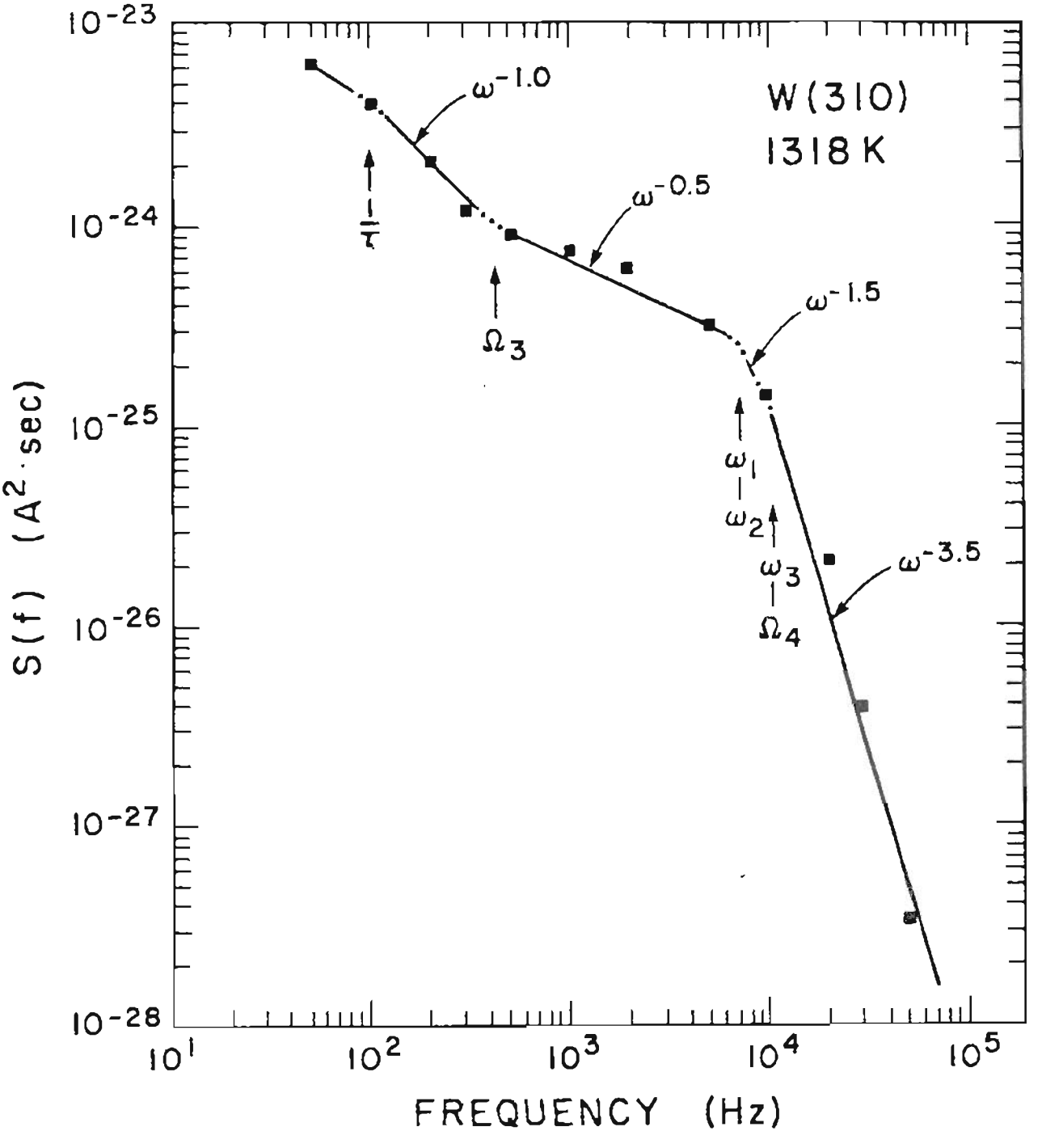

Fig.22. Graph of the variation of the spectral density function $S(f)$ with frequency for W(310) at $1318K$. The solid squares correspond to the experimental data of ref.[1].

the empirical curve fitting method used previously it is instead found from the fractional area increase of the FN area upon buildup. This measurement used a separate emitter "C" from that employed in the noise spectrum measurement, "A". The area

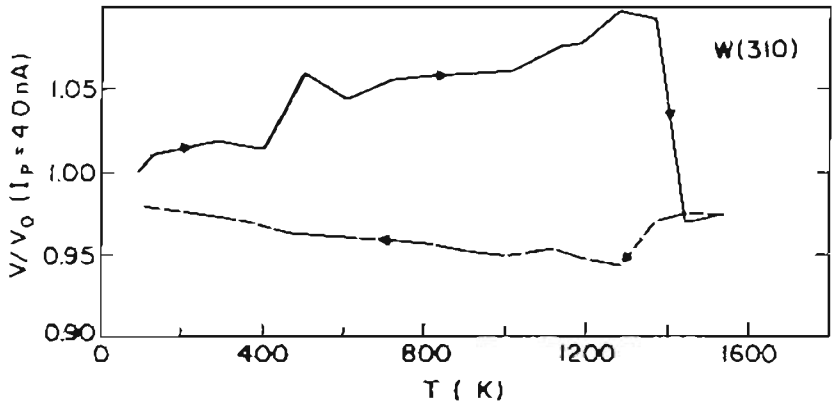

Fig.23. Graph of the variation of the voltage ratio required to maintain $i_p = 4.0\,nA$ on the W(310) plane. Dashed line results from thermal field build up of the surface. The figure is a reproduction of Fig.2 of ref.[1].

$A_p = 890$ Å . Therefore the estimated area at $1318K$ is $A_p(1318K) = 890$ Å $\times 1.95 = 1733$ Å . This value and Fig.22 imply $l_1 = l_2 = 42$ Å and $l_3 = 35$ Å . The resolution limit is $\delta = 77$ Å . Eq.(164) predicts $\delta = 64$ Å . The diffusion coefficient is $D(1318K) = 6.1\times10^{-10}\,cm^2/sec$. Combined with $D(870K)$ this latter value yields an activation energy $E_D = 0.1\,eV$. The defect activation energy cannot be calculated because the net plane area energetics are unknown.

iii) W(112).

Fig.24 graphs the noise spectrum from a W(112) emitter at $905K$. No higher temperature measurement of $S(\omega)$ was taken for this plane, which precludes a

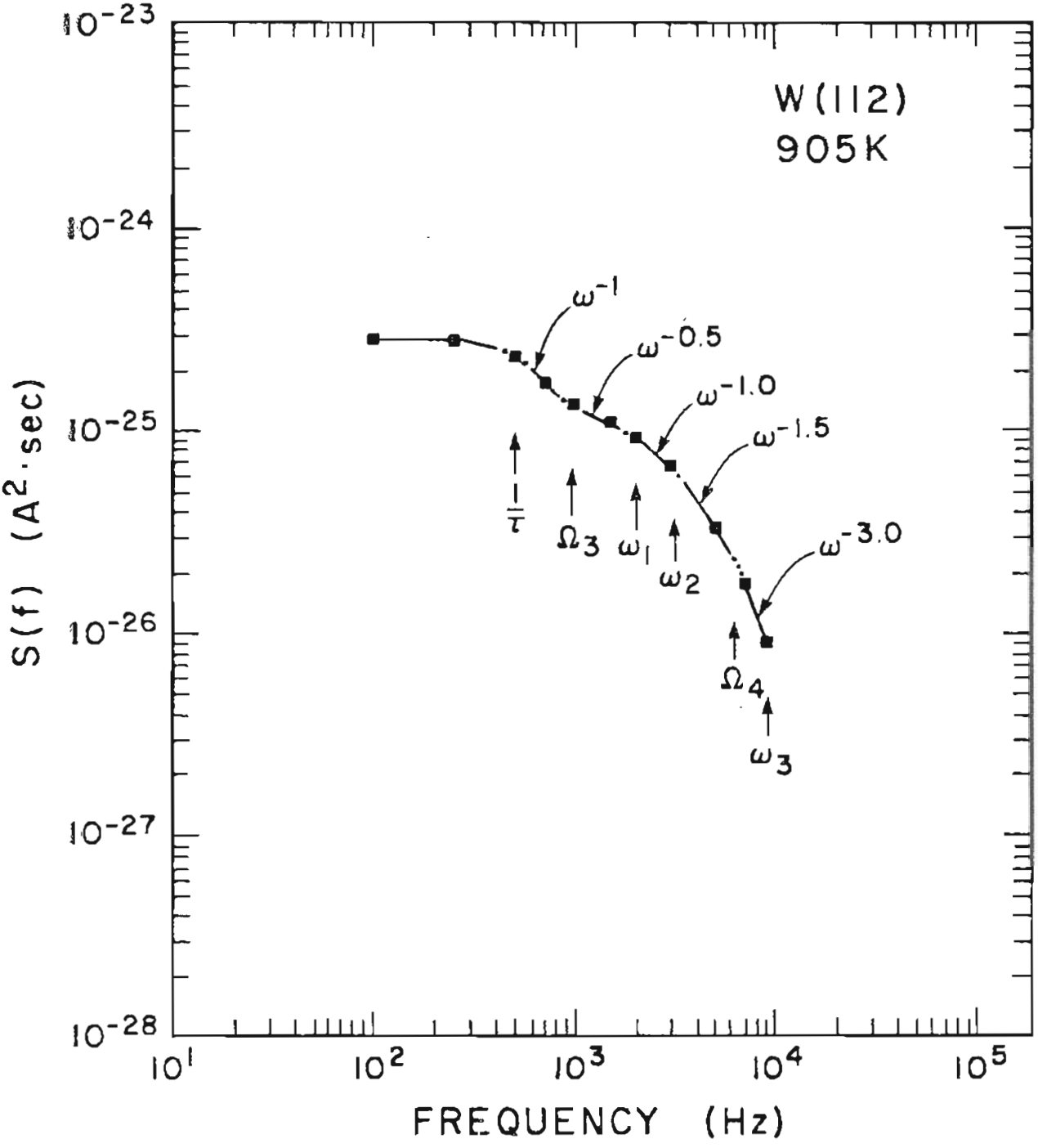

Fig.24. Graph of the variation of the spectral density function $S(f)$ with frequency. The solid squares correspond to the experimental data of ref.[1].

determination of $E_D(112)$. The characteristic frequencies are

$$1/\tau = 5\times10^2\,Hz,\ \Omega_3 = 10^3\,Hz,\ \omega_1 = 2\times10^3\,Hz,$$

$$\omega_2 = 3\times10^3\,Hz,\ \Omega_4 = 6.5\times10^3\,Hz,\ \omega_3 = 9\times10^3\,Hz.$$

The ω_2/ω_1 ratio indicates $l_1 = 1.2\,l_2$. This may be evidence for a slight anisotropy in the beam compression factor. The emitter used for the W(112) measurements had a (310) on-axis orientation, which would be consistent with this hypothesis. Also of the three planes, (310), (100), and (112), from which data was taken the (112) plane had the largest FN area. Coupled with the relatively small anisotropy factor this would explain why the effect is not seen on the other planes. The conclusion must remain tentative until a more precise check of the accuracy of the theory can be made.

The FN area and Fig.24 also show that $l_1 = 86$ Å , $l_2 = 71$ Å , $l_3 = 54$ Å , and Ω_4 implies $\delta = 106$ Å . Eq.(164) yields $\delta = 84$ Å . The diffusion coefficient is $D(905K) = 7.4\times10^{-10}\,cm^2/sec$.

2. Discussion.

The spectral analysis for the GCE developed in the previous sections has been applied to thermal field emission noise spectra taken from W(100), W(310), and W(112) planes at two sets of temperatures 870—905K and 1318K. The theory has been able to reproduce each of the five measured $S(\omega)$ spectra and accounted for temperature, emitter geometry, and diffusivity effects. Specifically the increase in net (hkl) plane due to thermal field buildup has been identified and distinguished from the temperature dependent diffusion coefficient.

Table 3. Summary of derived values for the W-thermal field emitter.

	W(100)		W(310)		W(112)
T (K)	905	1318	870	1318	905
β	2.6	60.	1.8	2.9	3.1
δ (A) (a)	37	920	27	49	106
(b)	58	1322	77	64	84
$D(cm^2/sec)$	2.8×10^{-10}	1.2×10^{-7}	3.8×10^{-10}	6.1×10^{-10}	7.4×10^{-10} 2.8×10^{-10} [18] 1.4×10^{-10} [19]
E_D(eV)	1.5		0.1		
Q(ev)	2.6 [c]2.4				

(a) This work

(b) From Eq.(32) of ref.[16]

(c) Orientation averaged, ref.[21].

Table 3 summarizes the quantities derived from this analysis. The diffusion coefficient found for the (112) plane is in close agreement with values obtained from two field ion microscopy (FIM) studies that were performed in the range $250K \leq T \leq 400K$. The values obtained from these studies have since been shown to

be the result of a combination of single and pair adatom motion, which separately have different diffusion coefficients [20]. Therefore it is likely that both single and pairwise surface diffusion of tungsten adatoms also occurred on the thermal field emitter surface. The defect formation activation energy for W(100), $Q = 2.6\,eV$, is very close to the value derived by Bettler and Charbonnier in their study of the thermal field induced buildup process [21]. Their value is the average contribution from several (hk) planes, but since the W(110) is the only *bcc* plane more densely packed than the W(100) the agreement is not fortuitous as these planes are the rate limiting regions for the buildup process.

The noise measurements occupy an intermediate position with respect to temperature when compared with FIM and the buildup experiments. Furthermore both Q and E_D are obtained here whereas the other two methods find one but not both of these quantities. The close agreement with the activation energies found by these other methods provides strong support for the present theory especially when it is recalled that the combined measurements occur over a $2000K$ temperature range, the agreement between the diffusivities is on the order of 1 part in 10^{12}, and the estimated defect activation energies are within 10% of each other.

Another interesting development of this work is that the resolution of the field emission microscope is derivable from the characteristic frequency Ω_4 when it appears in the measured $S(\omega)$ curves. As shown in Table 3 there is generally quite good agreement with the resolution estimate based on Eq.(164). The derivation of this equation relies on a consideration of the energy distribution transverse to the normal emission direction, which is governed by Fermi-Dirac statistics. It is curious that the fluctuation theory presented here proceeds from a classical statistical viewpoint of density fluctuations to derive the resolution whereas Eq.(164) is based on the quantum

mechanical properties of the emitted electrons.

3. The "ideal" $1/f$ spectrum.

The nature of $1/f$ noise spectra has remained a subject of fascination for more than thirty years continuing to the present as a perusal of the literature will show. Of course it is well known that a spectral density function cannot be purely $1/f$ since it results in logarithmic divergences of the noise power in both the low and high frequency limits. Nonetheless a considerable effort has been spent to understand what are the causes of such a spectrum and why it appears in so many systems. Here I speculate on why this is so and give the conditions that yield the largest frequency band, within the limits of the diffusion model for the GCE, leading to $S(f) \propto 1/f$.

Since $S(\omega) \propto C(x=0,\omega)\, N_c^{-1}(\omega)$, for any ω^{-1} region to appear the minimum conditions are that $\Omega_2 < \Omega_3$ and $\Omega_2 < \omega_1$, refer to Fig.17 and Table 2. The latter inequality implies $l_1 < \pi L_2/\sqrt{2}$. A large $S(\omega) \propto \omega^{-1}$ band appears when $\Omega_2 \ll \Omega_3$, i.e. when $L_2 \gg L_3$. In physical terms the ω^{-1} region is extended when $D \ll \omega_{min} L_2$, where ω_{min} is the smallest measured frequency. The band is further increased if $\omega_1 \approx \Omega_3$ and $\omega_2 \geq \Omega_4$. For this case $S(\omega) \propto \omega^{-1}$ in the broadest possible frequency band, which is $[\,\Omega_2\,,\,\Omega_4\,]$. The ratio $\Omega_4/\Omega_2 = (L_2/\delta)^2$ so the band is four decades wide if $L_2/\delta \approx 100$, which for a field emitter only requires a net plane diameter of 2,500 Å .

These geometrical limits are sketched in Fig.25. The broadest frequency band resulting in $S(\omega) \propto \omega^{-1}$ occurs with a large thin rectangular or square sample and a rectangular parallelepiped with small cross section of the order of the smallest sample

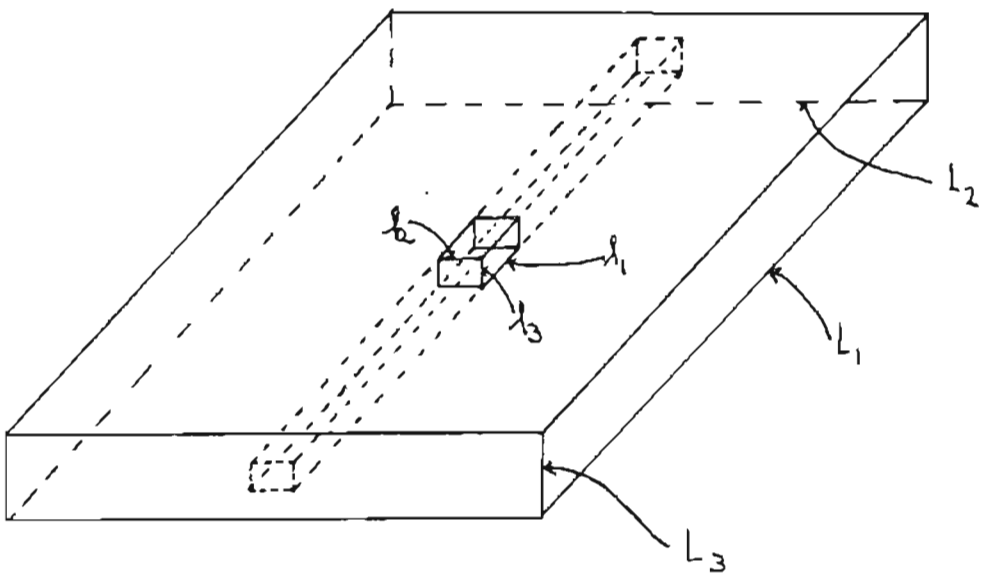

Fig.25. Diagram of the probe-sample geometry that produces a broad band spectrum of the form $S(\omega) \propto \omega^{-1}$.

dimension whose length does not exceed $2L_2/\sqrt{\pi}$.

It is now hypothesized that the prevalence of $1/f$ spectra is due to the detector interacting with relatively small portions of an essentially planar geometrical region coupled with an appropriate diffusion coefficient. As an example consider current noise produced at semiconductor contacts as a representative class of systems that exhibit this behavior, see chapter I references for a partial list of these studies.

Assuming Voss and Clarke's explanation that resistor flicker noise is induced by equilibrium temperature fluctuations [2] and also that the boundary of a metal-semiconductor system has a higher resistivity than the bulk regions then it follows that temperature fluctuations in this boundary region will be the dominant factor influencing fluctuations in charge transport. The noise is detected when current passes through the contact. Given good mechanical contact occurs within the boundary region over relatively small areas where the semiconductor metallization exists then the current will pass primarily through these areas. Hence the probed region will be much smaller than the planar region throughout which the temperature-resistance fluctuations are occurring. This corresponds to the situation described in Fig.25 therefore leading to broadband $1/\omega$ noise.

H. Summary of chapter IV.

The starting point for equilibrium field emission noise theory is the corresponding autocorrelation function

$$R(t) = C_{FN} \int\int < \delta n(\vec{r}_1, t)\, \delta n(\vec{r}_2, t) > d\vec{r}_1\, d\vec{r}_2, \qquad \text{(IV.1)}$$

which relates the current noise to surface density fluctuations $\delta n(\vec{r}, t)$. The difference between chapter I and the present one is in the method of evaluating this fluctuation. Here the density fluctuation satisfies a stochastic diffusion equation of the Langevin type

$$\left(\frac{\partial}{\partial t} - D\nabla^2 + \tau^{-1}\right) n(\vec{x},t) = \mathbf{Z}_+(\vec{x},t), \qquad \text{(IV.22)}$$

which allows for fluctuations in the total number of adatoms on a net plane. This property distinguishes the model from chapter I where the net plane adatom number is constant. The resulting difference in the mathematical formalism is considerable.

The solution to this differential equation was written in the compact form of a convolution product that includes a consideration of the finite size of the net plane,

$$n(\vec{x},t) = \mathbf{Z}_+(\vec{x},t) \;{}^{**}\; e^{-t/\tau} F(\vec{x},t). \qquad \text{(IV.30)}$$

This was a nontrivial task as the bounded fundamental solution to the diffusion equation is composed of an infinite series of terms. The utility of a convolution product solution becomes evident when the solution to Eq.(10) is Fourier transformed to get the corresponding spectral density function $S(\omega)$.

The local time dependent density is composed of the unbounded solution to the diffusion equation and a special set of Poisson impulse functions that appear in

Eq.(30). The statistics of these impulses are calculated so that the principal statistical functions $R(t)$ and $S(\omega)$ themselves can be computed. A method similar to one developed by Rice is used to calculate the Poisson statistics. Several standard results are derived by a different route. More importantly balance equations are derived by calculating the mean value of the density. The most significant aspect of this part of the work is that a finite lifetime τ must be imposed on the fluctuations for equilibrium to be maintained. This is the first time the necessity of including this factor has been fully appreciated. It also has important consequences for the subsequent spectral analysis. It was also shown that the type of boundaries, i.e. reflecting or absorbing, plays only a secondary role in determining the nature of the noise spectrum.

The correlated volume concept suggested by Voss and Clarke is placed on a firm foundation by a separate Fourier analysis of the fluctuating probe current. This idea is crucial in providing an approximation to a double spatial integration of the point frequency correlation $C(|\vec{x}_1 - \vec{x}_2|, \omega)$. The result is

$$S_o(\omega) \approx \frac{V_p^2 \; C(x=0,\omega)}{N_c(\omega)}, \tag{IV.97}$$

which expresses the noise spectrum in terms of the calculable number of correlated volumes $N_c(\omega)$ and $C(|\vec{x}_1 - \vec{x}_2|, \omega)$. It is stressed that the probe spatial averaging influences the former term while the sample boundary effect is contained in the latter.

The finite fluctuation lifetime produces a zero slope low frequency: correlation length Λ_r point correlation $C(x=0, \omega)$, and spectral density $S(\omega)$. These observations coupled with a detailed investigation of $N_c(\omega)$ also resolves an outstanding problem stated by Voss and Clarke concerning the appearance in their theory of a divergent noise power integral. A somewhat different divergence encountered by Bliek is

also removed by the presence of τ.

Out of the analysis of the correlated volume construction comes a potentially even more interesting result. There it was demonstrated that removal of the divergence requires introducing a lower length scale for distinguishing fluctuations. This introduces in a natural manner the resolution limit of the detector, which in the present case is the field emission microscope. Later comparison with experimental noise data proved it could indeed by measured and the values obtained were in good agreement with the theoretical prediction based on the transverse energy distribution of the field emitted electrons. One therefore has the interesting possibility of measuring detector resolution from spectral analysis of the current fluctuations.

Several methods are suggested for extracting the diffusion coefficient from spatial correlation measurements. However the more direct method is to evaluate $S(\omega)$ itself. The frequency dependence of $S(\omega)$ is delimited by two sets of characteristic frequencies $\{\Omega_i = \pi^2 D/L_i^2\}$ and $\{\omega_i = 2D/l_i^2\}$, which are respectively functions of net plane and probe geometry. These sets are used to curve fit the various theoretical $S(\omega)$'s to measured W - thermal field noise spectra. The procedure results in a determination of the diffusion coefficient, its corresponding activation energy, the activation energy for defect adatom formation, and the elucidation of the net plane buildup affect on this data. Close agreement with derived values for these quantities obtained by other techniques lends strong support to the validity of this construction.

As a final note the conditions for the broadest band $S(\omega) \propto \omega^{-1}$ possible within the diffusion model are given and a hypothesis is presented on the reasons for the ubiquitous nature of this type of spectra.

I. Chapter IV references.

[1] L. Swanson, "Current Fluctuations From Various Crystal Faces of a Clean Tungsten Field Emitter." *Surface Science.* **70** *(1978) 165.*

[2] R.F. Voss and J. Clarke, "Flicker (1/f) Noise: Equilibrium Temperature and Resistance Fluctuations." *Phys. Rev.* **B13** *(1976) 556.*

[3] L. Bliek, "A Diffusion Model for 1/f Noise for Samples of Finite Dimension." *"Recent Developments in Condensed Matter Physics" vol.3,* eds. DeVreese, Lemmens, Van Doren, Van Royen *(Plenum, 1981).*

[4] S.O. Rice, "Mathematical Analysis of Random Noise," *Bell System Technical Journal* **23,24** *(1944) 1.* Also in *"Selected Papers on Noise and Stochastic Processes"* ed. Wax *(Dover, New York 1954).*

[5] L.W. Swanson and A.E. Bell, "Recent Advances in Field Electron Microscopy of Metals." In *"Advances in Electronics and Electron Physics" vol. 32 (Academic Press, New York 1973).*

[6] I. Stakgold, *"Boundary Value Problems of Mathematical Physics" vol. II (Macmillan, 1968).*

[7] W. Feller, *"An Introduction to Probability Theory and Its Applications" vol. II (Wiley and Sons, New York 1966).*

[8] A. Papoulis, *"Probability, Random Variables, and Stochastic Processes." (McGraw - Hill, New York 1965).*

[9] G. Mazenko, J.R. Banavar, and R. Gomer, "Diffusion Coefficients and the Time Autocorrelation Function of Density Fluctuations." *Surface Sci.* **107** *(1981) 459.*

[10] E.T. Whittaker and G.N. Watson, *"A Course in Modern Analysis" chpt. XXI, 4th ed. (Cambridge Univ., 1980).*

[11] *"Tables of Integral Transforms" vol.1, ed.* Erdélyi *(McGraw-Hill, New York 1954).*

[12] J.R. Carson, "The Statistical Energy-Frequency Spectrum of Random Disturbances." *Bell System Technical Journal* **10** *(1931) 374.*

[13] A. van der Ziel, *"Noise: Sources, Characterization, Measurement." (Prentice-Hall, Englewood Cliffs, N.J. 1970).*

[14] M.J. Lighthill, *"Fourier Analysis and Generalised Functions." (Cambridge Univ., 1978).*

[15] A. Seeger, "Theorie der Gitterfehlstellen." In *"Handbuch der Physik" vol. VII/1 (Springer-Verlag, Berlin 1955).*

[16] R. Gomer, *"Field Emission and Field Ionization" (Harvard Univ., 1961).*

[17] L.W. Swanson and R.W. Strayer, "Field-Electron-Microscopy Studies of Cesium Layers on Various Refractory Metals: Work Function Change." *J. Chem. Phys.* **48** *(1968) 2121.*

[18] D.W. Bassett and M.J. Parsley, "Field Ion Microscope Studies of Transition Metal Adatom Diffusion on (110), (211), and (321) Tungsten Surfaces." *J. Phys. D* **3** *(1970) 707.*

[19] G. Ehrlich and F.G. Hudda, "Atomic View of Surface Self-Diffusion: Tungsten on Tungsten." *J. Chem. Phys.* **44** *(1966) 1039.*

[20] W.R. Graham and G. Ehrlich, "Surface Self-Diffusion of Atoms and Atom Pairs." *Phys. Rev. Lett.* **31** *(1979) 1407.*

[21] P.C. Bettler and F.M. Charbonnier, "Activation Energy for the Surface Migration of Tungsten in the Presence of a High-Electric Field." *Phys. Rev.* **119** *(1960) 85.*

Conclusion

"What I tell you three times is true."
Lewis Carrol The Hunting of the Snark

Noise power spectra have been derived for both adsorbate covered and clean field electron emitters. The current noise probes emitter surface density fluctuations and provides a measure of adatom static and dynamic properties. Previously unidentified adsorbate phase transitions have been detected. In the case of thermal field emission the spatial resolution of the detector can be determined. Formally the analysis is related to the general theory of $1/f$ noise governed by diffusive equilibrium fluctuations.

In the case of adsorbate covered emitters, corresponding to a canonical ensemble, the most general classical expression for the field emission autocorrelation function has been derived and shown consistent with the first one derived by Gomer. The first correct spectral density function has also been derived for this case. For unbounded diffusion, i.e. no net plane boundary effect, it is analogous to one derived by Burgess to explain contact noise in semiconductors. It also corresponds to Gomer's autocorrelation function. The first closed form solution of the spectral density has been derived that includes net plane boundary effects.

Thermal field emission noise has been placed in the context of a grand canonical ensemble and density fluctuation dynamics are described by a diffusion equation with stochastic inhomogeneous source term. Subsequent analysis yields the first divergence free spectral density function than includes net plane boundary, probe spatial averaging, and finite fluctuation lifetime effects. Balance equations required for maintaining

equilibrium are also developed. Details of experimental noise spectra are explained. Surface diffusion coefficients, defect vacancy activation energies, and the resolution of the field emission microscope are all derived from the spectral density functions. A hypothesis is also put forth explaining the frequent occurrence of $1/f$ type spectra for diffusive equilibrium systems and the broadest band purely $1/f$ spectra is stated in terms of probe-system geometry.

The fundamental dynamical quantity derived from analysis of the time variation of the noise is the density dependent diffusion coefficient. Field emission noise experiments measure equilibrium density fluctuations and so are placed in the same category as neutron scattering of liquids and light scattering by dilute suspensions. The diffusivities derived from this type of studies is compared to one derived from macroscopic decay of a density gradient involving irreversible thermodynamic relations and with ones obtained from Monte Carlo computer simulations, which model all of the above. The issues discussed can be stated as three related questions. One is, when does the diffusivity obtained in a nonequilibrium experiment equal that obtained by measuring equilibrium fluctuations? Two, under what conditions can it be ensured that irreversible thermodynamics is equivalent to microscopic equilibrium fluctuation theory? And three, under what conditions can the stability of a nonlinear partial differential equation be guaranteed and hence ensure a unique solution? As discussed in chapter II a truly comparative diffusion study of the density dependence of the diffusion coefficient has yet to be done. Theoretically the implications of nonequilibrium thermodynamic stability theory have yet to be completely elucidated as its range of validity is not completely clear for diffusive systems.

The relation between static and dynamic properties of a two dimensional system undergoing a phase transformation has been touched on within the context of field

emission noise studies. A number of experimental data are reinterpreted. Kinetic expressions included in the diffusion coefficient have been evaluated by a two level thermodynamic model.

Two of possibly the most interesting experiments that should be investigated concern the determination of the virtual source size of a thermal field emitter from the resolution estimate obtained from the spectral density function, and secondly extension of the noise analysis to liquid metal ion sources, which are of current research and technological interest.

The present work provides a framework for further experimental tests and extension in the abovementioned directions. A direct measure of the virtual source would be of use to those involved with electron optical problems. This work also firmly places field emission noise in the context of the general theory of diffusion mediated flicker noise and resolves several mathematical problems found there. Detailed fluctuation analysis and experiment presents a most sensitive probe of the internal dynamic mechanisms of the system under investigation.

BIOGRAPHICAL NOTE

The author was born 26 September 1955 in San Diego, California. He attended public schools in Oregon City, Oregon, was an American Field Service foreign exchange student to Belo Horizonte, Brazil in the summer of 1972 and graduated from Oregon City High School in June 1973. He then entered Reed College, majored in physics and received his Bachelor of Arts degree in June 1977. The latter part of 1977 was spent working as a technician in Professor Swanson's laboratory at the Oregon Graduate Center. During 1978 the author travelled throughout South America from the Amazon basin in northeast Brazil to Patagonia, Argentina and then up through the Andes including parts of the Inca trail in Peru. The winter of 1978-1979 was spent in Pennsylvania designing and building stained glass windows. In June 1979 he returned to the Oregon Graduate center as a technician and in September 1981 began study there as a graduate student where he completed the requirements for the degree of Doctor of Philosophy in June 1985.

The author is a member of Phi Beta Kappa, Sigma Xi, the American Physical Society, and the American Mathematical Society.